CHALMERS
UNIVERSITY OF TECHNOLOGY

Mineral Carbonation for Permanent Sequestration of CO_2

Experimental study of CO_2 capture and storage by mineral carbonation using mine tailings as starting material, followed by a technoeconomic assessment of a possible upscaled process.

Master's thesis in chemistry and chemical engineering, KBTX12

SIMON DUDA
IVAR KÖRNER ACEVEDO

DEPARTMENT OF CHEMISTRY AND CHEMICAL ENGINEERING
DIVISION FOR CHEMISTRY AND BIOCHEMISTRY

CHALMERS UNIVERSITY OF TECHNOLOGY
Gothenburg, Sweden 2023

Master's Thesis Report

Mineral Carbonation for Permanent Sequestration of CO_2

Experimental study of CO_2 capture and storage by mineral carbonation using mine tailings as starting material, followed by a technoeconomic assessment of a possible upscaled process.

Simon Duda, Ivar Körner Acevedo

Examiner: Henrik Leion, professor at Environmental Inorganic Chemistry, Chalmers University of Technology

Supervisors: · Marcus Hedberg, researcher at Nuclear Chemistry, Chalmers University of Technology
· Placid Atongka Tchoffor, researcher at Materials Design, RISE Research Institutes of Sweden

Department of Chemistry and Chemical Engineering
Chalmers University of Technology
Göteborg, Sweden 2023

Mineral Carbonation for Permanent Sequestration of CO_2

Experimental study of CO_2 capture and storage by mineral carbonation using mine tailings as starting material, followed by a technoeconomic assessment of a possible upscaled process.

Simon Duda, Ivar Körner Acevedo

Master's Thesis Report
Department of Chemistry and Chemical Engineering
Chalmers University of Technology
SE-412 96 Göteborg
Sweden
Telephone +46 31-772 10 00

The thesis was conducted in collaboration with:
RISE Research Institutes of Sweden AB
Division Built Environment
SE-412 79 Göteborg
Sweden
Telephone +46 10-516 50 00

Chalmers Library
Göteborg, Sweden 2023

Mineral Carbonation for Permanent Sequestration of CO_2

Experimental study of CO_2 capture and storage by mineral carbonation using mine tailings as starting material, followed by a technoeconomic assessment of a possible upscaled process.

Simon Duda, Ivar Körner Acevedo
Department of Chemistry and Chemical Engineering
Chalmers University of Technology

Abstract

Carbon Capture and Storage (CCS) is an important tool for combating the ongoing climate crisis. In this thesis, a CCS method known as mineral carbonation has been studied, with the aim to assess the feasibility of using mine tailings for CCS via indirect mineral carbonation, as well as to estimate the economic viability of a corresponding upscaled industrial process.

Mine tailings from three Swedish and Finnish mines were leached with HCl or NH_4HSO_4 at different temperatures. After filtration, pH was adjusted to 9 and 10 with NH_4OH, with filtering steps at pH 5, 7, 9 and 10 to investigate possibilities for byproduct recovery. Lastly, carbonation with 15 vol% CO_2 was conducted at 35 °C with solution alkalinity left to decrease to a stop condition of pH 8. Solid samples were analyzed with PXRD, liquid samples with ICP-OES. Carbonation efficiencies, amounts of captured CO_2 per tonne feedstock and CO_2 capture efficiencies were calculated.

Higher leaching temperature was found to promote extraction of Mg, whereas the correlation for Ca was unclear. HCl produced higher extraction yields than NH_4HSO_4. Byproduct recovery was not successful upon pH adjustment, partly due to insufficient amounts of solid precipitates for PXRD analysis. Carbonation of the extracted Ca was successful and relatively fast, while carbonation of Mg was slow and unsuccessful when starting at pH 9.

In the technoeconomic assessment, calculations were made in terms of operating expenses (OpEx) for an industrial process which mimics the laboratory procedure in this thesis. While heating was found to be the highest source of energy demand, the cost of chemicals for leaching and pH adjustment was identified as the single largest expense. Therefore, recycling the chemicals is crucial if an economically viable process is to be developed.

Mine tailings from the Kaunis Iron mine in Pajala and the Boliden mine in Garpenberg can be feasible for mineral carbonation, much depending on the reaction parameters. Future studies should focus on further mapping of the reaction parameters' influence on the carbonation and sequestration efficiencies, as well as on finding feasible ways to recycle at least 95 % of the make-up chemicals.

Keywords: mineral carbonation, CO_2 mineralization, mine tailings, carbon capture and storage, CCS, technoeconomic assessment

Mineral Carbonation for Permanent Sequestration of CO_2
Experimental study of CO_2 capture and storage by mineral carbonation using mine tailings as starting material, followed by a technoeconomic assessment of a possible upscaled process.
Simon Duda, Ivar Körner Acevedo
Department of Chemistry and Chemical Engineering
Chalmers University of Technology

Acknowledgmenets

We would like to express sincere gratitude to our examiner and supervisors, Henrik Leion, Marcus Hedberg and Placid Atongka Tchoffor, for their guidance throughout the project and their commitment to help us when things went difficult.

We would also like to thank Jonas Zetterholm at RISE in Sundsvall, Sweden, for kindly taking on a supervisor role for the technoeconomic assessment part of the project. These results would have been much more difficult to obtain without his guidance.

Last but not least, a word of appreciation to Ron Zevenhoven and his team at Åbo Akademi University (ÅA) in Turku, Finland, for their willingness to introduce us to the research at ÅA, and to show us the laboratory procedures conducted there. This experience provided a valuable insight in how the experiments can be done and ultimately made it much easier to start with the laboratory work after arriving back in Gothenburg.

Mineral Carbonation for Permanent Sequestration of CO_2

Experimental study of CO_2 capture and storage by mineral carbonation using mine tailings as starting material, followed by a technoeconomic assessment of a possible upscaled process.

Simon Duda, Ivar Körner Acevedo
Department of Chemistry and Chemical Engineering
Chalmers University of Technology

List of Abbreviations

ABS	Ammonium Bisulfate (NH_4HSO_4)
CapEx	Capital Expenses
CCE	CO_2 Capture Efficiency
CCS	Carbon Capture and Storage
CCGS	Carbon Capture and Geological Storage
CCUS	Carbon Capture, Utilization and Storage
CE	Carbonation Efficiency
DH	District Heating
DW	Distilled Water
ICP-OES	Inductively Coupled Plasma - Optical Emission Spectroscopy
IPCC	Intergovernmental Panel on Climate Change
LCA	Lifecycle Assessment/Analysis
MSWI-FA	Municipal Solid Waste Incineration Fly Ash
OpEx	Operational Expenses
PCC	Precipitated Calcium Carbonate
PES	Polyethersulfone
PFB	Pressurized Fluidized Bed (Reactor)
PXRD	Powder X-Ray Diffraction
XRF	X-Ray Fluorescence

Mineral Carbonation for Permanent Sequestration of CO_2
Experimental study of CO_2 capture and storage by mineral carbonation using mine tailings as starting material, followed by a technoeconomic assessment of a possible upscaled process.
Simon Duda, Ivar Körner Acevedo
Department of Chemistry and Chemical Engineering
Chalmers University of Technology

List of Figures

Simon Duda, Ivar Körner Acevedo
Department of Chemistry and Chemical Engineering
Chalmers University of Technology

List of Tables

Contents

1 Introduction

The ongoing climate crisis poses a threat to nearly all aspects of the modern society. More than 20 million people are already forced to relocate annually due to extreme weather events [1]. According to IPCC, an important threshold for a rapid climate change will be the 1.5 °C goal [2]. This goal, agreed upon by 196 countries in the Paris Agreement, determines that humanity should take all measures available to prevent the Earth's mean surface temperature from increasing more than 1.5 °C [3]. As human activity, such as the engineering and technology in use, is designated as the prime factor behind the accelerated climate change, it will also have to be part of the solution.

One of the many technological approaches to hamper the advancing climate change are strategies for permanent sequestration, i.e., binding and depository of carbon dioxide (CO_2), also known as Carbon Capture and Storage (CCS). This is an all growing area of interest and technological research, much due to human-enforced CO_2 emissions, and the subsequently augmented greenhouse effect, being the major contributor to the rising temperature on Earth. Moreover, the government of Sweden has set up its own goal for net zero greenhouse gas emissions by 2045. If that goal is to be reached, CCS will be a necessary tool.

Mineral carbonation is a promising method of CCS that aims at mimicking and accelerating its naturally occurring counterpart - weathering of rocks, where alkaline earth metals are converted into environmentally stable and benign carbonates. It is an especially interesting field for countries that lack vast and suitable capacities for underground storage of CO_2 gas (CCGS), such as Sweden, Finland, Estonia etc. [4]. The idea, originally presented in 1990 [5], has since seen an increase in research activity, and there is nowadays a variety of proposed process routes, reaction conditions and starting materials, which all aim at maximizing the CO_2 sequestration potential while minimizing energy/time penalties and overall costs [6].

An interesting starting material for mineral carbonation is a byproduct of the mining industry that has historically been shunned, i.e., mine tailings. These Ca- and Mg-rich residuals could, depending on their composition, be used for extraction of the alkaline earth metals and subsequent carbonation. As the ambitions presented by IPCC regarding decreasing CO_2 emissions are largely based upon electrification [2], the demand for metals is expected to increase. This poses a challenge since the mining industry of Sweden currently stands for approximately 7 % of Sweden's CO_2 emissions [7]. It also means, however, that the availability of mine tailings is set to increase further, while already being a well-accessible and cheap material. This motivates research in mine tailings as possible starting material for mineral carbonation, especially in countries like Sweden. Moreover, there is a trend in society and industry to minimize the amounts of waste produced as much as possible. As mine tailings are today being disposed of as waste, utilizing them for a useful application instead is of great interest to help minimize the production of waste.

This Master's thesis deals with the permanent sequestration of CO_2 through carbonation of Ca and Mg, extracted from Swedish and Finnish mine tailings, as well as a technoeconomic assessment of the upscaled process.

1.1 Aim

The aim of the experimental part of this thesis is to assess the feasibility of using mine tailings for CO_2 sequestration through mineral carbonation. To meet the aim of the study, the objective has been set to experimentally quantify the amount of CO_2 that can be captured and stored with mine tailings from Sweden and Finland during indirect carbonation.

As for the technoeconomic assessment part of the project, the aim is to estimate the economic viability of using tailings for CO_2 sequestration via indirect carbonation. To achieve this, an operating expenses (OpEx) estimation was calculated on an upscaled, industrial version of the carbonation route used in the experimental part.

1.2 Limitations

The scope of this study is focused on investigating possibilities for mineral carbonation via the indirect route, i.e., the direct route is omitted. Also, only tailings from certain mines will be examined, meaning that results may vary if tailings from other sources are used, as they may have different compositions. Ambient pressure and only slightly elevated temperatures (up to 80 °C) are used in the experiments. While there are many possible compounds that can be used as leaching agents and pH regulators, this study only uses HCl and NH_4HSO_4 as leaching agents and NH_4OH as pH regulator. Particle size is not varied, only particles $\leq$ 150 µm are studied.

The technoeconomic assessment in this study is limited to OpEx, i.e., operating expenses of a possible industrial application of the carbonation procedure examined experimentally. Capital expenses (CapEx) are thus omitted.

2 Background and state of research

Carbon Capture and Storage (CCS) has been a growing area of research for a few decades now and has since its beginnings seen important milestones in research, as well as commercialization at some sites. A variety of different techniques, methods and starting materials has been proposed [8]. Today, CCS can be roughly divided into four major ways to sequestrate carbon dioxide (CO_2). Geological storage (CCGS), where CO_2 is effectively pumped into vast underground storage spaces, but where future leakage, and thus a need for constant maintenance, are drawbacks to this method. It is, however, the to date most commercialized method of CO_2 sequestration. Oceanic storage and incorporation of CO_2 in industrial products are two other carbon storage methods, although only allowing short-term storage and, in the case of the oceanic storage, also possibly implying negative environmental effects [4, 6].

Mineral carbonation, also known as CO_2 mineralization, is the fourth carbon storage method, the only one to date that allows for permanent CO_2 sequestration without the risk of future leakage. This is because the carbonate products are stable under ambient conditions, environmentally benign, and abundant in nature, meaning they provide an inherently safe and permanent way to sequestrate CO_2 [6]. The setback here is the kinetics and the cost – mineral carbonation, as a naturally occurring process, is much slower than would be needed for efficient sequestration of large amounts of CO_2. Many of the attempts to accelerate the reactions have so far shown to be either too slow still, not efficient enough (low carbonation potential), or very energy intensive, thus driving up the cost of the process into non-justifiable numbers [4, 6].

This thesis, as part of a larger, international research project, aims at providing further clues into overall effectivization of the process for the research project. The project deals with mineral carbonation using a start material that is cheap, alkaline earth metal-rich and well-abundant in Sweden – mine tailings, i.e., rest-products of the mining industry, which are often regarded as waste and disposed of accordingly. The hope is to eventually present an industrially feasible way to make use of the tailings, while simultaneously binding and storing significant amounts of CO_2, and also, hopefully, recovering viable products along the way, that could be sold to other industries, thus lowering the operational costs of the process (also referred to as CCUS - Carbon Capture, Utilization and Storage) [9].

2.1 Natural carbonation

The reaction of CO_2 with alkaline earth metal ions, e.g., Ca^{2+} and Mg^{2+}, to form carbonates, MCO_3, where M = {Ca, Mg}, is a naturally occurring process that has a potential to bind some of the atmospheric CO_2. In nature, the process most often happens when alkaline silicate minerals are in contact with water. The reactive components, i.e., the metal ions, dissolve in water, along with atmospheric CO_2, forming the dissolved species Ca^{2+}/Mg^{2+}(aq) and CO_3^{2-} (or HCO_3^-), which then react to form solid, environmentally stable carbonates [10]. The process can be described with an overall, generalized chemical reaction as follows [11]:

$$MSiO_3 + CO_2 + nH_2O \longrightarrow MCO_3 + SiO_2 \cdot nH_2O \tag{2.1}$$

where M is an alkaline-earth metal ion, or even some of the divalent transition metal ions, e.g. Ca^{2+}, Mg^{2+} or Fe^{2+} [11].

The natural process, caused by various biogeochemical processes, is important for the Earth's surface and soil modelling, as well as climate control over geologic time scales [11]. It is, unfortunately, slow, therefore unable to handle the vast amounts of anthropogenic CO_2. Given the environmentaly benign and stable nature of the carbonate products, however, it is of interest for science to accelerate the reaction [10].

2.2 Mineral carbonation - choice of start material and process routes

There are various takes on a mineral carbonation process. First, the starting material must be chosen. This should be a mineral/rock that is rich in Ca and Mg, readily available and, preferably, cheap. So far, research has focused on steelmaking slags [12], municipal solid waste incineration fly ash (MSWI-FA) [13], mine tailings of different kinds, and other waste materials and industrial residues, e.g., cement kiln dust, waste cement, bauxite residue, or coal fly ash [6]. For this thesis, the research on mine tailings is of most interest, although others will be mentioned as well.

The chosen starting material may need to be processed in some way before moving forward with the reactions of interest. In the case of mine tailings, these may contain large amounts of water, which is preferably dried away to ease handling and avoid interference with other chemicals later in the process. Also, the dried sand should be sieved to achieve a somewhat uniform particle size in the material.

Nonetheless, there are two ways to perform the carbonation. It can be done directly, by reacting the material with gaseous or aqueous CO_2, or indirectly, i.e., by first extracting the earth metals from the material, then reacting the resulting matrix with CO_2 [6]. The extraction can be achieved in different ways, e.g., by leaching with an acid, or with an ammonium salt solution, or by other, less conventional ways [6]. After the extraction, more steps may be needed before the actual carbonation reaction can be performed. Figure 2.1 shows a visual representation of the different strategies for mineral carbonation.

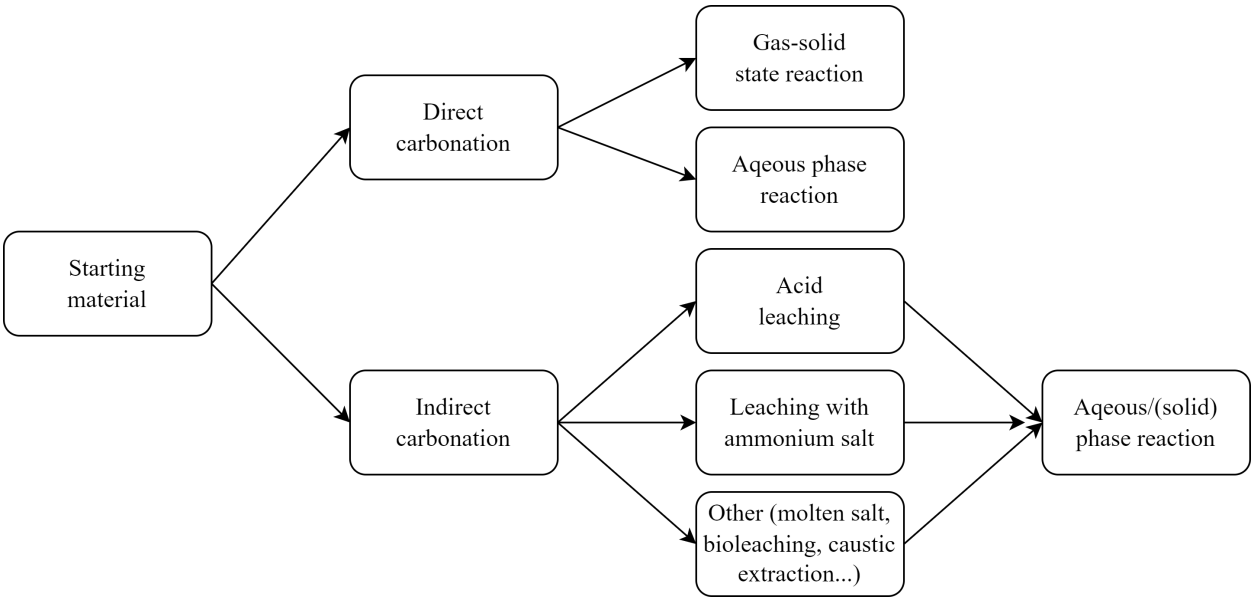

Figure 2.1: Rough map of possible routes of mineral carbonation (based on Bobicki et al. [6]).

2.3 Direct carbonation route

Direct mineral carbonation involves reaction of a chosen starting material with CO_2, either in gaseous or aqueous form. The main benefit with this route is the relatively simple process with few intermediate/pre-carbonation steps. The main problem seems to be the slow reaction kinetics, stemming from the fact that this direct route mimics the natural variant of carbonation the closest [6].

Direct carbonation with gaseous CO_2 has been demonstrated successfully, however, the kinetics seem to limit its practical utilization. The need for elevated temperatures and pressures comes with an upper limit, after which carbonation no longer works. The problem is that for common, naturally occurring silicates, this often means that the reaction kinetics cannot be sped up enough to make the process industrially feasible. On the other hand, carbonation of oxides or hydroxides has been demonstrated with acceptable rates; these materials are, however, less prevalent and are mostly found as industrial waste streams [6].

Direct carbonation in an aqueous suspension on the other hand, has been proven industrially feasible even with naturall silicates, like serpentine and olivine. The major obstacle here seems to be, apart from the more complex chemistry, the cost of the process. Acceptable reaction rates often come with requirements such as eleveated temperatures and pressures during the reaction, as well as extensive pre-treatments of the mineral prior to the reaction [6]. There is, however, progress being made in the present day to this type of carbonation. In a recent study, Zhao et al. [13] trialed direct aqueous carbonation on MSWI-FA. While using similar reaction conditions to this thesis, i.e., ambient pressure, added ammonium salt at 1 M, setting reaction temperature to 60 °C and a gas flow rate of 1 l/min, they achieved a carbonation efficiency of 78.49 %, rendering the direct carbonation route a promising method for CO_2 sequestration using an alkaline waste material as feedstock [13].

Since this thesis deals with the indirect carbonation route, the direct route will not be discussed further in this report.

2.4 Indirect carbonation route

Indirect mineral carbonation resembles the direct route, only with multiple steps in the process. Most often, this involves some pre-treatment of the starting material, followed by extraction of Mg^{2+} and Ca^{2+}, typically by leaching with an acid or an ammonium salt solution. Other extraction techniques have been demonstrated as well. The carbonation reaction only takes place after the extraction, and a possible intermediate step. Similarly to the direct route, the carbonation reaction can be done either in a gas-solid state, or in an aqueous suspension [14].

2.4.1 Gas-solid state reaction

Much of current research on mineral carbonation focuses on the indirect route conducted in aqueous suspenstions. There is, however, research done on the gas-solid state reaction as well. Zevenhoven et al. [14] have demonstrated this type of carbonation on serpentinite mine tailings using a pressurized fluidized bed reactor (PFB) at elevated temperatures and pressures, after first precipitating $Mg(OH)_2$ with ammonium hydroxide (NH_4OH). Only modest converstions (26%) and slow kinetics were obtained. However, large amounts of iron were obtained during the hydroxide precipitation step, pointing to possible implications within the Fe/steel producing sector [14].

Using a fluidized bed reactor, accelerated reaction could be achieved at elevated pressures, with the overall objective to make the reaction fast enough for the process to not require additional heat (for the hydroxide precipitation step). The main obstacle here was identified as the competition between $MgCO_3$ and MgO being formed [4]. Gas-solid conversion of the MgO into $MgCO_3$ has later been shown to be much slower than the conversion of $Mg(OH)_2$ [15]. Even a mechanochemical approach with a "CO_2-carrier" in the form of ammonium bicarbonate (NH_4HCO_3) has been trialed, yielding good extraction of Mg (>60%), but only modest converstions (30%) into nesquehonite ($MgCO_3 \cdot 3H_2O$). This indicated, though, that ammonium salts will probably be important for future research on CO_2 mineralization [16].

Later exergetic [17] and energy/environmental performance [18] assessments on this type of approach to CO_2 mineralization have shown that there is a need to avoid the energy penalty associated with CO_2 capture, should the process have a positive impact. This points to the need of optimizing the process for non-pure CO_2 as a reaction feedstock, e.g., by utilizing flue gases directly. It has also been identified as preferable if the process can produce waste heat, which could then be re-used in e.g. the extraction step [18]. This motivates the choice of a 15 vol% CO_2 gas used in this thesis, rather than a pure CO_2 gas.

2.4.2 Aqueous reaction

This is the type of carbonation process that is investigated in this thesis. Indirect aqueous carbonation involves extraction of Ca/Mg from a starting material, and a subsequent carbonation reaction done by exposing an aqueous slurry to gaseous CO_2. The overall reaction that occurs depends much on the starting material used, but can be generalized for Ca/Mg silicates as the following [19]:

$$(\mathrm{Mg,Ca})_x\mathrm{Si}_y\mathrm{O}_{x+2y+z}\mathrm{H}_{2z}(s) + x\mathrm{CO}_2(g) \longrightarrow x(\mathrm{Mg,Ca})\mathrm{CO}_3(s) + y\mathrm{SiO}_2(s) + z\mathrm{H}_2\mathrm{O}(l) \tag{2.2}$$

Since serpentine is a common mineral to make up mine tailings, and given that there is no available mineral analysis for the tailings used in this thesis, this overall reaction is assumed to describe the process in this project. There is, however, elemental analysis of the materials used in this project, indicating a Ca/Mg silicate material in the tailings.

Teir et al. [20] did experiments with a similar setup to this thesis, while using serpetinite mine tailings. Here, the sand was dissolved in acid at elevated temeperature (70 °C), followed by solvent evaporation, mixing with water, pH adjustment and an subsequent bubbling of CO_2 gas through the liquid matrix. HCl showed to be a feasible solvent for the tailings. Also, byproducts, such as amorphous silica and iron oxide, could be recovered during the process, pointing at possible byproduct recovery as an area of interest in the field [20]. If valuable products can be recovered during the mineralization process, perhaps those could later be purified and sold, lowering the overall cost of the process. Most importantly though, pH 9 (and 10) were identified as the most preferable for the highest precipitation of hydromagnesite ($Mg_5(CO_3)_4(OH)_2 \cdot 4H_2O$), stemming from the fact that there is a distribution of different carbonate species dissolved in an aqueous solution, depending on pH, which influences the interaction with the reactive components [20]. Later, Ebrahimi et al. carbonated acidic mine tailings treates with steel slag or coal fly ash under similar conditions, finding pH 9 to be the best for precipitation of hydromagnesite [21]. These results motivate the choice of pH 9 and 10 as the starting alkalinities in this thesis. Teir et al. controlled the alkalinity to keep it constant during the carbonation step. This thesis is, however, more oriented towards an industrial application of the

process and aims at mimicking a "real-life" industrial process, which would likely consider it easier to control reaction time rather than solution pH at every given time. Also, keeping the pH constant would increase the demand for base, thus increasing the overall cost of the process. Therefore, pH is not held constant here, only adjusted to a certain starting level, then let to decrease to a stop level.

Other research has been done on this topic. A continuous reactor process has been built for steel converter slag to be used as feedstock for carbonation into calcium carbonate ("slag2PCC"; PCC = Precipitated Calcium Carbonate). Particle size, as well as type and amount of ammonium salt during the extraction have been identified as important parameters in extraction of Ca from the slag [22]. Dahmani et al. used Ca-sepiolite material for the carbonation instead, finding an open reactor system under conditions pH 8.5-9, 80 °C and 1 bar to be optimal for total carbonate precipitation after 45 min [23]. Molahid et al. demonstrated the feasibility of using Fe-rich mine tailings for mineral carbonation, where small particle sizes (30 µm), alkaline pH and slightly elevated reaction temperature (80 °C) were shown to favor the carbonation [24].

Most research trialled the carbonation reaction with pure CO_2 gas. In an industrial application, however, it is of interest to be able to utilize exhaust gases directly for the carbonation in order to avoid expensive and energy-intensive separation of the CO_2. This is why in this thesis, 15 vol% CO_2, 85 vol% N_2 is used. In a recent paper, Wang et al. produced pure (>98 %) and fine (2 µm) PCC from wollastonite (Ca-silicate mineral) using CO_2 from an industrial exhaust in a looping process which enables reuse of a base medium (ammonium chloride), thus demonstrating the feasibility to utilize non-purified CO_2 [25]. This has also been demonstrated at Åbo Akademi University in Finland, as a partner institute in the research project, where a carbonation process called "the ÅA route" was developed, as described above [14]. An alternative ÅA route was developed, where flue gas CO_2 can be utilized [26]. Later lifecycle analysis (LCA) showed that this route may be preferable over the original ÅA route depending on the CO_2 source, waste heat availability and the targeted carbonate product [27].

2.4.3 Extraction of Ca and Mg from starting material

The extraction of the reactive components (Ca^{2+} and Mg^{2+}) from a starting material is such a major step in the indirect carbonation route, that there are research papers solely focused on this step of the process. Teir et al. did extraction experiments on natural serpentinite with several solutions of acids, finding that H_2SO_4, HCl and HNO_3 extracted all Mg, and a large part of iron, from the mineral at 70 °C after 1-2 h [28]. Since H_2SO_4 has the highest boiling point (338 °C), and therefore may deem an industrial process more energy-intensive, even if waste heat is utilized [20], and since HNO_3 is much more expensive than HCl [20], HCl seems to be the most feasible solvent from the three [20, 28].

Wang et al. did similar experiments, but with ammonium salts instead, finding that ammonium bisulfate (NH_4HSO_4) was the most efficient, being able to extract all Mg from serpentine at 100 °C after 3 h [29]. These results motivate the choice of solvents/leaching agents for this thesis.

Erlund et al. did similar experiments, comparing different mineral materials in their reactivity with ammonium bisulfate, ammonium sulfate ($(NH_4)_2SO_4$) and HCl, pointing out ammonium bisulfate as attractive for the extraction step from serpentine due to its high extraction yields. However, the reactivities with two other Mg-rich minerals, diopside and Mg-Horn, were found to be insufficient, extracting only modest amounts of Mg [30].

3 Methodology and laboratory work

Starting materials for the entire experimental section of this thesis are mine tailings in the form of wet sand from three mines. Pajala, located in the northernmost region of Norrbotten in Sweden, operated by Kaunis Iron. Garpenberg, located in the Dalarna region in Sweden, operated by Boliden AB. Lastly, Kevitsa, located in the Lappland region in Finland, operated by Boliden AB. The sand was stored in buckets sent directly from the respective mines. Below follows a detailed description of the different laborative procedures in their respective order.

3.1 Material composition

Total elemental analyses with X-Ray Fluorescense (XRF) conducted at RISE (Borås, Sweden) were used as guidance for the analyses of the leaching samples, as well as for calculations on the amount of leached-out elements. Table 3.1 presents amounts of the most abundant elements found in the three tailings samples. The complete list of measured element concentrations is available in Appendix A.

Table 3.1: Amounts of the most abundant of the detected elements in the three mine tailings in [wt%].

	Ca	**Mg**	**Fe**	**Si**
Pajala	9.4	14	4.6	16
Garpenberg	6.53	4.97	3.56	24.1
Kevitsa	9.19	13.5	8.48	22.4

3.2 Sample preparation

The first step in the preparation was to dry the sand, this was done in an oven at 70-80 °C for 1-2 days, with the objective to obtain constant weight. Although a limiting factor of drying the sand was the availability of the oven, and thus the available temperature, the samples were considered to be dry after 24 hours. Upon the drying step, a small piece of the sand was first weighed and then dried separately, then weighed again after drying, in order to obtain a measure of the amount of water that was evaporated from the sand.

After drying, the sand was sieved to obtain a suitable particle size. In this work, the particle size was not varied, instead, all samples were sieved to a particle size of ≤ 150 µm.

3.3 Leaching experiments

The prepared samples were first subjected to leaching experiments, in order to extract Mg and Ca from the sand and into a liquid solution. This was done by mixing 25 g of the sand with 250 ml of a leaching agent, this being either 1.5 M HCl or 1.5 M ammonium bisulfate (NH_4HSO_4), further referred to as ABS. For each combination of sand and leaching agent, the experiment was done at three different temperatures, namely room temperature (25 °C), 50 °C and 80 °C. All in all, this yields a matrix of 18 leaching experiments, presented in Table 3.2 below.

Table 3.2: Experiment matrix for the leaching experiments.

Run #	Mine location	Temperature [°C]	Leaching agent
1	Pajala (SE)	25	1.5 M HCl
2	Pajala (SE)	50	1.5 M HCl
3	Pajala (SE)	80	1.5 M HCl
4	Pajala (SE)	25	1.5 M NH_4HSO_4
5	Pajala (SE)	50	1.5 M NH_4HSO_4
6	Pajala (SE)	80	1.5 M NH_4HSO_4
7	Garpenberg (SE)	25	1.5 M HCl
8	Garpenberg (SE)	50	1.5 M HCl
9	Garpenberg (SE)	80	1.5 M HCl
10	Garpenberg (SE)	25	1.5 M NH_4HSO_4
11	Garpenberg (SE)	50	1.5 M NH_4HSO_4
12	Garpenberg (SE)	80	1.5 M NH_4HSO_4
13	Kevitsa (FI)	25	1.5 M HCl
14	Kevitsa (FI)	50	1.5 M HCl
15	Kevitsa (FI)	80	1.5 M HCl
16	Kevitsa (FI)	25	1.5 M NH_4HSO_4
17	Kevitsa (FI)	50	1.5 M NH_4HSO_4
18	Kevitsa (FI)	80	1.5 M NH_4HSO_4

The leaching itself was conducted in a 1 l three-necked round-bottom flask, partially submerged into a silicon oil bath in order to ease heating of the solution, which was placed on a magnetic stirrer/heater. A Dimroth condenser was connected to the middle neck, inhibiting evaporation of the solution. The rightmost neck was used for pH measurements, while the leftmost one was used for temperature measurements. When not in use, these were closed off to prevent loss of the solution.

When working at elevated temperatures, the silicon bath, and the leaching agent, were heated before the addition of the sand. When at the correct temperature, the sand was added to the round-bottom flask, then the mixture was left for 60 minutes while being continuously stirred at approximately 300 rpm. pH was measured at the beginning and the end of each experiment with Mettler-Toledo SevenCompact. The instrument was calibrated before each experiment to minimize measurement errors.

After the leaching experiments, the solutions were filtered using a traditional Büchner funnel. Approximately 30 ml of the solutions, however, were filtered through a PES hydrophilic membrane filter with a pore size of 0.22 µm using a Leybold-Heraeus Minni A vacuum pump. This was done for enhanced purity/decreased uncertainty of the filtrates for the subsequent ICP-OES analysis. The filtrates were then used in further experiments, while the filter cakes were dried in an oven at 70-80 °C for approximately 24 hours, then analyzed with PXRD. See section 3.6 for details on the analysis methods.

3.4 pH adjustment

Given the results of the leaching experiments, the Kevitsa sand was eliminated from all subsequent experiments, as the results were least satisfactory for this mine (see section 4.1.1). Furthermore, as the leaching results showed a positive trend in terms of increasing temperature, only filtrates from leaching experiments conducted at 80 °C were considered for the pH lift and subsequent carbonation. Along with moving forward with both leaching agents, this yields the experiment matrix shown in Table 3.3 below.

Table 3.3: Experiment matrix for pH lifts.

Run #	Mine location	Temperature [°C]	Leaching agent	pH levels
1	Pajala	80	1.5 M HCl	5, 7, 9, 10
2	Pajala	80	1.5 M NH_4HSO_4	5, 7, 9, 10
3	Garpenberg	80	1.5 M HCl	5, 7, 9, 10
4	Garpenberg	80	1.5 M NH_4HSO_4	5, 7, 9, 10

As CO_2 is known to behave acidically in an aqeous solution, and given results from previous research (see section 2.4.2), the filtrates from the leaching experiments were pH-adjusted to alkaline. Given the strongly acidic nature of the leaching agents, 5 M ammonium hydroxide (NH_4OH) was used for the pH lift under continuous pH measurement and stirring at about 200 rpm.

For later analysis, the solutions were filtered at pH 5, 7, 9 and 10, while putting aside approximately 5 ml at each pH step, and drying and saving the filter cakes. This was done to obtain information about what is being precipitated at the different pH levels, ultimately aiming for byproduct recovery. At pH 9, approximately 90-100 ml of the filtrates were put aside for later carbonation, then the pH lift was continued up to pH 10. The solutions with pH 9 and 10 were later used in the carbonation experiments. The filtration was done through disposable, single-use PES membrane filters with a pore size of 0.2 µm from Fisherbrand, using the Leybold-Heraeus Minni A pump from the leaching step.

3.5 Carbonation experiments

All the samples from the pH adjustment experiments were used for the final carbonation step, although only the filtrates from pH 9 and 10. This yields the experiment matrix shown in Table 3.4 below.

Table 3.4: Experiment matrix for carbonation.

Run #	Mine location	Temperature [°C]	Leaching agent	pH
1	Pajala	80	1.5 M HCl	9
2	Pajala	80	1.5 M HCl	10
3	Pajala	80	1.5 M NH_4HSO_4	9
4	Pajala	80	1.5 M NH_4HSO_4	10
5	Garpenberg	80	1.5 M HCl	9
6	Garpenberg	80	1.5 M HCl	10
7	Garpenberg	80	1.5 M NH_4HSO_4	9
8	Garpenberg	80	1.5 M NH_4HSO_4	10

The samples were first heated to 35 °C along with the silicon oil bath from the leaching step. As pH decreases with increased temperature, the pH of the solutions was re-adjusted to 9 or 10 using the same base as during the pH adjustment, i.e., 5 M NH_4OH. When at the correct temperature and pH, 80 ml of the solutions were transferred into the carbonation setup, the rest was saved for later analysis. Note that in most cases, there was visible precipitated matter present in the samples after refrigeration for a few days. Therefore, the heating and re-adjustment of pH were preceded by filtration using disposable, single-use PES membrane filters with a pore size of 0.45 µm from Fisherbrand, with the vacuum pump from the leaching step.

The carbonation setup, much like in the leaching step, consisted of a smaller, 100 ml three-necked round-bottom flask, partially submerged into a silicon oil bath, and connected to a Dimroth condenser. The rightmost neck was used for continuous pH measurements, which were logged and saved in 60 second intervals.

The leftmost neck was used for the introduction of the CO_2 gas. The CO_2 at a concentration of 15 vol%, mixed with N_2 from Air Liquide Gas AB, i.e., mimicking conventional flue gases, was introduced at a rate of 500 ml/min directly into the solution.

The carbonation was carried out until the pH reached 8, or during a maximum of four hours, while maintaining 35 °C. The product was filtered using the disposable filters mentioned above.

The experimental setups for both the leaching and the carbonation steps are shown in Figure 3.1 below. The figures were made in ChemDraw.

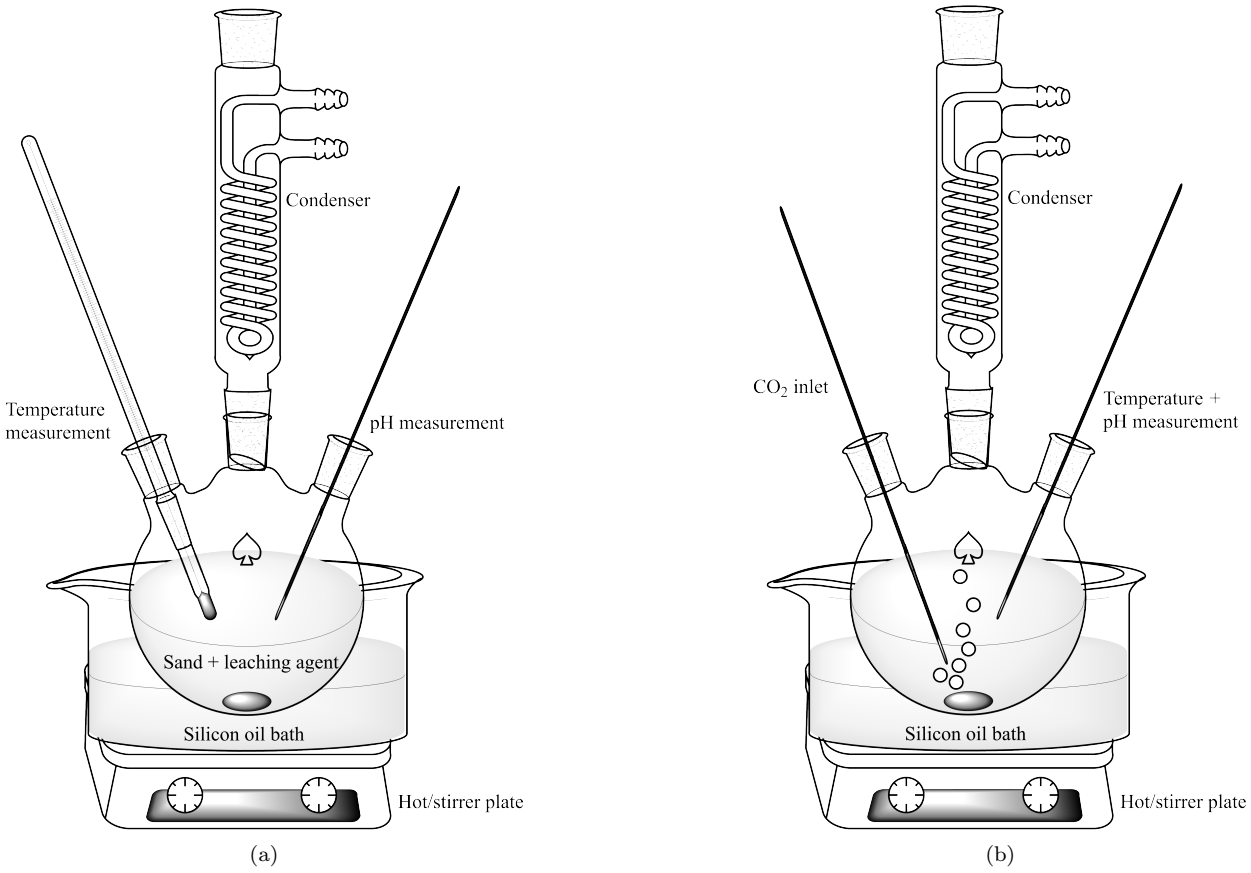

Figure 3.1: Experimental setup for (a) leaching, (b) carbonation.

After the carbonation experiments, the solid products were dried and weighed before being analyzed with PXRD, while filtrates were analyzed with ICP-OES.

3.6 Sample and data analysis

Liquid samples from the laboratory experiments, i.e., filtrates from the leachings, pH lifts and carbonations, were analyzed by Inductively Coupled Plasma Optical Emission Spectroscopy (ICP-OES). Solid samples, i.e., filter cakes from the leachings, pH lifts and carbonations, were analyzed using Powder X-Ray Diffraction (PXRD). In the following subsections, the procedures of these analysis methods are described.

3.6.1 ICP-OES

The ICP-OES analyses were done using the Thermo Scientific iCAP PRO ICP-OES. In total 17 elements were searched for and measured in terms of concentration. The main elements of interest were Al, Ca, Fe, K, Mg, Na and Si. Also trace elements were measured, i.e., As, Cd, Co, Cr, Cu, Mo, Ni, Pb, V and Zn. Internal standard solutions were made for each element in dilution series at concentrations of 0.1, 0.5, 1, 5, 10 and 20 ppm (also 40 ppm for the trace elements), made from 1000 ppm standards. The solutions were prepared with 50 vol% 0.3 M HNO_3 with 2 ppm Y, and filled up with 0.3 M HNO_3 as volume compensation. A reference solution (blank) was prepared as 50 vol% 0.3 M HNO_3 with 2 ppm Y and 50 vol% 0.3 M HNO_3.

All leaching samples were diluted with factors 1000, 100 and 10 with respect to volume and prepared into 10 ml vials with 50 vol % HNO_3 with 2 ppm Y and filled up with HNO_3. The factor 1000 and 100 vials were used for measurements of the main elements, whereas the x10 diluted samples were used for measurements of the trace elements. The measurements were conducted in ascending concentration orders for all samples. Washing steps with 0.3 M HNO_3 were included in the beginning and the end of the measurements, as well as after every 2-3 samples. Samples from the pH lift experiments and the carbonation experiments were only diluted with factors 100 and 10, as the x100 diluted samples from the leaching experiments proved to be sufficient in the data analysis.

The measurements yielded a number of counts for each elements with respect to two frequencies. Linear functions were fitted to the series of measurement points from the standard solutions, where the frequency with the best fit, i.e., R^2-value closer to unity, was chosen for further calculations. The linear functions were then extrapolated to the measured counts for each element, from which the concentrations of the elements in the samples in terms of weight-ppm were obtained. Generally, the calculated concentrations from the x1000 diluted samples are presented as results, although for some samples the measured concentrations were too low (below 0.1 ppm), therefore the x100 samples were used instead. For samples from the pH lift and carbonation steps, only dilution factors x100 and x10 were used.

The measured concentrations in weight-ppm were calculated into [g/l leaching agent] in order to be presented in a more industrially feasible unit. The calculation was done according to equation (3.1):

$$C_x = \frac{C_{ppm} \cdot V_v \cdot f_V}{V_s \cdot f_m} \text{ [g/l]} \tag{3.1}$$

where C_{ppm} is the measured concentration in [ppm], $V_v = 10$ ml is the total volume of the sample vial, $f_V = 10^3$ is a volume correction factor to transition to [l], V_s is the volume of sample into the vial, depending on the dilution factor, i.e., $f = x1000 \Rightarrow V_s = 0.01$ ml, $f = x100 \Rightarrow V_s = 0.1$ ml and $f = x10 \Rightarrow V_s = 1$ ml. Finally, $f_m = 10^6$ is a mass correction factor to transition into [g].

In the case of the pH adjustment step, the samples were diluted between each filtration by addition of base. Therefore, the calculations were tweaked to take the volume changes into account. Here, the calculation for each pH-level was done according to equation (3.2):

$$C_x = \frac{C_{ppm} \cdot V_v \cdot f_V}{V_s \cdot f_m} \cdot \frac{V_i + V_b}{V_i} \text{ [g/l]} \tag{3.2}$$

where V_i is the initial volume of the sample before addition of base and V_b is the volume of added base.

3.6.2 PXRD

The PXRD analyses were done using the Bruker D8 Discover PXRD. The samples with sufficient quantities ($>\sim$ 0.5 g) were hand-ground into fine powders, then placed in plastic sample holders in the machine's automated sample dispenser. Three samples with lower quantities but high importance were instead placed in zero-background Si-holders. These were the following: carbonation product for Garpenberg, ABS at pH 9 and Garpenberg, ABS at pH 10, as well as precipitate from Garpenberg, ABS at pH 5. Results were analyzed in Bruker DIFFRAC.EVA software with the built-in databases.

3.6.3 Calculations on captured CO_2

From the obtained ICP-OES data, calculations were done on various types of efficiencies that were obtained during the laboratory work. First, a carbonation efficiency (CE) was calculated to show how efficient the carbonation reaction was for each sample and element. This was done according to equation (3.3):

$$CE_x = \frac{C_{x,i} - C_{x,f}}{C_{x,i}} \times 100 \text{ [\%]} \tag{3.3}$$

where $C_{x,i}$ is the initial concentration of element $x = \{\text{Ca, Mg}\}$, i.e., measured prior to carbonation, and $C_{x,f}$ is the final concentration of element x, i.e., measured after carbonation (Table 4.7).

Next, the amount of CO_2 captured per tonne feedstock (sand) was calculated in two ways. Since there appeared to be losses of the reactive components during storage time in between the different experiments (see section 4.2.1), the amount of CO_2 captured was calculated both experimentally, i.e., taking the losses into account, and theoretically, i.e., ignoring the losses. This is of interest to know, since in an industrial application, the samples would most likely not be stored for several days to weeks in between the different stages of the process, and so the material losses would likely be prevented. The calculations were done under the assumption that the stoichiometric relations are preserved, i.e., 1 mol x $\leftrightarrow$ 1 mol xCO_3 $\leftrightarrow$ 1 mol CO_2 captured.

Material losses occurred during storage time between leaching and pH adjustment, as well as between pH adjustment and carbonation. Therefore, two loss factors (F_1 and F_2) were calculated. First, the amounts of Ca and Mg were calculated and extrapolated to the uniform volume of 250 ml according to equation (3.4):

$$m_{xj} = C_{xj} \cdot 0.250 \cdot 40000 \text{ [g/tonne sand]} \tag{3.4}$$

where j represents an index for the different stages, i.e., after leaching, prior to pH adjustment, post-pH adjustment and prior to carbonation. C_{xj} is thus the measured concentration of x at stage j (Tables 4.1, 4.4 and 4.7). Furthermore, 0.250 is the uniform volume of 250 ml and 40000 is a scaling factor to transition from amount of x per 25 g sand into amount of x per tonne sand.

Next, the two loss factors could be calculated according to equations (3.5) and (3.6):

$$F_{1x} = \frac{m_{x,\text{ post-leaching}} - m_{x,\text{ prior to pH-adjustment}}}{m_{x,\text{ post-leaching}}} \times 100 \text{ [\%]} \tag{3.5}$$

$$F_{2x} = \frac{m_{x,\text{ post-pH-adjustment}} - m_{x,\text{ prior to carbonation}}}{m_{x,\text{ post-pH-adjustment}}} \times 100\ [\%] \tag{3.6}$$

Finally, the amount of CO_2 captured per tonne dry sand experimentally ($m_{CO_2,e}$) was calculated according to equation (3.7):

$$m_{CO_2,e} = \sum_x \frac{m_{x,pl} \cdot (1 - F_{1,x}) \cdot (1 - F_{2,x}) \cdot CE_x \cdot M_{CO_2}}{M_x \cdot 1000}\ [\text{kg/ton dry sand}] \tag{3.7}$$

where pl = post-leaching, $M_{CO_2} = 44.009$ g/mol, $M_{Ca} = 40.078$ g/mol and $M_{Mg} = 24.305$ g/mol are the corresponding molar masses, and 1000 is a scaling factor to transition from mass CO_2 in [g] to [kg].

Next, the corresponding amount of CO_2 that would be captured if no material losses occurred in the process, i.e., $m_{CO_2,t}$ where t = theoretical, was calculated according to equation (3.8):

$$m_{CO_2,t} = \sum_x \frac{m_{x,pl} \cdot CE_x \cdot M_{CO_2}}{M_x \cdot 1000}\ [\text{kg/ton dry sand}] \tag{3.8}$$

where the indices and scaling factors are identical to the previous equations ((3.3) to (3.7)).

Also the theoretical maximum of the amount CO_2 captured per tonne dry sand was calculated given the amounts of Ca and Mg measured in the dry sand, as provided in Table 3.1. Assuming leaching efficiency of 100 %, stoichiometric conversion, no material losses in the process, and carbonation efficiency of 100 %, the theoretical max of CO_2 captured ($m_{CO_2,tm}$) was calculated according to equation (3.9):

$$m_{CO_2,tm} = \sum_x \frac{m_x}{M_x} \cdot M_{CO_2} \times \frac{10^4}{10^3}\ [\text{kg/ton dry sand}] \tag{3.9}$$

where the scaling factor of 10^3 is to transition from [g] to [kg] and the factor 10^4 is to transition from [(100 g sand)$^{-1}$] to [(1 ton sand)$^{-1}$], both stemming from the measured amounts of Ca and Mg (m_x) being given in [wt%] $\Leftrightarrow$ [g/100 g sand].

Note that all of the above calculations were done per unit weight dry sand. If the corresponding information per unit weight wet sand is desired instead, the amounts can be weighed with the amount of water in the sand, obtained by weighing the sand before and after drying. This calculation follows equation (3.10):

$$m_{CO_2}\ [\text{kg/ton wet sand}] = m_{CO_2}\ [\text{kg/ton dry sand}] \cdot (1 - m_{H_2O,i}) \tag{3.10}$$

where $m_{H_2O,i}$ is the weight fraction of water in the sand.

From the theoretical max and the experimentally captured CO_2 (equation (3.7)), the CO_2 capture efficiency (CCE) was calculated according to equation (3.11):

$$CCE = \frac{m_{CO_2,e}}{m_{CO_2,tm}} \times 100\ [\%]. \tag{3.11}$$

3.7 Technoeconomic assessment

This thesis had the objective to study and estimate a primary operational expenditure (OpEx) for an upscaled version of the experimental procedure described above.

Figure 3.2 below is an illustration of the process with material and energy flows.

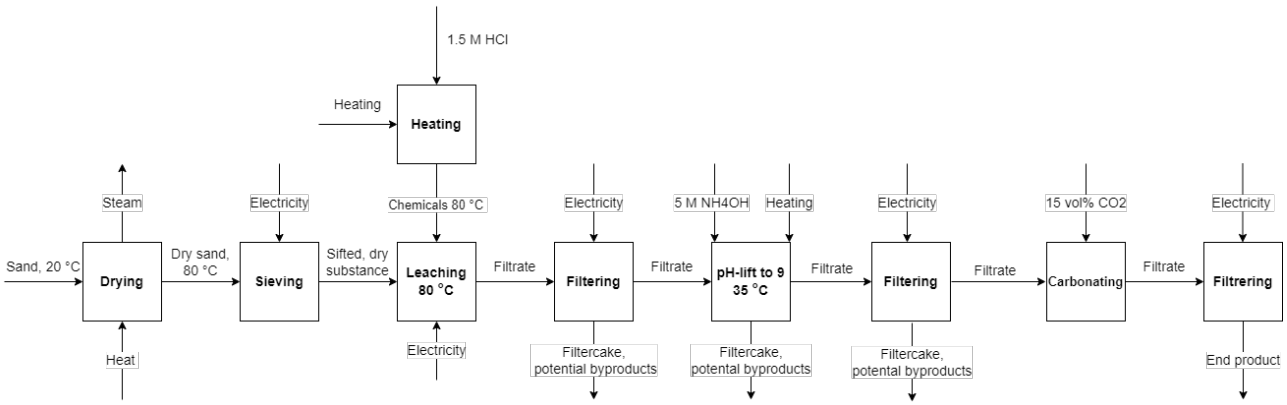

Figure 3.2: Material and energy flows of the process

An energy balance was made for each of the boxes presented in figure 3.2.

The calculations were done for 1 ton wet and dry sand for the Garpenberg and Pajala samples at 80 °C for the leaching step using HCl and with carbonation at pH 9 at 35 °C. The energy price for district heating (further DH) was assumed to be 20 €/MWh and the electricity price 30 €/MWh. The reason for making the two cases, i.e, wet and dry sand, is to obtain information about how parameters such as weather condition at sample collection could effect the cost and energy consumption of the process. The following calculations were done for 1 ton wet sand, the calculations for dry sand were done in the same manner but without any water content at start. Furthermore, no Ca or Mg is assumed to dissipate in between the leaching and carbonation steps. The OpEx cost is presented in € per kg sequestrated CO_2.

Table 3.5 below lists assumed constants and prices for the calculations.

Table 3.5: Overview of constants and prices for calculations.

C_{p,H_2O}	4.18 kJ/kgK [31]
$\Delta H_{vap,H_2O}$	2258 kJ/kg [31]
Deionized water, price	0.33 €/ton [32]
Concentrated HCl, price	25 €/ton [33]
Concentrated NH_4OH, price	130.2 €/ton [34]
District heating, price	20 €/MWh
Electricity, price	30 €/MWh [35]
EU CO_2 credit market, price	0.09 €/ton [36]

In the first drying step, it was assumed that the sand was dried at 100 °C, where the inlet ambient temperature was estimated to be 20 °C. The energy consumed for the heating steps was assumed to be supplied by DH. The first energy balance was calculated according to equation (3.12):

$$\dot{Q}_{drying} = m_w C_{p_w}(T_{out} - T_{amb}) + m_w h_{vap} \text{ [kJ/kg]} \tag{3.12}$$

where m_w was obtained by weighing a sample of the enriched sand before and after the drying step. The heat capacity C_{p_w} was used for water at 20 °C. The evaporation enthalpy h_{vap} was taken at 100 °C.

The next step, i.e., sieving the sand, was assumed to have rather low energy consumption and was therefore neglected in terms of energy. It is also assumed that no mass is lost since no large particles were found when executing this step in the laboratory. After sieving the sand, the chemicals needed for the leaching, i.e., HCl, were expected to be heated to 80 °C according to equation (3.13):

$$\dot{Q}_{HCl} = m_{HCl} C_{p,HCl}(T_{out} - T_{amb}) \text{ [MJ/kg]} \tag{3.13}$$

where m_{HCl} was 10 times the weight of the dried sand, i.e., 10 ton in this case, and the C_p value for 1.5 M HCl was estimated to be the same as for water at 20 °C since the solution is diluted in distilled water. T_{out} was set to 80 °C. To execute the leaching process, the solution was stirred for an hour at a constant temperature. While the energy consumption during this step was not explicitly measured, the assumption was made that it corresponds to $\sim$ 10 % of the previous heating step. This is because the solution's high heat capacity, combined with the system's good isolation, meant that the temperature change during stirring would be minimal.

For the filtering step, a filter press was thought to be an appropriate mechanism due to the ratio of the solvent and the enriched sand. In order to estimate energy consumption for an industrial process the filter press Q345B from Jingjin was used as a reference [37]. Based on the product details, the energy consumption for the step was calculated as:

$$E_{batch} = P \cdot 60 \cdot t \text{ [kJ]} \tag{3.14}$$

where P is the power of the machine and t is the time that it takes for filtering a batch. The time for this step was set to 30 min based on the mean filtration time that was required in the laboratory experiments. With a total volume capacity of 10.404 m^3 the energy per kg was calculated according to equation (3.15) by assuming that the density of the leachate is the same as for water, i.e., 1000 kg/m^3 which gives a mass capacity m_{cap} of 10 404 kg/batch.

$$\dot{E} = \frac{E}{m_{cap}} \text{ [kJ/kg]} \tag{3.15}$$

The pH lift was performed in several stages, each with multiple objectives. Initially, the pH was raised from the previous filtering to pH 5 by adding 5 M NH_4OH, after which the solution was filtered to check for the presence of any valuable precipitate. This process was repeated for pH values of 7, 9 and 10. Although the rest-products were not assumed to contribute to a reduction in OpEx for this report, it is possible that they could do so in the future, but due to uncertainties presented in the results, they are excluded. Therefore the only filtration that was taken into consideration for this step was the filtration that took place when the solution reached pH 9, with the purpose of removing the precipitate that came with the pH lift. The energy

for this step was calculated with the equations (3.14) and (3.15) but the time was reduced to 15 min since this filtration generally went faster during the laboratory work for this step.

In the second stage, the solution with pH of 9 was heated to 35 °C where the energy was obtained based on equation (3.16), and the pH was adjusted by adding more NH_4OH because the increase in temperature caused a slight decrease in pH:

$$Q = m_9 C_p (T_{out} - T_{amb}) \text{ [kJ/kg]} \tag{3.16}$$

where m_9 is the total mass of the solution at pH 9.

The carbonation was, as explained above, done by adding 15 vol% CO_2 mixed with N_2 until the solution reached pH 8. The time for this was 60 min for the Garpenberg sample and 35 for Pajala. With a gas flow of 500 ml/min, which is equivalent to a mass flow $\dot{g} = 77.92$ kg/min for 1 ton dry sand, assuming the density of CO_2 to be 1.87 [kg/m^3], the mass of CO_2 inserted in the system was then obtained according to equation (3.17)

$$m_{CO_2} = \dot{g} \cdot t \cdot \frac{f_{CO_2}}{1 - f_{H_2O}} \text{ [kg]} \tag{3.17}$$

where f_{CO_2} is the CO_2 fraction and f_{H_2O} is the fraction of water in the respective samples. After the carbonation, another filtration was done in order to separate the carbonates from the solution. The estimated time for this on an industrial scale was set to 15 min. The energy consumption was for this step therefore the same as for the filtration done at pH 9. Lastly, the carbonates were dried, but since the solvent content was quite low after the filtration and no data of evaporated weight were collected, the energy for this step was not included in the calculations. In order to obtain the mass sequestrated CO_2 per ton wet enriched sand the equation (3.8) was used.

4 Experimental results

In the following sections, results from the laboratory part of the work are presented in chronological order. Results of the technoeconomic assessment are presented in a separate chapter.

4.1 Leaching experiments

4.1.1 ICP-OES data

Below are the results from the ICP-OES analysis on filtrates from the leaching experiments presented. The primary results, obtained in weight-ppm, were translated into g/l leaching agent for the main elements, and into mg/l leaching agent for the trace elements. Table 4.1 shows the results for the main elements.

Table 4.1: Amounts of leached-out elements in g/l leaching agent.

Sample	**Al**	**Ca**	**Fe**	**K**	**Mg**	**Na**	**Si**
Pajala, 1.5 M HCl @ 25 °C	0.39	4.00	0.57	0.65	2.47	0.25	0.24
Pajala, 1.5 M HCl @ 50 °C	0.49	5.08	1.39	0.75	6.01	0.15	0.64
Pajala, 1.5 M HCl @ 80 °C	1.02	5.41	2.06	0.96	9.15	0.28	0.71
Pajala, 1.5 M NH_4HSO_4 @ 25 °C	0.06	0.62	0.29	0.43	1.42	0.04	0.24
Pajala, 1.5 M NH_4HSO_4 @ 50 °C	0.06	0.59	0.80	0.27	4.43	0.03	0.43
Pajala, 1.5 M NH_4HSO_4 @ 80 °C	0.08	0.60	0.98	0.28	6.11	0.03	0.48
Garpenberg, 1.5 M HCl @ 25 °C	0.10	2.66	0.21	0.46	1.05	0.24	0.24
Garpenberg, 1.5 M HCl @ 50 °C	0.21	4.85	0.28	0.33	1.70	0.35	0.49
Garpenberg, 1.5 M HCl @ 80 °C	0.38	4.35	0.50	0.50	1.90	0.24	0.60
Garpenberg, 1.5 M NH_4HSO_4 @ 25 °C	0.07	0.83	0.14	0.43	0.88	0.24	0.20
Garpenberg, 1.5 M NH_4HSO_4 @ 50 °C	0.08	0.59	0.20	0.26	1.60	0.15	0.42
Garpenberg, 1.5 M NH_4HSO_4 @ 80 °C	0.13	1.81	0.23	0.29	5.46	0.05	0.99
Kevitsa, 1.5 M HCl @ 25 °C	0.09	0.39	0.32	0.45	0.52	0.03	0.34
Kevitsa, 1.5 M HCl @ 50 °C	0.13	0.46	1.25	0.29	2.06	0.03	1.10
Kevitsa, 1.5 M HCl @ 80 °C	0.25	0.56	3.90	0.30	4.71	0.02	3.05
Kevitsa, 1.5 M NH_4HSO_4 @ 25 °C	0.03	0.38	0.39	0.29	0.59	0.02	0.42
Kevitsa, 1.5 M NH_4HSO_4 @ 50 °C	0.06	0.44	1.19	0.26	1.96	0	1.93
Kevitsa, 1.5 M NH_4HSO_4 @ 80 °C	0.10	0.48	2.13	0.25	3.41	0.02	2.94

The most important observation in terms of an eventual industrial application that can be made from the table, is that the amount of leached-out element generally increases with increased leaching temperature. Especially, this trend is clearly seen for Mg, but also for Al, Fe and Si. For Ca, the trend is a bit less clear. For instance, in the case of Pajala being leached with ABS, it appears as if the temperature essentially does not influence the amount of Ca obtained. In other cases, e.g., Garpenberg with ABS and Kevitsa with ABS, the trend seems to be weak. More specifically, the amount of Ca in these cases seems to increase with temperature increase from 25 °C to 50 °C, but not upon the increase from 50 °C to 80 °C.

Since the leaching of Ca and Mg is the main focus of the leaching experiments, the measured concentrations of these elements were calculated into [%] leached out element, given the amount of the element present in the sand, as given by the elemental analysis from Table 3.1. The result is shown in Figure 4.1 below.

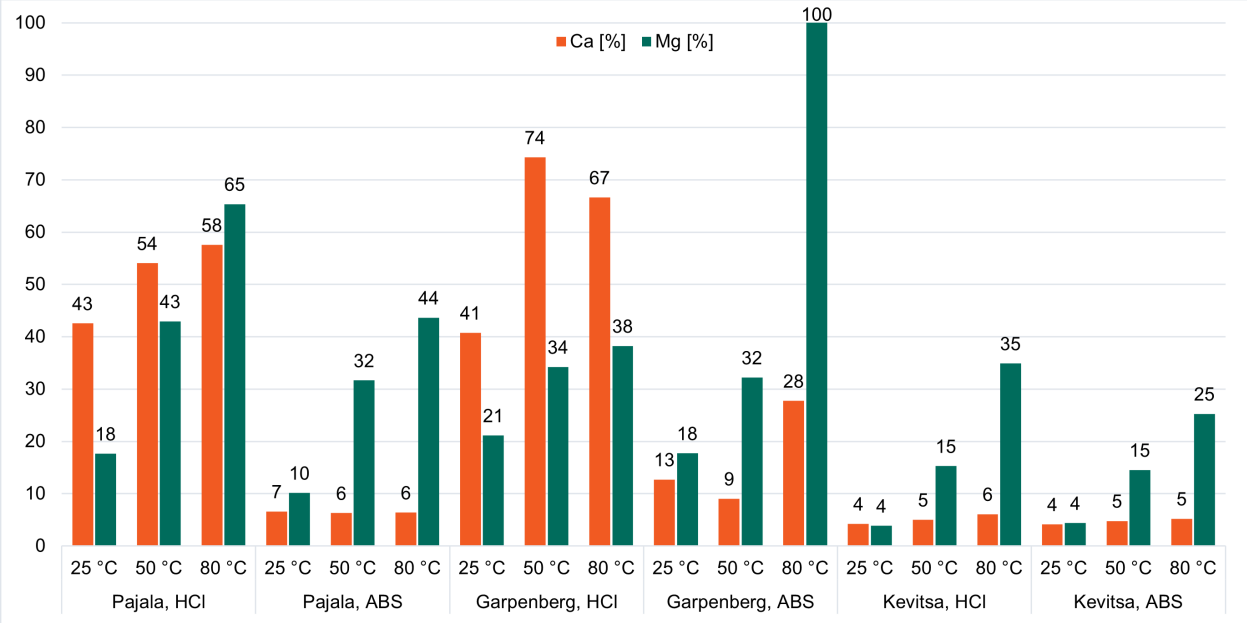

Figure 4.1: Amounts of leached out Ca and Mg as wt% of the amounts in the starting material. Rounded-off calculated percentages are shown above the bars.

The figure illustrates what can be seen from Table 4.1, i.e., sand from the Pajala mine leached with HCl gives generally the highest extraction yields of Ca and Mg, followed by Garpenberg with the same leaching agent. The effect of higher temperature can also be seen for Mg, where 50 °C and 80 °C generally give notably higher amounts of the element than room temperature. For the extraction of Ca, the temperature effect is less apparent, except for one sample (Pajala, HCl). ABS shows to be less efficient as a leaching agent than HCl, except for sand from the Kevitsa mine, where neither of the two gave substantial amounts of Ca and Mg. There is also a special case, where the amount of Mg obtained was calculated to almost 110 %, i.e., Garpenberg with ABS as the leaching agent at 80 °C. There is obviously en error, either in the measurements or in the calculations in this case. It is also possible that the sample used for leaching contained more Mg than the sample used in the elemental analysis. Therefore, the amount was rounded off to the highest possible amount, i.e., 100 %, still being probably wrong given the rest of the measurement series.

As for the alkali metals K and Na, it is difficult to find a certain trend. Generally speaking, the amounts of these elements found are low; in one case, Na was not detected at all. In some cases, the above mentioned trend is followed, whereas in others, it appears to be reversed, i.e., less leached-out element at higher temperatures. There are also cases, where no trend can be seen. Consequently, no clear trend can be observed for leaching of K and Na under the given circumstances.

There is another observable trend in the analysis of the ICP-OES results for the main elements, which may be of particular interest for a potential industrial application. When comparing the three mines, the general trend, especially regarding Ca and Mg, is that the highest amounts were leached out from the Pajala sample, followed by Garpenberg. The lowest amounts of Ca and Mg were obtained from the Kevitsa sample. Also, there is a notable difference between the two leaching agents. With some exceptions, HCl shows a general ability to extract higher amounts than ABS, especially regarding Ca in the Pajala and Garpenberg samples.

Table 4.2 shows corresponding results from ICP-OES calculations for the trace elements.

Table 4.2: Amounts of leached-out trace elements in mg/l leaching agent. n.d. = not detected.

Sample	**As**	**Cd**	**Co**	**Cr**	**Cu**	**Mo**	**Ni**	**Pb**	**V**	**Zn**
Pajala, HCl @ 25 °C	0	n.d.	n.d.	0.58	0.26	0.34	1.30	0.30	0.26	0.68
Pajala, HCl @ 50 °C	0	n.d.	n.d.	0.84	1.19	0.35	3.15	0.46	1.12	1.15
Pajala, HCl @ 80 °C	0	n.d.	n.d.	1.13	3.03	0.35	41.46	0.46	1.26	1.30
Pajala, NH_4HSO_4 @ 25 °C	0.08	n.d.	n.d.	0.70	0.12	0.36	1.47	0.17	0.13	0.85
Pajala, NH_4HSO_4 @ 50 °C	0.03	n.d.	n.d.	0.94	0.43	0.36	2.37	0.28	0.38	1.12
Pajala, NH_4HSO_4 @ 80 °C	0.10	n.d.	n.d.	1.00	1.34	0.44	20.05	0.33	0.54	1.20
Garpenberg, HCl @ 25 °C	0.68	n.d.	n.d.	4.62	0	0.34	0.19	94.98	0.16	42.44
Garpenberg, HCl @ 50 °C	0.92	n.d.	n.d.	5.01	0.05	0.34	0.48	105.35	0.30	50.72
Garpenberg, HCl @ 80 °C	0.17	n.d.	n.d.	0.58	1.59	0.32	24.92	101.18	0.39	43.05
Garpenberg, NH_4HSO_4 @ 25 °C	0.70	n.d.	n.d.	4.76	0	0.35	0.20	7.20	0.08	48.53
Garpenberg, NH_4HSO_4 @ 50 °C	0.89	n.d.	n.d.	5.23	0.04	0.34	0.31	8.05	0.20	52.40
Garpenberg, NH_4HSO_4 @ 80 °C	0.96	n.d.	n.d.	5.02	0.07	0.36	0.37	9.44	1.00	52.59
Kevitsa, HCl @ 25 °C	0	n.d.	n.d.	3.17	1.34	0.35	6.86	0.10	0.11	0.21
Kevitsa, HCl @ 50 °C	0	n.d.	n.d.	4.26	4.05	0.35	15.45	0.19	0.33	0.75
Kevitsa, HCl @ 80 °C	0	0.18	n.d.	2.05	15.44	0.70	56.26	0.52	1.58	1.69
Kevitsa, NH_4HSO_4 @ 25 °C	0.80	0.43	n.d.	3.46	1.55	1.16	8.14	0.58	0.60	0.74
Kevitsa, NH_4HSO_4 @ 50 °C	0	n.d.	n.d.	4.02	2.48	0.34	14.85	0.16	0.15	0.66
Kevitsa, NH_4HSO_4 @ 80 °C	0	n.d.	n.d.	5.37	4.54	0.39	21.10	0.17	0.43	1.04

As for the trace elements, there is an evident variety in the results. While Co was not detected in any of the 18 samples, and Cd was only above the detection limit in two of the Kevitsa samples, other elements were found in greater abundance. Notable examples of this are Pb and Zn in the Garpenberg samples. Cr, V, and especially Mo, showed relatively low diversity in terms of extracted amounts over the sample matrix, while As, Cu and Ni showed much larger variety. The trend observed in the analysis of the main elements, i.e., that higher leaching temperature generally permits larger quantities of extracted elements, persists in the case of trace elements. In most of the samples, no clear contrast between the two leaching agents can be observed. A remarkable exception to this is Pb in the Garpenberg samples, where HCl allowed for extraction of up to 13 times higher quantities of the element. It is worth mentioning that there seemed to be some measurement interference for the signals for Co, meaning that the element not being detected may have been influenced by this.

A trend that could be of great importance for an industrial application arises when comparing the three mines. It stands clear that the Garpenberg sand yielded the highest amounts of trace elements out of the three, especially regarding Ni, Pb and Zn. Since in particular Ni and Zn have commercial value, it is of interest to investigate whether these elements could be feasibly separated from the material. A downside of this trend is the fact that also As is a trace element that is much more abundant in leachates from the Garpenberg sand. Since As is well known to be hazardous, toxic and carcinogenic [38], this may pose a hindrance for this type of commercialization of the Garpenberg sand.

4.1.2 PXRD analysis of the sand after leaching

Table 4.3 below presents all detected crystalline phases from the leaching experiments. All structures were matched against the DIFFRAC.EVA software's attached databases. In most cases, only database matches marked as high-quality measurements were used. Corresponding diffractograms, along with the detected

structures, are attached in Appendix B.

Table 4.3: XRD analysis of the sand after leaching.

Sample	**Identified structures**	**Chemical composition**
Pajala, HCl, 25°C	Edenite	$NaCa_2Mg_5AlSi_7O_{22}(OH)_2$
	Lizardite-1T	$Mg_3Si_2O_5(OH)_4$
	Dehydroxylated muscovite	$KAl_3Si_3O_{11}$
	Actinolite	$Ca_2(Mg,Fe^{2+})_5Si_8O_{22}(OH)_2$
	Lizardite-1T	$Mg_{2.7}Fe_{0.3}Si_2O_5(OH)_4$
Pajala, HCl, 50°C	Tremolite	$Ca_2Mg_5Si_8O_{22}(OH)_2$
	Antogorite	$Mg_3Si_2O_5(OH)_4$
	Nepouite	$(Ni_{0.92}Mg_{0.08})_3Si_2O_5(OH)_4$
	Riebeckite	$Na_2Fe^{2+}_{4.6}Fe^{3+}_2Mg_{0.4}Si_8O_{22}(OH)_2$
Pajala, HCl, 80°C	Tremolite	$Ca_2Mg_5Si_8O_{22}(OH)_2$
	Pargasite	$NaCa_2Mg_4Al_3Si_6O_{22}(OH)_2$
	Magneseio-homblende	$(Ca,Na)_{2.26}(Mg,Fe,Al)_{5.15}(Si,Al)_8O_{22}(OH)_2$
	Lizardite-1T	$Mg_{2.7}Fe_{0.3}Si_2O_5(OH)_4$
Pajala, ABS, 25°C	Potassium Aluminum Silicate	$KAlSiO_4$
	Edenite	$NaCa_2Mg_5AlSi_7O_{22}(OH)_2$
	Lizardite-1T	$Mg_3Si_2O_5(OH)_4$
	Tremolite	$Ca_2Mg_5Si_8O_{22}(OH)_2$
Pajala, ABS, 50°C	Tremolite	$Ca_2Mg_5Si_8O_{22}(OH)_2$
	Actinolite	$Ca_2(Mg,Fe^{2+})_5Si_8O_{22}(OH)_2$
	Nepouite	$(Ni_{0.92}Mg_{0.08})_3Si_2O_5(OH)_4$
Pajala, ABS, 80°C	Edenite	$NaCa_2Mg_5AlSi_7O_{22}(OH)_2$
	Tremolite	$Ca_2Mg_5Si_8O_{22}(OH)_2$
	Actinolite	$Ca_2(Mg,Fe^{2+})_5Si_8O_{22}(OH)_2$
	Pargasite	$NaCa_2Mg_4Al_3Si_6O_{22}(OH)_2$
	Lizardite-1T	$Mg_{2.7}Fe_{0.3}Si_2O_5(OH)_4$
Garpenberg, HCl, 25°C	Quartz	SiO_2
	Tremolite	$Ca_2Mg_5Si_8O_{22}(OH)_2$
	Magneseio-homblende	$(Ca,Na)_{2.26}(Mg,Fe,Al)_{5.15}(Si,Al)_8O_{22}(OH)_2$
Garpenberg, HCl, 50°C	Quartz	SiO_2
	Richterite	$Na_2(MgFeFe)_6Si_8O_{22}(OOH)_2$
	Sodium Cobolt Oxide Hydrate	$Na_{0.27}CoO_2{\cdot}2.6H_2O$
Garpenberg, HCl, 80°C	Quartz	SiO_2
	Magneseio-homblende	$(Ca,Na)_{2.26}(Mg,Fe,Al)_{5.15}(Si,Al)_8O_{22}(OH)_2$
Garpenberg, ABS, 25°C	Quartz	SiO_2
	unidentified peaks	n/a
Garpenberg, ABS, 50°C	Quartz	SiO_2
	Magneseio-homblende	$(Ca,Na)_{2.26}(Mg,Fe,Al)_{5.15}(Si,Al)_8O_{22}(OH)_2$
Garpenberg, ABS, 80°C	Quartz	SiO_2
	Magneseio-homblende	$(Ca,Na)_{2.26}(Mg,Fe,Al)_{5.15}(Si,Al)_8O_{22}(OH)_2$

Kevitsa, HCl, 25°C	Diopside	$CaMgSi_2O_6$
	Tremolite	$Ca_2Mg_5Si_8O_{22}(OH)_2$
Kevitsa, HCl, 50°C	Diopside	$CaMgSi_2O_6$
	Tremolite	$Ca_2Mg_5Si_8O_{22}(OH)_2$
Kevitsa, HCl, 80°C	Tremolite	$Ca_2Mg_5Si_8O_{22}(OH)_2$
	Diopside, Ni^{2+} bearing	$CaMg_{0.8}Ni_{0.2}Si_2O_6$
	Augite	$Ca_{0.90}Mg_{0.71}Fe_{0.25}Si_2O_6$
Kevitsa, ABS, 25°C	Diopside	$CaMgSi_2O_6$
	Tremolite	$Ca_2Mg_5Si_8O_{22}(OH)_2$
Kevitsa, ABS, 50°C	Diopside	$CaMgSi_2O_6$
	Tremolite	$Ca_2Mg_5Si_8O_{22}(OH)_2$
	Augite, Al^{3+} bearing	$Ca(Mg,Fe,Al)(Si,Al)_2O_6$
Kevitsa, ABS, 80°C	Diopside	$CaMgSi_2O_6$
	Tremolite	$Ca_2Mg_5Si_8O_{22}(OH)_2$
	Edenite	$NaCa_2Mg_5AlSi_7O_{22}(OH)_2$

There are some clear differences between the different materials tested. The samples stemming from the Pajala tailings are clearly the most complex ones, often consisting of 4-5 different structures, possibly even more, since the diffractograms were complex themselves. Generally, the Pajala samples consist of Ca/Mg silicates, such as tremolite, edenite, or lizardite-1T. The findings of tremolite in almost every Pajala sample, and actinolite in some, is especially interesting, as they are two of the six identified types of asbestos [39]. A recent internal asbestos evaluation done during the time of making this thesis by ALS Global on the three materials has in fact detected trace amounts of those minerals in one of two Pajala samples, as well as in a Kevitsa sample. Finding these in the PXRD measurements after the leaching experiments confirms this result and imply much more precaution and care than has been taken in any further handling of these tailings within the project.

As for the Garpenberg samples, these were much less complex and generally easier to identify. Simple quartz was found in each of the six samples, as well as magnesio-hornblende, which was found in most of them. One of the samples contained peaks that could not be matched against any structure in the database, and another contained structures not found in any other sample. This may be the result of a measurement error, or perhaps was the sample not loaded correctly into the machine. Nonetheless, one of the samples seemed to contain tremolite, which is unexpected given that the internal asbestos evaluation did not detect any type of asbestos in the Garpenberg sand. Again, this may be attributed to a measurement error or poor matching against the database, or perhaps was the mineral found in a non-fibrous form, but rather in a ”bulkier” crystalline form.

The internal asbestos evaluation did detect trace amounts of several asbestos types in the Kevitsa samples, rendering the findings of tremolite in each of the six samples expected. Again, this implies caution in any further handling of the material within the project. Aside from tremolite, also the Ca/Mg silicate diopside was detected in all of the Kevitsa samples, along with signs of augite and edenite in three of the samples.

4.2 pH adjustment

4.2.1 ICP-OES data

In the following section, the ICP-OES data from the pH lift step are presented. Table 4.4 shows the results for the main elements. The measured concentrations have been calculated into [g/l leaching agent], in the corresponding way as for those in section 4.1.1. Since the pH lift was done by addition of base, the concentrations were weighed with the volume change of the samples (see equation (3.2)). For the sample of Garpenberg leached in HCl, pH 5 is not present due to accidental overshooting of added base during the experiment.

Table 4.4: Amounts of elements in g/l leaching agent after each pH-lift stage.

Sample	**Al**	**Ca**	**Fe**	**K**	**Mg**	**Na**	**Si**
Garpenberg, HCl, pH native	0.23	3.20	0.34	0.11	1.36	0.01	0.40
Garpenberg, HCl, pH 7	0	3.58	0.13	0.12	1.44	0.02	0.09
Garpenberg, HCl, pH 9	0	2.88	0	0.10	1.17	0.01	0.07
Garpenberg, HCl, pH 10	0	2.94	0	0.09	0.83	0.02	0.09
Garpenberg, ABS, pH native	0.13	0.57	0.21	0.02	1.48	0.01	0.30
Garpenberg, ABS, pH 5	0.09	0.58	0.16	0.02	1.53	0.01	0.18
Garpenberg, ABS, pH 7	0	0.47	0.10	0.02	1.25	0.01	0.10
Garpenberg, ABS, pH 9	0	0.46	0	0.02	1.23	0.01	0.07
Garpenberg, ABS, pH 10	0	0.44	0	0.02	1.12	0.01	0.11
Pajala, ABS, pH native	0.07	0.55	0.80	0.03	4.57	0.02	0.36
Pajala, ABS, pH 5	0.04	0.57	0.28	0.03	4.72	0.02	0.25
Pajala, ABS, pH 7	0	0.52	0.21	0.03	4.32	0.02	0.16
Pajala, ABS, pH 9	0	0.51	0.12	0.03	4.32	0.02	0.11
Pajala, ABS, pH 10	0	0.49	0	0.03	4.12	0.02	0.10
Pajala, HCl, pH native	0.47	2.83	1.24	0.56	5.19	0.03	0.44
Pajala, HCl, pH 5	0.02	2.96	0.61	0.56	5.32	0.04	0.10
Pajala, HCl, pH 7	0	2.72	0.49	0.53	4.87	0.03	0.08
Pajala, HCl, pH 9	0	2.80	0.04	0.53	4.97	0.03	0.08
Pajala, HCl, pH 10	0	2.84	0	0.50	2.55	0.03	0.08

Several trends can be observed from the table. Most notably, the concentration of Al and Fe found in the solutions seem to be strongly influenced by the pH, as most of the elements seems to have precipitated away already at pH 5 or 7, and since no Al or Fe at all was detected at pH 10, and in most cases, already at pH 9. Judging only from the ICP-OES data, this may mean a possibility to recover Al- or Fe oxides, which would be added-value products, as intended. However, this could not be confirmed (see section 4.2.2 below). Also Si seems to be influenced by the same trend, although there is still some Si left even at pH 10. The alkali metals Na and K were not influenced by the change of pH, as their measured concentrations are more or less constant at all the pH levels. Only in two cases, where HCl was the leaching agent, did small amounts of K seem to precipitate.

As for the reactive alkaline earth metals Ca and Mg, these should not precipitate, as they are needed in the solution for the carbonation step. Judging from the ICP-OES data, they are indeed still in the solution after the pH lift. Only in two exceptional cases, where HCl was the leaching agent, did some Mg seem to precipitate at pH 10. In some cases, there seems to have been a slight increase in the measured concentration of the elements between two steps of the pH lift. This is obviously not possible, but is instead attributed to measurement errors, calculation uncertainties, or measurement interferences.

What is worth noticing is the fact that the measured concentrations of Ca and Mg seem to have decreased in some cases, as compared to the post-leaching measurements (see Table 4.1 and 4.7). Given that there often was a precipitate in many samples, both prior to the pH adjustment step, and prior to the carbonation step, this suggests that some of the Ca and Mg may have precipitated from the solution during storage time. Further, this indicates that the liquid solutions are unstable and have a limited shelf life, within which they should be handled further in order to prevent losses of the reactive components. In an industrial application, this should not be a problem, as the throughput of material through the process would probably be relatively high, it should nonetheless be noted. It may also have to do with measurement errors or different measurement dates.

Table 4.5 shows the corresponding results for the trace elements. Since Co was never detected in any of the post-leaching samples, it is not considered further and therefore not included in the table.

Table 4.5: Amounts of trace elements in mg/l leaching agent after each pH-lift stage.

Sample	**As**	**Cd**	**Cr**	**Cu**	**Mo**	**Ni**	**Pb**	**V**	**Zn**
Garpenberg, HCl, pH native	0.68	0.34	0.62	2.69	0.73	19.25	92.44	0.78	42.87
Garpenberg, HCl, pH 7	0.46	0.33	0.60	0.49	0.65	17.90	9.91	0.51	14.05
Garpenberg, HCl, pH 9	0.33	0.24	0.44	0.26	0.55	13.75	0.33	0.25	10.09
Garpenberg, HCl, pH 10	0.34	0.26	0.49	0.27	0.62	14.43	0.24	0.33	10.93
Garpenberg, ABS, pH native	1.16	0.22	3.64	0.51	0.37	0.44	4.49	0.49	53.36
Garpenberg, ABS, pH 5	0.43	0.23	3.69	0.37	0.41	0.41	3.86	0.55	54.92
Garpenberg, ABS, pH 7	0.31	0.19	3.03	0.23	0.34	0.33	0.35	0.34	40.55
Garpenberg, ABS, pH 9	0.20	0.19	3.19	0.15	0.41	0.32	0.14	0.18	40.57
Garpenberg, ABS, pH 10	0.32	0.23	3.08	0.22	0.57	0.43	0.20	0.24	39.56
Pajala, ABS, pH native	0.19	0.11	0.69	2.07	0.38	14.38	0.36	0.62	1.32
Pajala, ABS, pH 5	0.22	0.12	0.71	0.44	0.42	14.74	0.19	0.19	1.32
Pajala, ABS, pH 7	0.17	0.11	0.62	0.32	0.37	13.04	0.12	0.17	0.89
Pajala, ABS, pH 9	0.19	0.11	0.63	0.25	0.39	12.68	0.12	0.18	0.85
Pajala, ABS, pH 10	0.28	0.14	0.70	0.19	0.52	13.15	0.17	0.23	0.92
Pajala, HCl, pH native	0.13	0.11	0.69	4.17	0.36	27.39	0.43	1.27	1.36
Pajala, HCl, pH 5	0.19	0.11	0.71	0.67	0.40	27.52	0.20	0.19	1.29
Pajala, HCl, pH 7	0.15	0.11	0.66	0.58	0.37	25.36	0.13	0.17	0.60
Pajala, HCl, pH 9	0.18	0.10	0.10	0.23	0.38	22.86	0.14	0.17	0.46
Pajala, HCl, pH 10	0.24	0.13	0.14	0.18	0.46	24.81	0.16	0.20	0.32

The general trend seen here is that in most cases, the measured concentrations of the elements decrease with increasing pH, indicating precipitation. Mostly, the decrease is not dramatic, with one exception being Pb in the Garpenberg, HCl sample. An observation made before become very clear in this case, i.e., the measured concentrations tend to increase in the step from pH 9 to pH 10. This is of course not physically reasonable, and it is not clear why this phenomenon arises and is so pronounced. It can most likely be attributed to measurement errors or interferences from the signals.

There are some trace elements that could potentially be separated into value-added products, such as Zn, Ni and Cu. These seem indeed to be precipitated away from the solution upon increase in pH, but being present in low quantities to begin with, this would most probably not work for generating significant profit in an industrial application.

An unexpected observation is the detection of Cd, albeit in low concentrations. In most cases, Cd was not detected after leaching (see Table 4.2). It is not clear why this is the case. Perhaps was Cd indeed detected

after leaching, but measurement interferences or errors made it seem as if it was not present.

4.2.2 PXRD analysis of precipitates from the pH lift

Precipitates from the pH lift steps were sparse and in very low quantities - in fact, most of them could not be analyzed with PXRD at all because of this. Table 4.6 presents the results of PXRD analysis for the handful of the samples that were of sufficient quantities.

Table 4.6: XRD analysis of some filter cakes from the pH lift step. "*" = extensive background noise detected.

Sample	**Identified structures**	**Chemical composition**
Garpenberg, HCl, pH 7 *	Salammoniac	$(NH_4)Cl$
Garpenberg, HCl, pH 9	*non-crystalline*	n/a
Garpenberg, HCl, pH 10 *	*no match identified*	n/a
Garpenberg, ABS, pH 5	Mascagnite	$(NH_4)_2SO_4$
	Ammonium sulfate	$(NH4)_2SO_4$
Pajala, ABS, pH 5	*non-crystalline*	n/a
Pajala, HCl, Native *	Tremolite	$Ca_2Mg_5Si_8O_{22}(OH)_2$
	Diopside	$CaMgSi_2O_6$
Pajala, HCl, pH 5	*non-crystalline*	n/a
Pajala, HCl, pH 9	*non-crystalline*	n/a
Pajala, HCl, pH 10	*non- crystalline*	n/a

As can be seen in the table, many of the samples were identified as amorphous, thus no crystalline structure could be found. A possible explanation to this may be that extensive amounts of the filter paper were mixed with the precipitates, after the precipitates were scraped off the paper and into vials for storage after drying. In other cases, the samples seemed mostly crystalline, but with extensive amounts of background noise, making analysis and structure matching difficult. In one case, no structures could be identified at all because of this. The few samples that could be identified did not seem to contain any valuable products, as they mostly consisted of either ammonia salts or Ca/Mg silicates. One sample even seemed to contain tremolite, which could be outright dangerous, as it is a type of asbestos mineral (see section 4.1.2). This is unfortunate for attempts to separate value-added products from the pH adjustment step, as this does not seem to be feasible, judging from these results.

4.3 Carbonation experiments

4.3.1 ICP-OES data

Table 4.7 shows the calculated amounts of measured elements before and after the carbonation step. The word "initial" refers to the time frame after the sample was filtered after storage in a refrigerator (see section 3.5), but before it was heated to 35 °C and had the pH re-adjusted to the proper starting value. "Final" refers to the filtrate obtained after the carbonation step was completed. Note that due to the generally low obtained amounts of elements, all have been calculated to [mg/l] instead of [g/l].

Table 4.7: Amounts of elements in mg/l leaching agent before and after the carbonation reaction.

Sample	Al	Ca	Fe	K	Mg	Na	Si
Garpenberg, HCl, pH 9, initial	2.07	2548.00	0.40	88.24	1071.55	12.63	67.90
Garpenberg, HCl, pH 9, final	2.43	22.83	0.38	87.59	666.83	11.77	69.56
Garpenberg, HCl, pH 10, initial	2.33	1442.48	0.30	44.72	392.86	9.88	68.72
Garpenberg, HCl, pH 10, final	2.47	7.18	0.25	48.71	16.95	7.81	69.39
Garpenberg, ABS, pH 9, initial	2.50	430.96	0.31	15.61	1151.30	11.58	80.45
Garpenberg, ABS, pH 9, final	2.52	220.12	0.27	20.21	1163.70	11.38	79.52
Garpenberg, ABS, pH 10, initial	2.31	167.43	0.26	6.95	421.72	7.78	73.19
Garpenberg, ABS, pH 10, final	2.39	16.33	0.23	13.24	59.41	6.83	70.83
Pajala, ABS, pH 9, initial	2.31	471.13	0.19	24.09	3945.19	19.32	75.09
Pajala, ABS, pH 9, final	2.21	443.69	0.22	28.08	3893.91	19.24	75.70
Pajala, ABS, pH 10, initial	2.28	214.71	0.19	11.46	1738.67	11.99	72.01
Pajala, ABS, pH 10, final	2.37	10.51	0.21	17.84	83.69	10.31	74.24
Pajala, HCl, pH 9, initial	2.02	2681.23	0.10	498.16	4656.04	31.86	70.64
Pajala, HCl, pH 9, final	2.19	703.66	0.18	499.23	4565.17	31.93	70.49
Pajala, HCl, pH 10, initial	2.19	1512.16	0.18	247.76	1121.05	19.08	66.19
Pajala, HCl, pH 10, final	2.54	9.43	0.14	242.91	24.16	16.70	70.35

The table shows a drastic decrease in concentrations of Ca and Mg upon carbonation in most cases, indicating that these elements were indeed part of the reaction happening during the experiments. There are exceptions, the most notable one being the sample of Pajala, ABS at starting pH of 9, where more or less no Ca or Mg seemed to leave the matrix. This is also seen in Table 4.9 below, which shows that practically no solid product at all was obtained for this sample. It is not clear why some of the samples had much better yields than others.

As for the other elements, i.e., Al, Fe, K, Na and Si, those seem more or less uninfluenced by the carbonation reaction. The same can be said about the trace elements, whose concentrations before and after carbonation are shown in Table 4.8 below. This is an expected result, as these elements were neither expected nor supposed to participate in the reaction during the carbonation step.

Table 4.8: Amounts of elements in mg/l leaching agent before and after the carbonation reaction.

Sample	As	Cd	Cr	Cu	Mo	Ni	Pb	V	Zn
Garpenberg, HCl, pH 9, initial	0.18	0.16	0.38	0.14	0.37	13.59	0.11	0.16	10.05
Garpenberg, HCl, pH 9, final	0.17	0.15	0.40	0.14	0.37	14.12	0.11	0.16	10.21
Garpenberg, HCl, pH 10, initial	0.18	0.13	0.25	0.14	0.37	7.34	0.12	0.16	5.66
Garpenberg, HCl, pH 10, final	0.13	0.12	0.27	0.14	0.37	7.16	0.12	0.16	5.56
Garpenberg, ABS, pH 9, initial	0.17	0.17	2.67	0.14	0.38	0.29	0.11	0.16	34.01
Garpenberg, ABS, pH 9, final	0.13	0.16	2.65	0.14	0.38	0.30	0.11	0.16	34.00
Garpenberg, ABS, pH 10, initial	0.19	0.13	1.14	0.14	0.37	0.20	0.11	0.16	14.33
Garpenberg, ABS, pH 10, final	0.11	0.12	0.89	0.13	0.37	0.19	0.12	0.16	10.71
Pajala, ABS, pH 9, initial	0.18	0.10	0.62	0.13	0.37	12.09	0.11	0.17	0.87
Pajala, ABS, pH 9, final	0.13	0.10	0.61	0.14	0.37	11.87	0.11	0.16	0.79
Pajala, ABS, pH 10, initial	0.18	0.10	0.35	0.13	0.37	5.83	0.11	0.16	0.47
Pajala, ABS, pH 10, final	0.10	0.10	0.29	0.13	0.37	4.21	0.11	0.16	0.39
Pajala, HCl, pH 9, initial	0.17	0.10	0.11	0.13	0.38	20.18	0.12	0.16	0.37
Pajala, HCl, pH 9, final	0.17	0.10	0.11	0.13	0.37	20.22	0.12	0.16	0.31
Pajala, HCl, pH 10, initial	0.19	0.10	0.11	0.13	0.37	10.61	0.11	0.16	0.21
Pajala, HCl, pH 10, final	0.12	0.10	0.11	0.14	0.37	10.49	0.11	0.17	0.21

4.3.2 Decrease in pH upon carbonation and obtained carbonation products

There was a distinct difference in the behavior of the pH between samples carbonated with the initial pH of 9 and those with the initial pH of 10. The samples starting at pH 9 reached the final pH-value of 8 without issue, although with varying time frames. The samples starting at pH 10, however, stagnated around pH $8.3 - 8.45$, wherefore the experiments were discontinued after four hours. Figure 4.2 shows plots of the pH lowering process during carbonation as a function of time, where pH was logged every 60 s. Samples with initial pH 9 are plotted together in Figure 4.2a, while those with initial pH 10 are plotted in Figure 4.2b.

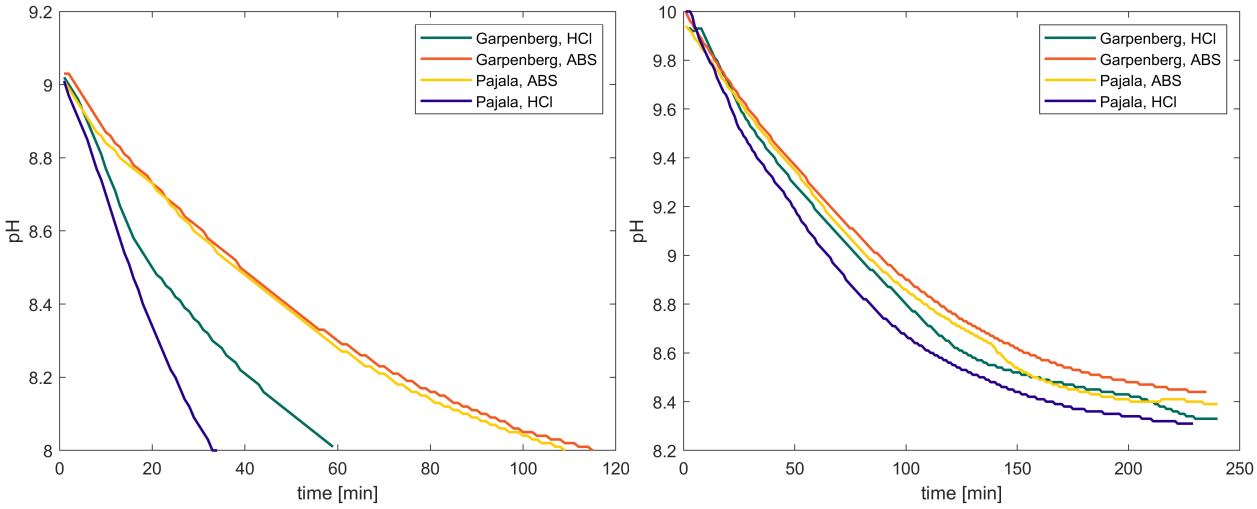

Figure 4.2: Logged pH lowering routes upon carbonation when starting at (a) pH 9, and (b) pH 10.

For the samples starting at pH 9, the pH clearly descends in an exponential manner. The time at which it reaches pH 8, however, widely differs for the different samples. There is a notable trend, where the samples that were originally leached with ABS, follow close to identical paths, both taking just short of 2 h to reach pH 8. This time is reduced to less than half for the samples where HCl was the leaching agent. More specifically, the sample with Pajala sand leached with HCl seems to provide the least amount of hindrance towards the pH drop, reaching pH 8 in about 35 min, while the Garpenberg sample leached with HCl reached pH 8 in just under 1 h. While this may indicate that faster reduction in pH to 8, or that starting at pH 9, yields more product, Table 4.9, where the weights of the obtained carbonation products are listed, shows that this is not necessarily the case.

Table 4.9: Weights of obtained carbonation products.

Sample (mine + leaching agent)	Initial pH	Mass of obtained product [g]
Garpenberg, HCl	9	0.51
Garpenberg, HCl	10	0.31
Garpenberg, ABS	9	0.02
Garpenberg, ABS	10	0.01
Pajala, ABS	9	7E-5
Pajala, ABS	10	0.48
Pajala, HCl	9	0.40
Pajala, HCl	10	0.61

As can be seen from the table, the samples with ABS as leaching agent yielded mostly much smaller amounts of product than those leached with HCl, when comparing samples from the same mine. When comparing the two different initial pH-values, then the Garpenberg samples starting at pH 9 yielded higher amounts of product than those starting at pH 10. Surprisingly, this trend is reversed for the Pajala samples, where the lower initial pH gave less product; in the case of ABS as leaching agent, there was effectively no product to be collected at all at pH 9. Also, comparing the two fastest samples with initial pH 9 from the pH curves in Figure 4.2a, the Garpenberg sample leached with HCl gave higher amount of product than the corresponding Pajala sample, although taking about double the time to reach the final pH of 8. Given all of the above, the time needed for the samples to reach pH 8, and whether or not pH 8 is at all reached, does not seem to have much effect on the amount of product obtained. Instead, the origin of the mine tailing, and the leaching agent used to extract the earth metals, seem to be of much more importance.

As for the samples starting at pH 10, there is again an exponential decrease in the pH. There is, however, no longer a clear distinction between the two leaching agents, although the samples, where HCl was the leaching agent, do decrease in pH slightly faster than those leached with ABS. For the Pajala sample leached with ABS, there is even a slight increase in pH towards the end of the measurement, which is unexpected. While this might be a measurement error, variations in temperature may also have had an impact, as in most carbonation experiments, the temperature was held at 35 °C to the best of efforts, but in practice varied between 33 to 37 °C. What is nonetheless important to observe, is that the pH seems to be unable to reach 8.3. It is not clear why this is the case. What can be said about the preparation of these samples, is that the pH needed to be adjusted back to the proper starting value upon the samples being heated up to 35 °C. While for the samples starting at pH 9, this was done by adding about $10 - 20$ ml NH_4OH, the amounts of NH_4OH needed to adjust the pH back to 10 were in the order of $100 - 170$ ml. Given that the initial volumes of the samples were in the order of $150 - 200$ ml, this meant an extensive dilution with the base, which may have ultimately affected the pH decrease ability.

4.3.3 PXRD analysis of precipitates before heating and carbonating

Some of the precipitated matter that arose during shelf time between the pH adjustment step and the carbonation step, could be collected in sufficient amounts as to be analyzed with PXRD. The results from this analysis are shown in Table 4.10 below.

Table 4.10: XRD analysis of some filter cakes from before the carbonation reaction.

Sample	**Identified structures**	**Chemical composition**
Garpenberg, HCl, pH 9	*non-crystalline*	n/a
Garpenberg, HCl, pH 10	Iowate	$Mg_{0.75}Fe_{0.25}Cl_{0.25}(OH)_2(H_2O)_{0.5}$
Garpenberg, ABS, pH 9	*non-crystalline*	n/a
Garpenberg, ABS, pH 10	*non-crystalline*	n/a
Pajala, HCl, pH 10	Brucite	$Mg(OH)_2$

In three of the five cases, the precipitate was not identified as crystalline, and in one of the cases, a rather complex Mg-Fe-Cl hydroxide (iowate) was identified. An interesting finding is that of brucite ($Mg(OH)_2$) in the Pajala, HCl sample at pH 10. It is interesting since in some research on mine tailings for mineral carbonation, this was the product that was precipitated in order to later be reacted into $MgCO_3$ [14, 15]. As can be seen in the following section, this seems not to have helped in the attempts to precipitate $MgCO_3$ during the carbonation step.

4.3.4 PXRD analysis of the carbonation products

All carbonation products, except for the Pajala, ABS sample at starting pH 9 (see Table 4.9), were able to be analyzed with PXRD. The results from this anaysis are presented in Table 4.11.

Table 4.11: XRD analysis of the carbonated products. "*" = extensive background detected.

Sample	**Identified structures**	**Chemical composition**
Garpenberg, HCl, pH 9	Calcium carbonate	$CaCO_3$
	Aragonite	$CaCO_3$
Garpenberg, HCl, pH 10	Calcite	$CaCO_3$
	Aragonite	$CaCO_3$
Garpenberg, ABS, pH 9	Mascagnite	$(NH_4)_2SO_4$
	Ammonium sulfate	$(NH4)_2(SO_4)$
	Calcite, Mg-bearing	$(Mg_{0.03}Ca_{0.97})CO_3$
	Calcium carbonate	$CaCO_3$
Garpenberg, ABS, pH 10 *	Aragonite	$CaCO_3$
	Mascagnite	$(NH_4)_2SO_2$
	Kieserite	$MgSO_4{\cdot}H_2O$
Pajala, ABS, pH 10 *	Mascagnite	$(NH_4)_2SO_2$
	Aragonite	$CaCO_3$
Pajala, HCl, pH 9	Calcite, Mg-bearing	$(Ca_{0.875}Mg_{0.125})CO_3$
Pajala, HCl, pH 10 *	Aragonite	$CaCO_3$

As can be seen from the table, various crystalline forms of $CaCO_3$ were identified in all of the carbonation products. In three of the samples, only $CaCO_3$ was in fact detected. This may entail possibilities for relatively cheap and easy purification of the product, after which it may be sold further as a value-added product, rather than disposed of. As for precipitation of $MgCO_3$, this seems to not have been particularly successful, as traces of the product were only identified in two samples, even then as parts of a Mg-bearing Calcite mineral. It was expected that the precipitation of $MgCO_3$ would be more difficult to achieve than that of $CaCO_3$, as this is a well-known issue in mineral carbonation of mine tailings; the almost complete lack of it is, however, was rather unanticipated. It is not clear why this is the case, but perhaps did the gradual lowering of the pH, rather than a constant pH in previous studies [20, 21], influence the outcome. As stated in section 2.4.2, the gradual lowering of pH until a stop value of 8 was a test to see how well the carbonation would work in reaction conditions closer to an industrial setting.

Note also that Mg was found in one of the samples, but in the form of the sulfate mineral kieserite, rather than a carbonate. Furthermore, impurities in the form of the ammonium salts mascagnite and ammonium sulfate were identified in some of the samples, suggesting that a potential purification of the $CaCO_3$ present in these samples would most probably be much more complex and expensive, than for the samples without these impurities. Also worth mentioning is that two of the samples contained large amounts of background noise, which may have influenced the structure matching. It also indicates that the samples may have had hardly identifiable, or even amorphous, impurities.

4.3.5 Calculations on CO_2 capture efficiencies

Table 4.12 presents results of calculations on the amounts of CO_2 captured per kg dry feedstock, both experimentally and as a theoretical max value, as well as the calculated CO_2 capture efficiencies and carbonation efficiencies for each of the carbonation samples. Calculations were done according to equations

(3.3) to (3.11). For CCE, index e represents calculations on the experimentally captured CO_2, while index t represents theoretical calculations on the captured CO_2 if no material losses were regarded. Note that the calculations were done on the assumption that the Mg that was lost during carbonation, as seen in Table 4.7, was indeed converted to $MgCO_3$, even if it mostly could not be detected with PXRD.

Table 4.12: Calculated and amounts of CO_2 captured per tonne dry feedstock given in [kg/ton dry sand], along with calculated efficiencies.

Sample	$\mathbf{CE_{Ca}}$ [%]	$\mathbf{CE_{Mg}}$ [%]	$\mathbf{m_{CO_2,e}}$	$\mathbf{m_{CO_2,t}}$	$\mathbf{m_{CO_2,tm}}$	$\mathbf{CCE_e}$ [%]	$\mathbf{CCE_t}$ [%]
Garpenberg, HCl, pH 9	99.1	37.8	39.3	60.3	161.7	24.3	37.3
Garpenberg, HCl, pH 10	99.5	95.7	28.3	80.4	161.7	17.5	49.8
Garpnberg, ABS, pH 9	48.9	0.0	2.9	9.7	161.7	1.8	6.0
Garpnberg, ABS, pH 10	90.2	85.9	10.8	102.9	161.7	6.7	63.6
Pajala, ABS, pH 9	5.8	1.3	1.3	1.8	356.7	0.4	0.5
Pajala, ABS, pH 10	95.1	95.2	35.8	111.6	356.7	10.0	32.3
Pajala, HCl, pH 9	73.8	2.0	23.7	47.0	356.7	6.6	13.2
Pajala, HCl, pH 10	99.4	97.8	56.9	221.1	356.7	15.9	62.0

The most notable trend that can be observed from the table is how the carbonation efficiencies differ between the different samples when comparing the starting pH. Namely, CE is higher for the samples where carbonation started at pH 10; drastically higher in fact for Mg. This may explain the leveling-off of the pH as seen in Figure 4.2, as it suggests that when starting at pH 10, the system had enough time to reach and carbonate the Mg, while for pH 9, it seems as if the reaction happened too fast for the Mg to be carbonated sufficiently. Note also that the difference in CE between the two pH-levels is not as high for Ca, suggesting that the carbonation of Ca happens faster than that of Mg. This is expected, since Ca is known to be easier to carbonate than Mg.

This trend also influences the amount of CO_2 captured per unit weight sand, and thus also the calculated CO_2 capture efficiencies, except for the case of the Garpenberg sample leached with HCl. Here, the amount of CO_2 captured, and thus also the experimental CCE, is higher for pH 9. This is due to higher material loss in between the pH adjustment step and the carbonation step. Indeed, the sample with pH 10 was stored for 5 days longer than that with pH 9 before carbonation, meaning there was a larger time frame for material loss through precipitation to happen. Overall, the material losses in between the different steps of the process have influenced the end result to a high extent. It is clear that avoiding them increases the CO_2 capture efficiency, greatly so in some cases.

Letting the theoretical CCE be the end result representing the efficiency of the process as a whole, two samples reached CO_2 capture efficiency higher than 60 %, namely the Garpenberg sample leached with ABS and carbonated at pH 10, and the Pajala sample leached with HCl and carbonated at pH 10. Since the technoeconomic assessment was done prior to these calculations, these samples were not represented there. They suggest, however, that the results of the TEA would be somewhat more favorable if these two samples were represented instead. Worth noticing is also that these calculations do not match the actual obtained products from Table 4.9, as they were made under the assumption that the precipitated Mg formed $MgCO_3$, as in "it had to go somewhere". It could, however, not be confirmed with PXRD, where almost no $MgCO_3$ was identified (Table 4.11). It thus remains unclear in what way/phase the Mg precipitated and the efficiency calculations should be interpreted with this in mind.

5 Technoeconomic assessment

Table 5.1 below presents some general assumptions of the process, a more rigorous description is provided under the section 3.7 in the method.

Table 5.1: Main assumptions.

Operation	**Assumptions**
General assumptions.	No Ca or Mg losses in between leaching and carbonation.
Drying sand	Drying the sand at 100 °C.
Sieving	Negligible energy consumption, no mass loss.
Heating HCl	From 20 °C to 80 °C. Mass of HCl 10x the amount of dry sand. The physical properties of HCl is the same as for water.
Leaching	Constant temperature at 80 °C for 1h. 10 % of the energy required to heat HCl to 80 °C.
Filtrating	30 min filtration time.
pH-lift to 9 at 35 °C	No byproduct extracted from the lift, NH_4OH is used as the base. The physical properties of NH_4OH is the same as for water.
Filtrating	15min filtration.
Carbonation	Flue gas with 15 vol% CO_2, 60 min for Garpenberg and 35 for Pajala.
Filtration	15 min.

5.1 Case 1

The first case presents the results of the calculations for 1 ton wet sand. Table 5.2 provides a comprehensive summary of the anticipated masses necessary for processing 1 ton of wet sand. Additionally, it presents the estimated heating and drying energy to be provided by district heating (DH), along with the corresponding total. Similarly, the electrical energy required for the filtration process is also displayed.

Table 5.2: Results mass flows and energy flows per ton wet sand

	Pajala, HCl, pH 9	**Garpenberg, HCl, pH 9**
m_{H_2O} [kg]	354	178.8
m_{HCl}(12 M) [kg]	6455	8210
m_{NH_4OH}(17 M) [kg]	287.479	993.466
m_{DW} [kg]	6127.181	9576.549
m_{CO_2} [kg]	432.438	701.25
m_{CO_2} sequestrated [kg]	4.542	7.367
Drying wet sand, required energy [MWh]	0.255	0.129
Heating, pre-leaching, required energy [MWh]	0.450	0.572
Heating during leaching, required energy [MWh]	0.045	0.057
Heating, carbonation, required energy [MWh]	0.129	0.202
Filtering, post-leaching, required energy [MWh]	0.003	0.004
Filtering, pH lift, required energy [MWh]	0.002	0.002
Filtering, post-carbonation, required energy [MWh]	0.002	0.002
Total heating energy consumption [MWh]	0.879	0.960
Total electricity energy consumption [MWh]	0.006	0.008

Table 5.2 highlights that the most significant energy consumption in the process is attributed to the heating and drying of the leachate for both samples. Furthermore, it is evident that the Pajala sample has a higher water content compared to Garpenberg, resulting in a greater energy demand for drying. However, this lower water content in the Garpenberg sample also implies a greater consumption of the leaching agent (HCl) and base (NH_4OH), thus increasing the energy requirements for the heating steps. As a result, Garpenberg exhibits a higher total energy consumption in the process compared to Pajala.

Table 5.3 summarizes the material costs and energy costs for the given process per kg CO_2 sequestrated.

Table 5.3: Result economics per kg CO_2 sequestrated.

	Pajala, HCl, pH 9	**Garpenberg, HCl, pH 9**
HCl, estimated cost [€]	4.383	3.437
NH_4OH, estimated cost [€]	7.580	17.369
Deionized water, estimated cost [€]	0.461	0.429
Heating energy, estimated cost [€]	3.871	2.606
Electricity energy, estimated cost [€]	0.040	0.031
CO_2 sequestrated , estimated income recent EU ETS 90€ [€]	0.932	0.737
OPEX [€]	16.125	21.38

The table shows that the most cost-intensive aspect of the process is the chemicals, followed by the cost of DH as the second most expensive factor. The electricity cost, as presented in this thesis, is comparable in magnitude to the estimated income from the sequestration of CO_2. However, these values are approximately three orders of magnitude smaller and can be considered negligible in comparison to the aforementioned factors.

When comparing Garpenberg to Pajala, a notable difference in cost arises from the higher demand for NH_4OH in the Garpenberg sample. This discrepancy significantly contributes to the overall price variation between the two samples.

Figure 5.1 illustrates a cumulative bar chart based on the energy consumption and costs of the OpEx.

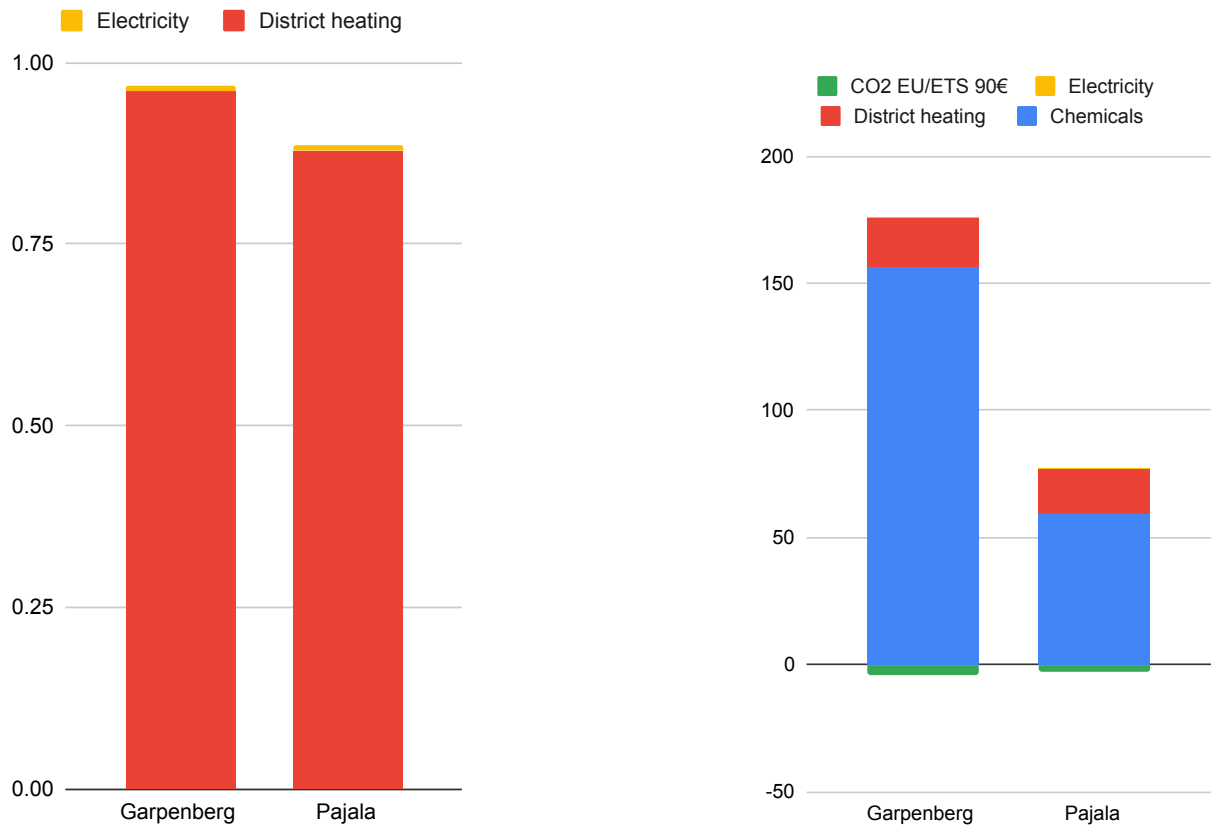

(a) (b)

Figure 5.1: Energy consumption [MWh/ton wet sand] in (a) and potential costs and income [€/kg CO_2 sequestered] of the process in (b).

The figure provides a visual representation of the various prices and energy consumption in relation to each other. Notably, the heat demand is approximately 100 times greater than that of electricity. Moreover, the costs associated with the process are predominantly influenced by the chemical expenses, which are approximately three times higher than the second largest cost, namely the heating cost. Furthermore, the income from CO_2 sequestration is relatively small and does not have a significant impact on the OpEx costs for this case.

5.2 Case 2

The second case presents the results for 1 ton dry sand which excludes the drying step of the previous section and also includes Figure 5.3, where 95 % of the chemical costs are neglected due to recirculation of the chemicals.

Table 5.4 offers a comprehensive overview of the projected quantities required to process 1 ton of dry sand. Furthermore, it provides estimates of the heating demand that will be supplied by DH, along with the corresponding total energy consumption. Similarly, the table presents the electrical energy demand for the filtration process.

Table 5.4: Results mass flows and energy flows per ton dry sand.

	Pajala, HCl, pH 9	**Garpenberg, HCl, pH 9**
m_{HCl}(12 M) [kg]	1239.669	1239.669
m_{NH_4OH}(17 M) [kg]	444.358	1210.068
m_{DW} [kg]	9829.191	11664.493
m_{CO_2} [kg]	432.438	701.25
m_{CO_2} sequestrated [kg]	47.049	60.333
Heating, pre-leaching, required energy [MWh]	0.697	0.697
Heating during leaching, required energy [MWh]	0.070	0.070
Heating, carbonation, required energy [MWh]	0.201	0.246
Filtering, post-leaching, required energy [MWh]	0.005	0.005
Filtering, pH lift, required energy [MWh]	0.002	0.002
Filtering, post-carbonation, required energy [MWh]	0.002	0.002
Total heating energy consumption [MWh]	0.967	1.012
Total electricity energy consumption [MWh]	0.009	0.009

The results presented in the above table exhibit a similar trend to the findings for the 1 ton wet sand. However, this table clearly demonstrates that the primary reason for Pajala's lower energy consumption is the lower demand for base during the pH lift process for the Pajala sample.

Table 5.5 provides a summary of the costs associated with materials and energy for the given process, calculated per kg sequestrated CO_2.

Table 5.5: Result economics per kg CO_2 sequestration.

	Pajala, HCl, pH 9	**Garpenberg, HCl, pH 9**
HCl, estimated cost [€]	0.296	0.231
NH_4OH, estimated cost [€]	1.232	2.583
Deionized water, estimated cost [€]	0.069	0.064
Heating energy, estimated cost [€]	0.411	0.336
Electricity energy, estimated cost [€]	0.006	0.005
CO_2 sequestrated , estimated income recent EU ETS 90€ [€]	0.090	0.090
OPEX [€]	2.235	3.128

From the table, it can be concluded that the main factor of the difference in OpEx prices arises from the higher consumption of base that Garpenberg has and that the most influential price of this process comes from the base (NH_4OH).

Figure 5.2 gives an illustration of the energy and costs per kg CO_2 sequestrated.

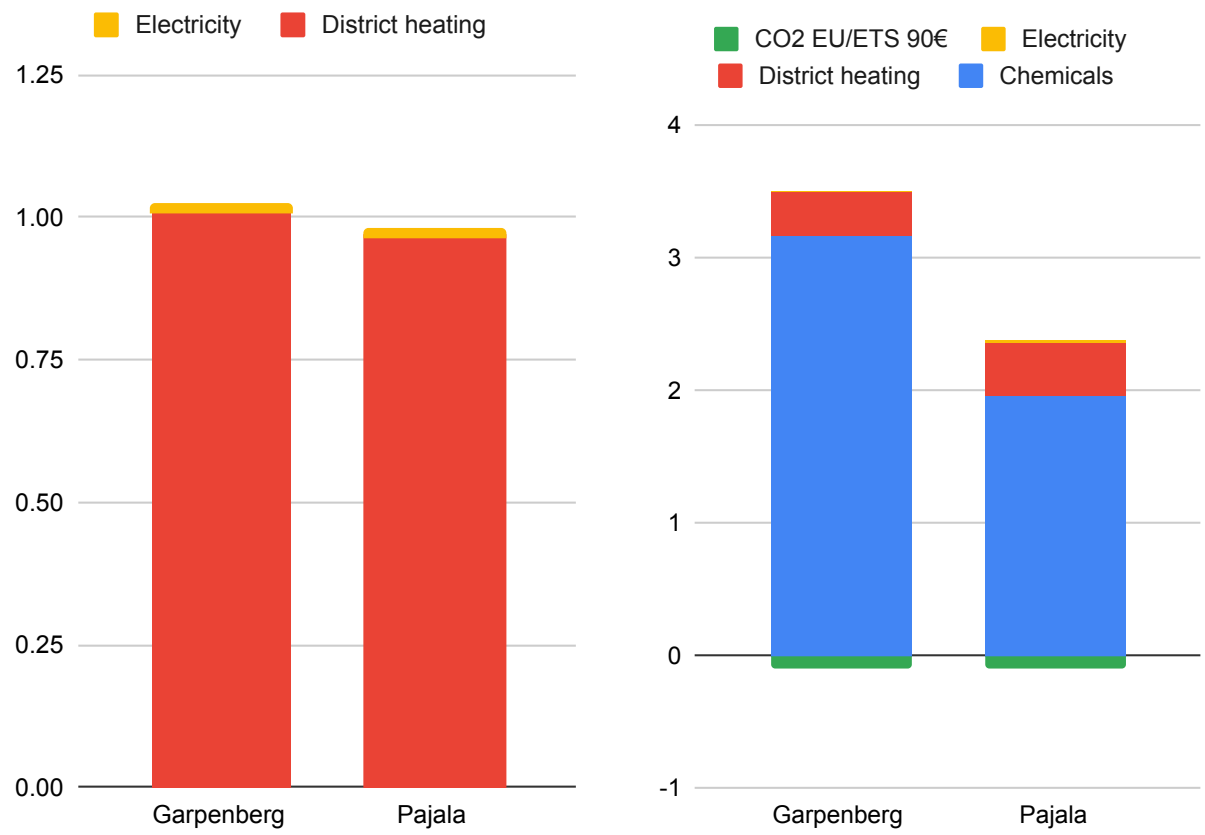

(a) (b)

Figure 5.2: Energy consumption [MWh/ton dry enriched sand] in (a) and potential costs and income of the process in (b) with the unit [€/kg CO_2 sequestrated]

The figure illustrates, in a similar manner to Figure 5.1, that the heating demand is 100 times larger than that for electricity and that the costs of the chemicals are approximately 3 times larger than the heating cost.

Figure 5.3 illustrate the results presented in table 5.5 if 95 % of the chemicals would be recirculated and therefore excluded as an operational cost.

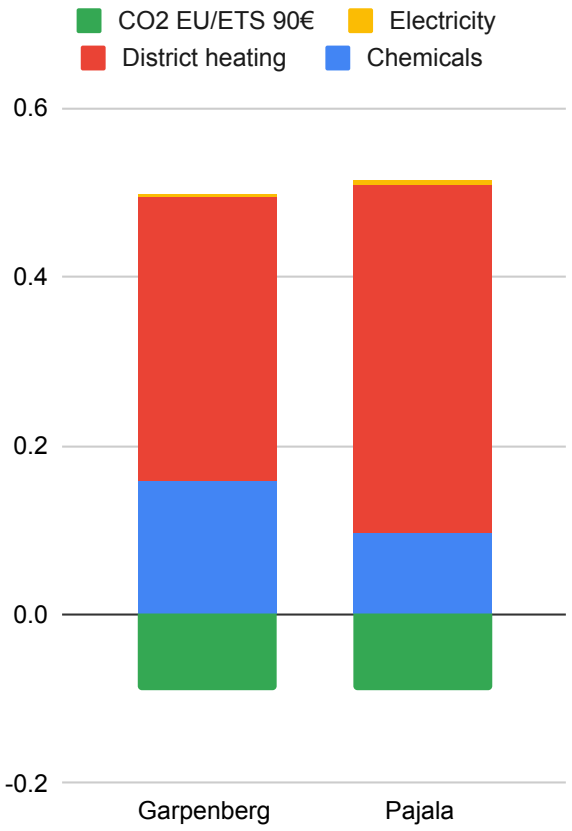

Figure 5.3: Costs and income of the process where 95 % of the chemical cost are excluded in €/kg CO_2 sequestrated.

The figure shows the case of chemical recirculation. Based on it, it is evident that this affects the operating cost and makes the income from CO_2 comparable in size to the chemical costs. The operating cost for the process, assuming 95 % reduction of cost from the chemicals, would give a OpEx cost of 0.408 €/kg CO_2 for Garpenberg and 0.425 €/kg CO_2 for Pajala. Making the OpEx cost for Pajala more expensive. This is due to the fact that Garppenberg sequestrated more CO_2 combined with the reduced chemical costs for the two samples.

6 Discussion

6.1 Extraction of Ca and Mg from the mine tailings

The results of the leaching process clearly indicate that temperature plays a significant role in the leaching of Mg, as higher temperatures lead to a greater yield of leached Mg. However, the trend regarding Ca extraction is not as apparent, although the Pajala sample treated with HCl follows a similar pattern. From this, it can be concluded that an operating temperature of 80 °C is crucial, and running the process at this temperature could potentially increase the value of the operation, particularly if the focus is on Mg extraction. However, the same cannot be said for Ca, as the cost of additional heat does not seem to significantly enhance the yield of Ca. Furthermore, the results suggest that HCl is a superior leaching agent for extraction of both Ca and Mg. However, HCl may be unattractive for some industries, as chlorinated solvents may cause corrosion of technical appliances, thus driving the cost of the process upwards.

Another noteworthy observation is the unusually high amount of extracted Mg from the Garpenberg sample treated with ABS at 80 °C. This result is likely an anomaly caused by the effect of cluster sampling, where the specific sample possibly contained a higher concentration of Mg compared to the overall batch. Further investigation should prioritize studying the effects of leaching time since this study only examined a leaching duration of 1 hour. Such investigation would greatly contribute to expanding our understanding of the process.

6.2 pH adjustment and byproduct recovery

Apart from being a chemical prerequisite for the carbonation reaction to work, an objective with the pH adjustment step was also to assess the possibility of recovering value-added byproducts. The ambition was to precipitate salable products at different pH steps, which would then compensate for some of the expenses associated with the mineral carbonation process. While some products have been recovered in previous studies, this was not successful during the work on this thesis.

From the ICP-OES data, it is clear that some elements have been precipitated to some extent, such as Al, Fe, Si, Cu and Pb. The amounts of precipitated products were, however, not sufficient to reliably analyze their contents with PXRD, and the few that did contain enough matter for the analysis seemed not to contain any products of value. The message taken from this result is that for any future work of a similar nature, 25 g of dried sand as a starting point for the experiments is not enough - at least the double amount should probably be used to obtain sufficient amounts of precipitates. Nevertheless, the fact that some potentially valuable elements seemed to have precipitated during the pH adjustment step, suggests that it may be worthwhile trying to assess in what forms and quantities this happens. Perhaps there are some value-added products in the precipitates, which, on an industrial scale, could be separated in fair amounts.

Another observation from this stage of the process appears from the PXRD analysis of the few successfully analyzed samples. Namely, precipitates from samples that had been pH adjusted contained ammonium salts, even when HCl was previously used as the leaching agent. This indicates that the precipitated ammonium

salts likely come from the pH regulator, i.e., NH_4OH. If any value-added product can be precipitated during the pH adjustment step, the presence of ammonium salts could make its purification difficult and expensive, possibly rendering the byproduct recovery idea economically infeasible. Moreover, the demand for NH_4OH greatly contributes to the overall cost of the process, as can be seen from the technoeconomic assessment. Therefore, trying a different base as the pH regulator could be useful in future experiments.

A last observation here relates also to the carbonation step, as well as to the technoeconomic assessment part of the thesis. Raising the pH to 9 for the carbonation required much less base than in the cases where the starting pH was set to 10. However, the samples, where the carbonation started at pH 10, yielded higher CO_2 capture efficiencies (Table 4.12). Regarding the results of the technoeconomic assessment, the chemicals, if not recycled, represent the highest cost item, even when doing the calculations on samples where pH 9 was the starting alkalinity for the carbonation. Therefore, a future study should attempt to make a more in-depth assessment of whether or not the extensive amounts of base needed to adjust the pH to 10, instead of 9, could improve the CO_2 capture efficiency enough to overshadow the higher expenses related to the higher demand for base.

6.3 Carbonation reaction

The most notable result from the carbonation step is the fact that carbonation of Ca was successful in all samples, mostly to a high degree, while carbonation of Mg was only successful in 5 of the 8 carbonation samples. Even so, the carbonation of Mg could in most cases not be confirmed by PXRD. Instead it was assumed that the precipitated Mg during the carbonation reaction, as seen from the ICP-OES data, was precipitated as $MgCO_3$. This is in contrast with ongoing research at the partner university within the project, i.e., Åbo Akademi University in Finland, where much of the experimental procedures were similar to the ones used in this thesis, and where the carbonation of Mg reached higher yields. The most notable difference in the experimental procedures is probably the fact that the pH of the solution was let to decrease to a stop-value during the work on this thesis, rather than kept constant for a specified amount of time. As mentioned in the background chapter, there is a distribution of different carbonate species dissolved in an aqueous solution at different pH levels. This may mean that there also is a distribution of different crystalline phases of $CaCO_3$ and $MgCO_3$ being favored at different alkalinities. There were indeed several different crystalline phases of $CaCO_3$ detected, in some cases more than one per sample. Perhaps this had an impact on the precipitation of $MgCO_3$, given that Mg is known to be more difficult to carbonate than Ca. This would then suggest that letting the pH decrease during carbonation may not be a preferable option. Therefore, a future study should assess the difference in results after the solution pH had been left to decrease, as compared to the case where it had been kept constant. Also, the impact of the purity of the CO_2 gas on the result should be assessed. This is an important knowledge, as it will dictate the way an industrial application of the process will be implemented in practice.

There is also a question of time efficiency vs. CO_2 capture efficiency. Looking at the calculated CO_2 capture efficiencies (Table 4.12), carbonation reactions that started at pH 10 yielded notably higher CO_2 capture efficiencies compared to the ones that started at pH 9, especially when disregarding the material losses during the process. However, the pH 10 samples were also carbonated more than 4 times longer than the pH 9 samples. This, along with comparing the calculated carbonation efficiencies, suggests that carbonation of Ca was relatively fast, followed by a slow carbonation of Mg (see section 4.3.5). While an industry that adapts

the process should aim for the highest possible CO_2 capture efficiencies, there may be a trade-off in terms of the time it takes to run a batch of the reactions, the energy it takes to maintain the reaction conditions for the required amount of time, and the demand for chemicals along the route. Especially the demand for base is much higher if pH 10 is the starting point, as compared to the case where pH 9 is the starting point. Therefore, it would be of interest for a future study to compare these parameters and their impact on the overall effectiveness and economy of the process.

6.4 Techoeconomic assessment

Based on the technoeconomic assessment results, it is evident that Garpenberg sand incurs higher operational costs in both cases, involving both wet and dry sand with the exception of the case with recirculated chemicals for the dry sand, where Garpenberg had a lower OpEx cost. In Case 1, the water content of the samples influences the amount of sand processed. Higher water content leads to a smaller amount of sand per ton, resulting in reduced mass of HCl and base (NH_4OH), ultimately impacting the overall cost. This implies that a process with higher water content appears "cheaper" per ton of wet sand but also captures less CO_2. Case 2, on the other hand, provides a more accurate representation for comparing costs and CO_2 sequestration based on the raw material, i.e., mine tailings. However, Case 1 presents a more realistic depiction of the potential industrial process as the current sand is stored in landfills exposed to precipitation. Depending on the weather conditions during sand collection, the water content can vary. Therefore, comparing water content between the Garpenberg and Pajala mines should not be considered a general trend for respective tailings from the mines. It serves as an example of possible water content variations. For a comparative analysis between the mines, Case 2 (€/kg CO_2 sequestrated from dry sand) offers a more representative approach.

The results from Case 2 clearly demonstrate that Garpenberg incurs higher costs when no chemicals are recirculated due to its greater demand for base (NH_4OH), which is consistent across all laboratory samples. It would be interesting to explore alternatives and evaluate the feasibility of using a less expensive base, thereby narrowing the price gap between the enriched sands. Additionally, Figure 5.3 represents a scenario where process chemicals are recirculated, leading to a substantial reduction in total OpEx costs and making Garpenberg the sample with less OpEx costs. Assuming a 95 % recirculation rate, the excluded chemical costs would be considered an investment cost rather than part of OpEx calculations. This representation provides a more realistic assessment of total OpEx costs and offers valuable insights into the potential impact of the chemical costs. For this case, it can be concluded that Garpenberg has the lower OpEx cost since it had a higher amount of CO_2 sequestrated combined with the fact that the chemicals have a smaller impact on the total OpEx Cost. This was an unexpected result based on composition data provided on the samples; the reason for a higher CO_2 sequestration for Garpenberg comes from the carbonation efficiencies. Furthermore, further examination and potential sale of the end product could enhance process income and further reduce costs. The ICP-OES results suggest that extraction of Al, Fe, Cu, and Zn could also increase income and reduce OpEx costs. However, more studies are needed to determine the profitability of this extraction. Parameters effecting the carbonation efficiencies should also be evaluated and studied in order to obtain higher carbonation efficiencies, which in turn would decrease the OpEx costs. It is important to note that the values presented in this report are preliminary estimations of potential OpEx based on scaling laboratory work and assumptions that we deemed reasonable for industrial implementation.

7 Conclusions and future work

This study aimed at assessing the feasibility of using mine tailings for CO_2 sequestration through indirect mineral carbonation. During extraction of the reactive components, i.e., Ca^{2+} and Mg^{2+}, the sand from the Kevitsa mine did not yield satisfactory amounts of the elements, and was therefore eliminated from further experiments. Hydrochloric acid as the leaching agent was found to be superior to ammonium bisulfate. Higher temperature was found to improve the leaching of Mg; the effect of temperature on the leaching of Ca was unclear. In the subsequent pH adjustment step, no value-added products could be recovered, while most of the solid precipitates contained insufficient quantities of product to be analyzed with PXRD. For the ones that were successfully analyzed, the pH regulating agent (NH_4OH) seemed to have precipitated as different ammonium salts, suggesting a different base to be used in future studies. Carbonation of Ca was successful, while carbonation of Mg had mixed and unclear results. This may have been influenced by the fact that the solution pH was let to decrease during the carbonation step, or perhaps by the use of diluted (15 vol%) CO_2 gas. The tailings from the Garpenberg and Pajala mines yielded comparable results with respect to CO_2 capture efficiencies, which were generally higher when carbonation was started at pH 10.

Based on the technoeconomic assessment results, several key findings can be derived. The technoeconomic assessment reveals that Garpenberg incurs higher operational costs compared to Pajala for both wet and dry sand processing when the chemicals are not recirculated. Case 2 provides a more accurate comparison of costs and CO_2 sequestration based on the raw material, enriched sand. Garpenberg's higher costs primarily stem from its greater consumption of base (NH_4OH) across all laboratory samples. Exploring alternatives and evaluating the feasibility of using a less expensive base could help narrow the price gap between the enriched sands. The representation of recirculating process chemicals (Figure 5.3) demonstrates a substantial reduction in total OpEx costs and makes Garpenberg the cheaper alternative due to its higher CO_2 sequestration. Assuming a high recirculation rate provides a more realistic assessment of total OpEx costs. Further examination, potential product sale, the extraction of other valuable elements like Al, Fe, Cu, and Zn, and increasing the carbonation efficiencies could enhance process income and reduce OpEx costs. However, additional studies are required to evaluate the profitability of these extraction processes. Further research is necessary to refine and validate these findings. A future study should focus on finding a method to recirculate at least 95 % of the make-up chemicals in order to decrease the operational costs to acceptable levels.

As an overall conclusion, mine tailings from the Pajala and Garpenberg mines can be feasible to be used in a CO_2 sequestration process. The end result in terms of CO_2 capture efficiency is much dependent on the chosen reaction parameters. Therefore, future work should focus on more in-depth mapping of the influence of different parameters on the results. Such parameters are the choice of leaching agent, temperature and time, pH regulator, carbonation pH and whether or not it should be kept constant, as well as purity of the CO_2 gas. At least 50 g of dried sand as a starting point is recommended to obtain sufficient amounts of precipitates for PXRD analysis. Lastly, in all future work should the mine tailings be handled with care and caution, given the findings of small amounts of asbestos in the Pajala and Kevitsa tailings.

References

[1] UNHCR. *Climate change and disaster displacement*. Accessed 2023-01-31. 2001-2023. URL: https://www.unhcr.org/climate-change-and-disasters.html.

[2] IPCC. *Climate Change 2022: Impacts, Adaptation and Vulnerability*. Cambridge, UK and New York, NY, USA, 2022. DOI: 10.1017/9781009325844.

[3] *Paris Agreement*. COP 21. United Nations. UNFCCC, 2015.

[4] Fagerlund J. and Zevenhoven R. "An experimental study of $Mg(OH)_2$ carbonation". In: *International Journal of Greenhouse Gas Control* 5 (2011), pp. 1406–1412. DOI: 10.1016/j.ijggc.2011.05.039.

[5] Seifritz W. "CO_2 disposal by means of silicates". In: *Nature* 345.486 (1990). DOI: 10.1038/345486b0.

[6] Bobicki E.R., Liu Q., Xu Z., and Zeng H. "Carbon capture and storage using alkaline industrial wastes". In: *Progress in Energy and Combustion Science* 38 (2012), pp. 302–320. DOI: 10.1016/j.pecs.2011.11.002.

[7] Fossilfritt Sverige. *Mining and minerals industry*. Accessed 2023-01-31. 2018. URL: https://fossilfrittsverige.se/en/roadmap/the-mining-and-minerals-industry-2/.

[8] Santos R.M. and Khalidy R. "The fate of atmospheric carbon sequestrated through weathering in mine tailings." In: *Minerals Engineering* 163.106767 (2021). DOI: 10.1016/j.mineng.2020.106767.

[9] RISE Research Institutes of Sweden AB. *Carbon capture, utilization and storage with Swedish mine tailings*. Accessed 2023-05-13. 2022. URL: https://www.ri.se/en/what-we-do/projects/carbon-capture-utilization-and-storage-with-swedish-mine-tailings.

[10] Quaghebeur M., Nielsen P., Horckmans L., and Van Mechelen D. "Accelerated Carbonation of Steel Slag Compacts: Development of High-Strength Construction Materials". In: *Frontiers in Energy Research* 3.52 (2015). DOI: 10.3389/fenrg.2015.00052.

[11] Monasterio-Guillot L., Fernandez-Martinez A., Ruiz-Agudo E., and Rodriguez-Navarro C. "Carbonation of calcium-magnesium pyroxenes: Physical-chemical controls and effects of reaction-driven fracturing". In: *Geochimica et Cosmochimica Acta* 304 (2021), pp. 258–280. DOI: 10.1016/j.gca.2021.02.016.

[12] Rank C. *Permanent sequestration of CO_2 using LD slag*. Munich, DE: Technical University of Munich, 2022.

[13] Zhao Y., Zhang J., Miao E., Du Y., Zheng X., and Zhang X. "CO_2 sequestration by direct mineral carbonation of municipal solid waste incinerator fly ash in ammonium salt solution: Performance evaluation and reaction kinetics". In: *Separation and Purification Technology* 309.123103 (2023). DOI: 10.1016/j.seppur.2023.123103.

[14] Zevenhoven R., Fagerlund J., Nduagu E., and Romão I. "A stepwise process for carbon dioxide sequestration using magnesium silicates". In: *Frontiers of Chemical Engineering in China* 4 (2010), pp. 133–141. DOI: 10.1007/s11705-009-0259-5.

[15] Fagerlund J., Highfield J., and Zevenhoven R. "Kinetics studies on wet and dry gas-solid carbonation of MgO and $Mg(OH)_2$ for CO_2 sequestration". In: *RSC Advances* 2 (2012), pp. 10380–10393. DOI: 10.1039/c2ra21428h.

[16] Highfield J., Lim HQ., Fagerlund J., and Zevenhoven R. "Mechanochemical processing of serpentine with ammonium salts under ambient conditions for CO_2 mineralization". In: *RSC Advances* 2 (2012), pp. 6542–6548. DOI: 10.1039/c2ra20575k.

[17] Zevenhoven R., Romão I., Slotte M., and Gando-Ferreira L.M. "CO_2 sequestration with magnesium silicates - Exergetic performance assessment". In: *Chemical Engineering Research and Design* 92 (2014), pp. 3072–3082. DOI: 10.1016/j.cherd.2014.05.016.

[18] Nduagu E., Romão I., Fagerlund J., and Zevenhoven R. "Performance assessment of producing $Mg(OH)_2$ for CO_2 mineral sequestration". In: *Applied Energy* 106 (2013), pp. 116–126. DOI: 10.1016/j.apenergy.2013.01.049.

[19] Goldberg P., Chen Z.-Y., O'Connor W., Walters R., and Ziock H. "CO_2 Mineral Sequestration Studies in US". In: (2001). Accessed 2023-05-25. URL: https://www.osti.gov/biblio/1208898.

[20] Teir S., Kuusik R., Fogelholm C.-J., and Zevenhoven R. "Production of magnesium carbonates from serpentinite for long-term storage of CO_2". In: *International Journal of Mineral Processing* 85 (2007), pp. 1–15. DOI: 10.1016/j.minpro.2007.08.007.

[21] Ebrahimi A., Saffari M., Hong Y., Milani D., Montoya A., and Valix M. et al. "Mineral sequestration of CO_2 using saprolite mine tailings in the presence of alkaline industrial wastes". In: *Journal of Cleaner Production* 188 (2018), pp. 686–697. DOI: 10.1016/j.jclepro.2018.04.046.

[22] Mattila H.-P. and Zevenhoven R. "Design of a Continuous Process Setup for Precipitated Calcium Carbonate Production from Steel Converter Slag". In: *ChemSusChem* 7 (2014), pp. 903–913. DOI: 10.1002/cssc.201300516.

[23] Dahmani J., Kharchafi A., El-Khalfaouy R. and El Gaidoumi A., Addaou A., and Lahsini A et al. "Sequestration of Carbon Dioxide by a Mineral Residue: Application on the Ca-Sepiolite Material Composite". In: *Chemistry Africa* 5 (2022), pp. 1703–1713. DOI: 10.1007/s42250-022-00444-y.

[24] Molahid V.L.M., Kusin F.M., Hasan S.N.M.S., Ramli N.A.A., and Abdullah A.M. "CO_2 Sequestration through Mineral Carbonation: Effect of Different Parameters on Carbonation of Fe-Rich Mine Waste Materials". In: *Processes* 10.432 (2022). DOI: 10.3390/pr10020432.

[25] Wang Q., Jin Z., Yu C., Wang R., Wei W., and Jing Y. "Preparation of precipitated calcium carbonate using wollastonite and CO_2 from industrial exhaust". In: *Brazilian Journal of Chemical Engineering* 39 (2022), pp. 661–669. DOI: 10.1007/s43153-021-00200-8.

[26] Zevenhoven R., Slotte M., Åbacka J., and Highfield J. "A comparison of CO_2 mineral sequestration processes involving a dry or wet carbonation step". In: *Energy* 117 (2016), pp. 604–611. DOI: 10.1016/j.energy.2016.05.066.

[27] Zevenhoven R., Slotte M., Koivisto E., and Erlund R. "Serpentinite Carbonation Process Routes using Ammonium Sulfate and Integration in Industry". In: *Energy Technology* 5 (2017), pp. 945–954. DOI: 10.1002/ente.201600702.

[28] Teir S., Revitzer H., Eloneva S., Fogelholm C.-J., and Zevenhoven R. "Dissolution of natural serpentinite in mineral and organic acids". In: *International Journal of Mineral Processing* 83 (2007), pp. 36–46. DOI: 10.1016/j.minpro.2007.04.001.

[29] Wang X. and Maroto-Valer M.M. "Dissolution of serpentine using recyclable ammonium salts for CO_2 mineral carbonation". In: *Fuel* 90 (2011), pp. 1229–1237. DOI: 10.1016/j.fuel.2010.10.040.

[30] Erlund R., Koivisto E., Fagerholm M., and Zevenhoven R. "Extraction of magnesium from four Finnish magnesium silicate rocks for CO_2 mineralisation—part 2: Aqueous solution extraction". In: *Hydrometallurgy* 166 (2016), pp. 229–236. DOI: 10.1016/j.hydromet.2016.07.004.

[31] Mörtstedt S. and Hellsten. *DATA OCH DIAGRAM*. Energi- och kemitekniska tabeller. Liber, 2016. ISBN: 078-91-47-00805-6.

[32] Xitong L, Sneha S, Timothy B V., Jay W F., and Meagan M S. "Cost Comparison of Capacitive Deionization and Reverse Osmosis for Brackish Water Desalination". In: *ACS ES&T Engineering* 1.2 (2021). DOI: doi:10.1021/acsestengg.0c00094.

[33] Duan W., Wu Q., Li P, and Cheng P. "Techno-economic analysis of a novel full-chain blast furnace slag utilization system". In: *Energy* 2422 (2022). DOI: doi.org/10.1016/j.energy.2021.123049.

[34] Antonio E., Mandelli F., Kolling D., Matsusato J S., Alberto C O F., and Mateus R S. et al. "Development of an economically competitive Trichoderma-based platform for enzyme production: Bioprocess optimization, pilot plant scale-up, techno-economic analysis and life cycle assessment". In: *Bioresource Technology* 364 (2022). DOI: doi.org/10.1016/j.biortech.2022.128019.

[35] Nord Pool. *Price Development*. 2023. URL: https://www.nordpoolgroup.com/en/.

[36] Carbon credits. *Live Carbon Prices Today*. 2023. URL: https://carboncredits.com/carbon-prices-today/?gclid=CjwKCAjwpuajBhBpEiwA_ZtfhfRF0MNwM4cU1pExp_d2aH8fRkbf4ggYM-3cH5jC6Vn9K_ouVVA97BoCsUUQAvD_BwE.

[37] *Jingjin Equipment*. 2020. URL: https://www.jingjinequipment.com/product/energy-saving-and-efficient-water-washing-vibrating-filter-press/.

[38] World Health Organization (WHO). *Arsenic*. Accessed 2023-05-29. 2022. URL: https://www.who.int/news-room/fact-sheets/detail/arsenic.

[39] IARC Monographs on the Evaluation of Carcinogenic Risks to Humans Volume 100C. "Arsenic, Metals, Fibres, and Dusts". In: International Agency for Research on Cancer, WHO, 2012. Chap. Asbestos (Chrysotile, Amosite, Crocidolite, Tremolite, Actinolite and Anthophyllite). ISBN: 978-9283213208.

A Elemental composition of the used materials

The following appendix shows the results of an elemental analysis of the three used materials conducted at RISE, using XRF.

Table A.1: Results of elemental analysis of the used materials.

	Pajala	**Garpenberg**	**Kevitsa**
Moisture [wt%]	n/a	< 0.2	< 0.2
C [wt%]	2.8	2.3	0.14
S [wt%]	0.12	5.8	0.62
Leachable Cl^- [wt%]	0.01	< 0.01	0.02
Al [wt%]	2.2	2.25	1.38
Si [wt%]	16	24.1	22.4
Fe [wt%]	4.6	3.56	8.48
Ti [wt%]	0.18	0.06	0.19
Mn [wt%]	0.09	1.17	0.14
Mg [wt%]	14	4.97	13.5
Ca [wt%]	9.4	6.53	9.19
Ba [wt%]	< 0.05	< 0.05	< 0.05
Na [wt%]	0.50	< 0.1	0.29
K [wt%]	1.4	1.38	0.18
P [wt%]	< 0.1	< 0.1	< 0.1
As [mg/kg]	< 20	170	< 20
Cd [mg/kg]	< 1	4	< 1
Co [mg/kg]	34	7	75
Cr [mg/kg]	40	7	2100
Cu [mg/kg]	29	100	350
Mo [mg/kg]	< 10	< 10	< 10
Ni [mg/kg]	64	7	750
Pb [mg/kg]	14	1830	8
V [mg/kg]	43	12	150
Zn [mg/kg]	24	1840	57

B PXRD diffractograms

In this appendix, all obtained diffractograms from the PXRD analysis are presented. For all crystalline samples with sufficiently low background noise, the detected crystalline phases are shown in the diffractograms.

B.1 Leaching experiments

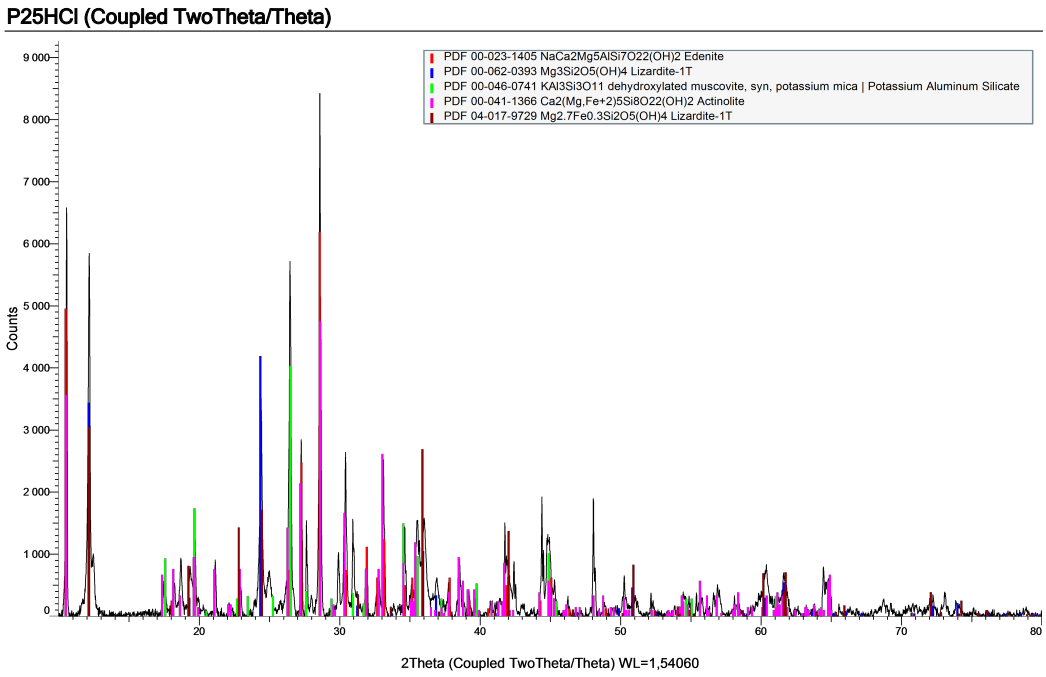

Figure B.1: Diffractogram for the leaching sample Pajala, HCl @ 25 °C.

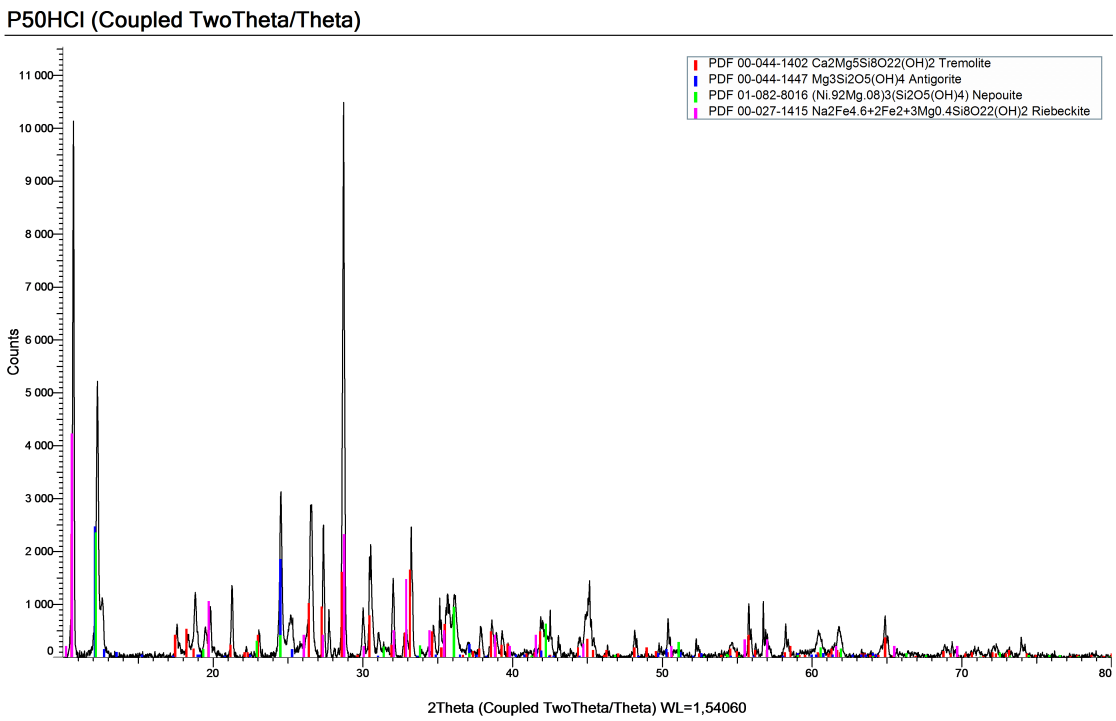

Figure B.2: Diffractogram for the leaching sample Pajala, HCl @ 50 °C.

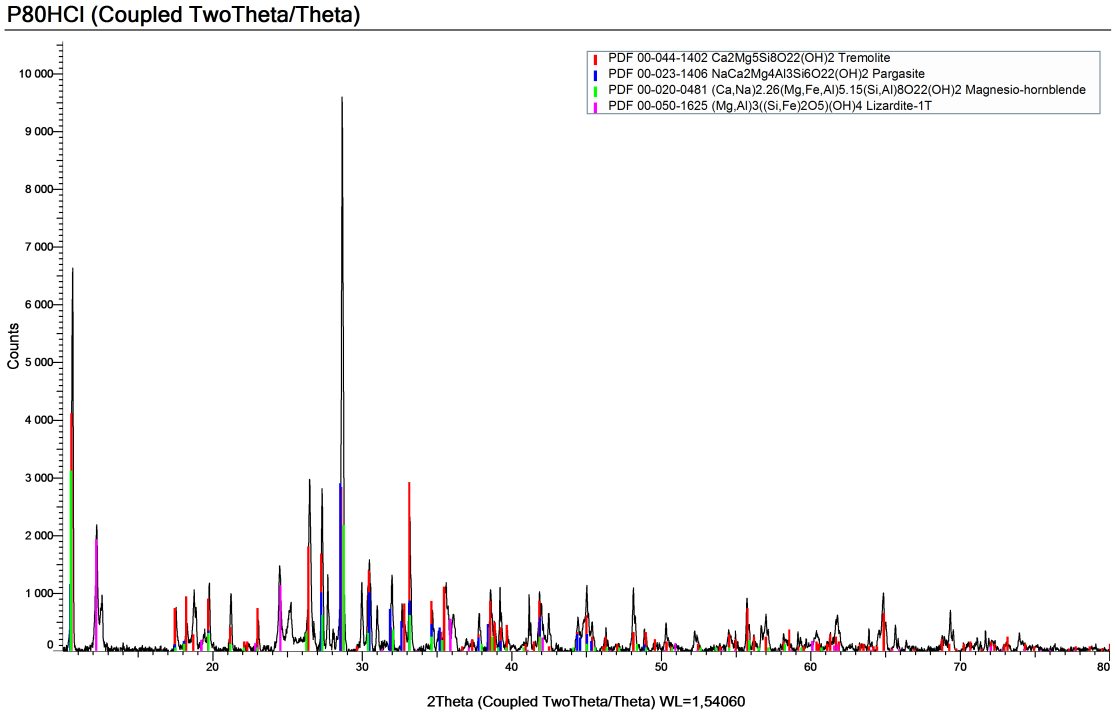

Figure B.3: Diffractogram for the leaching sample Pajala, HCl @ 80 °C.

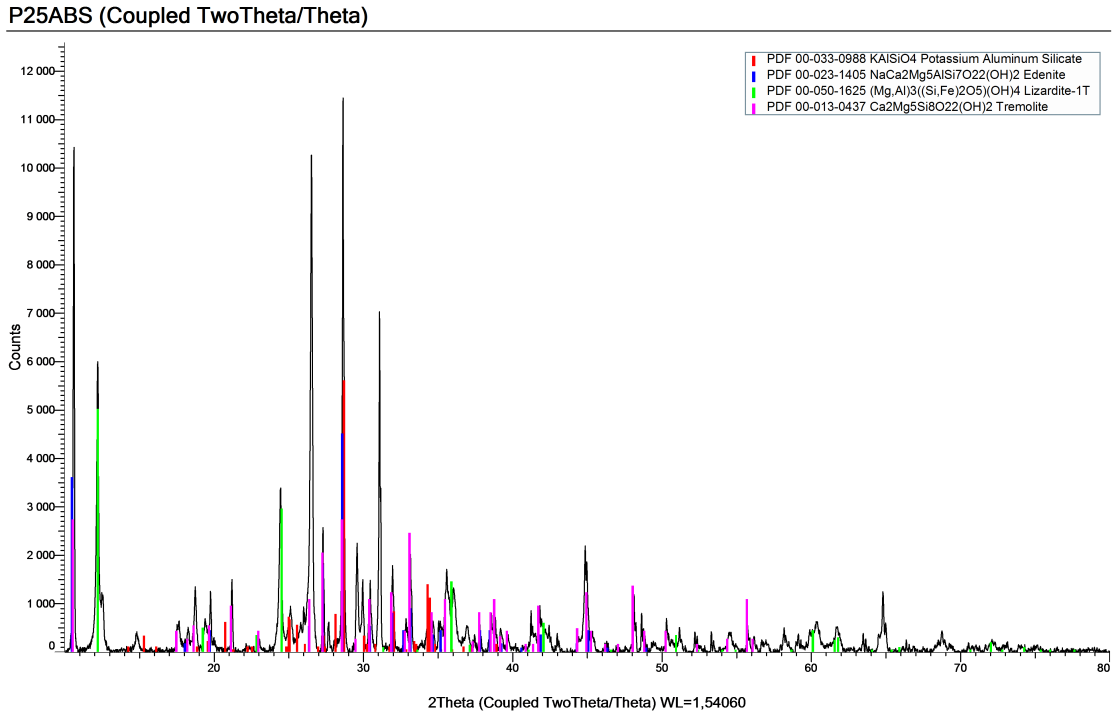

Figure B.4: Diffractogram for the leaching sample Pajala, ABS @ 25 °C.

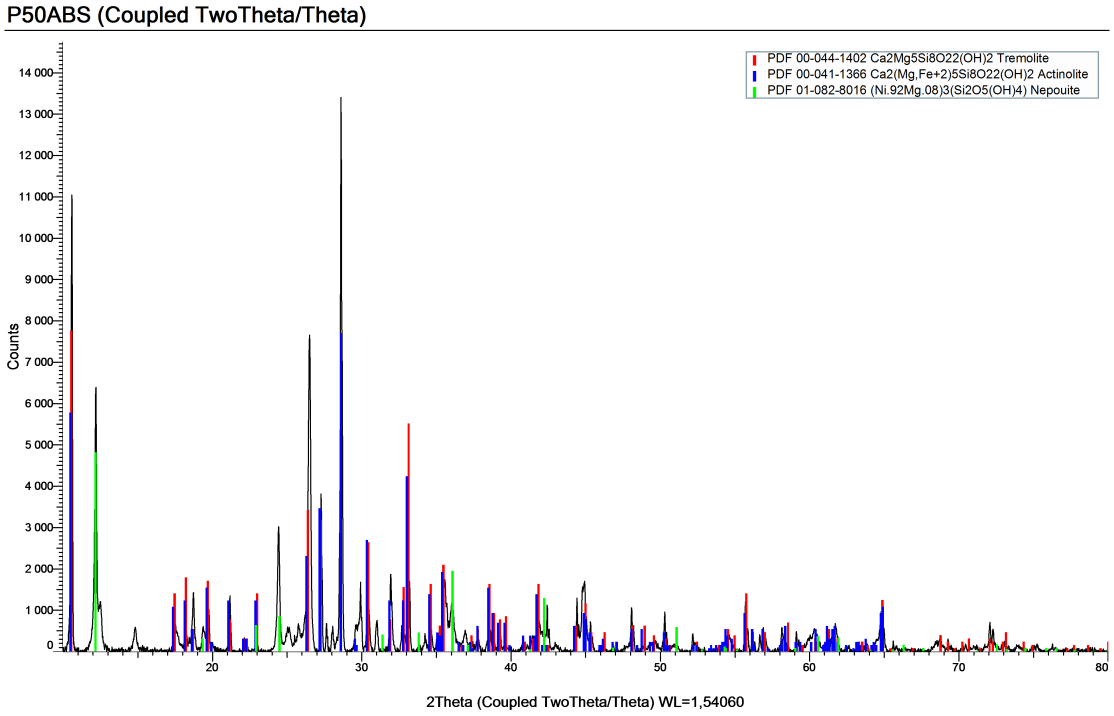

Figure B.5: Diffractogram for the leaching sample Pajala, ABS @ 50 °C.

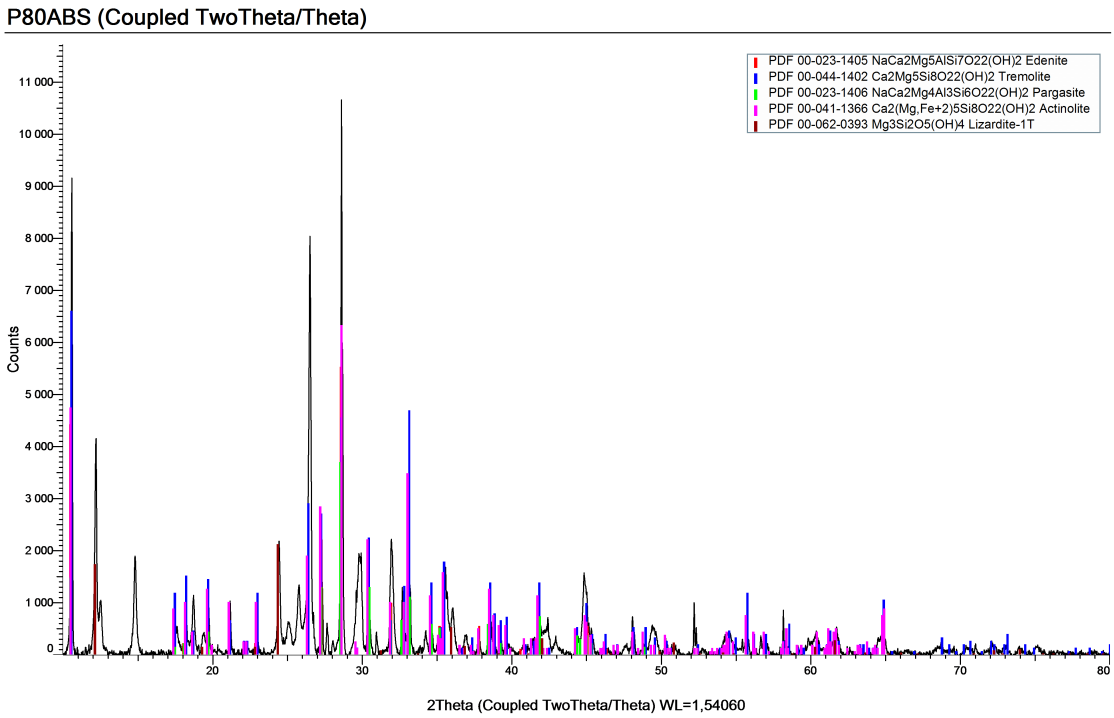

Figure B.6: Diffractogram for the leaching sample Pajala, ABS @ 80 °C.

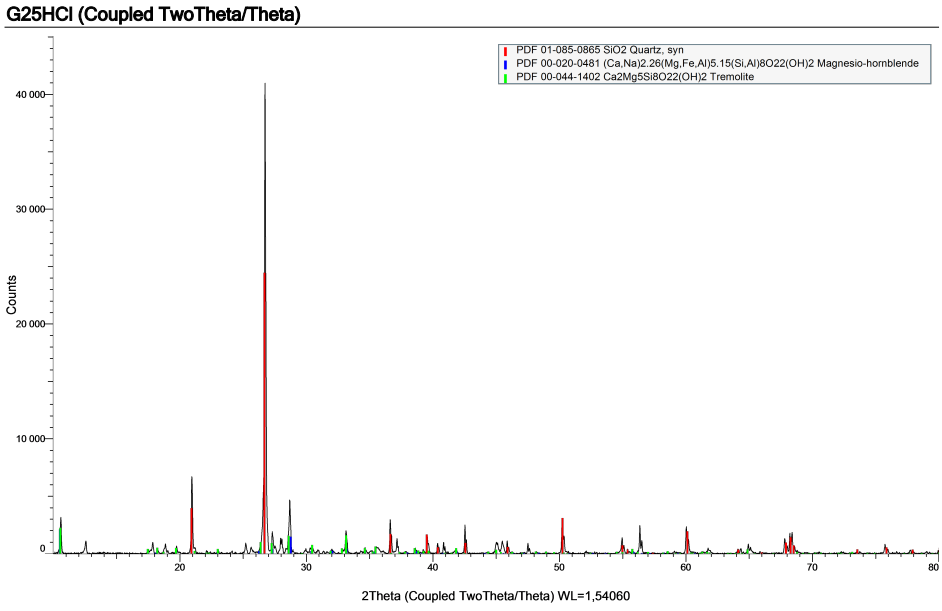

Figure B.7: Diffractogram for the leaching sample Garpenberg, HCl @ 25 °C.

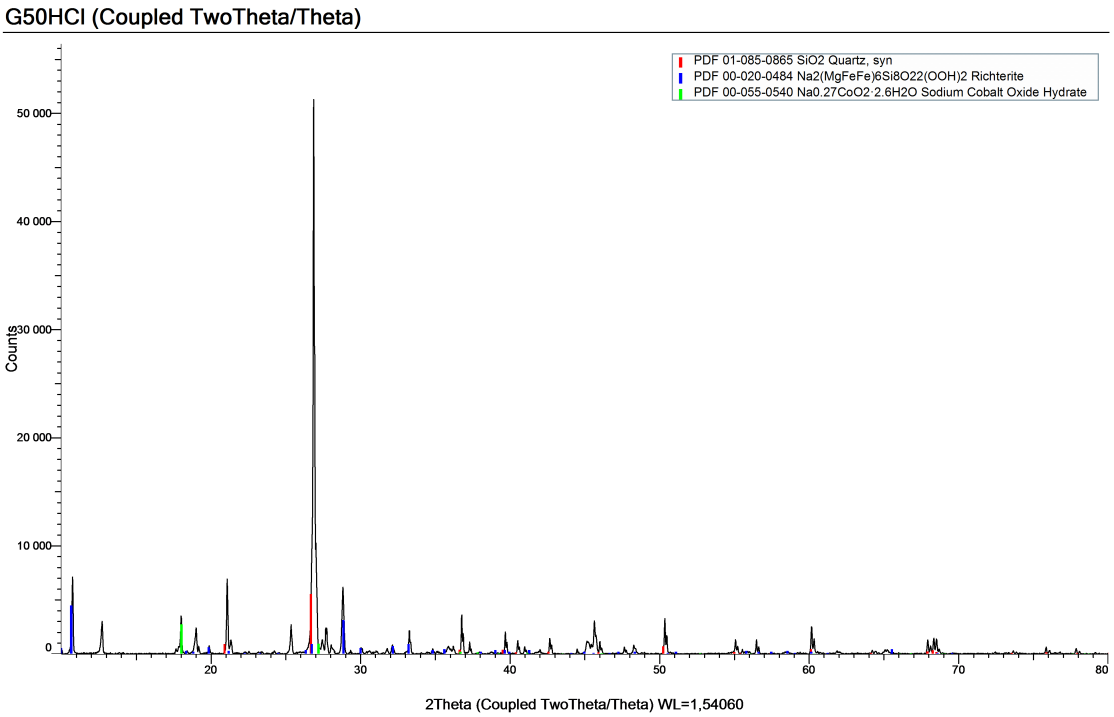

Figure B.8: Diffractogram for the leaching sample Garpenberg, HCl @ 50 °C.

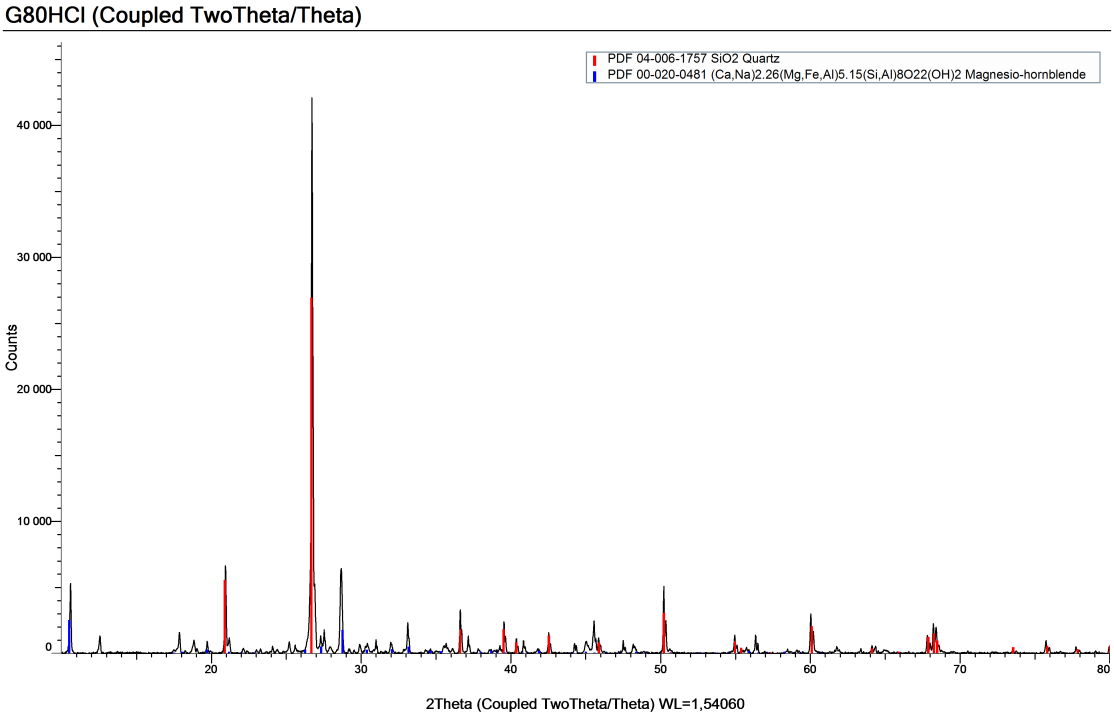

Figure B.9: Diffractogram for the leaching sample Garpenberg, HCl @ 80 °C.

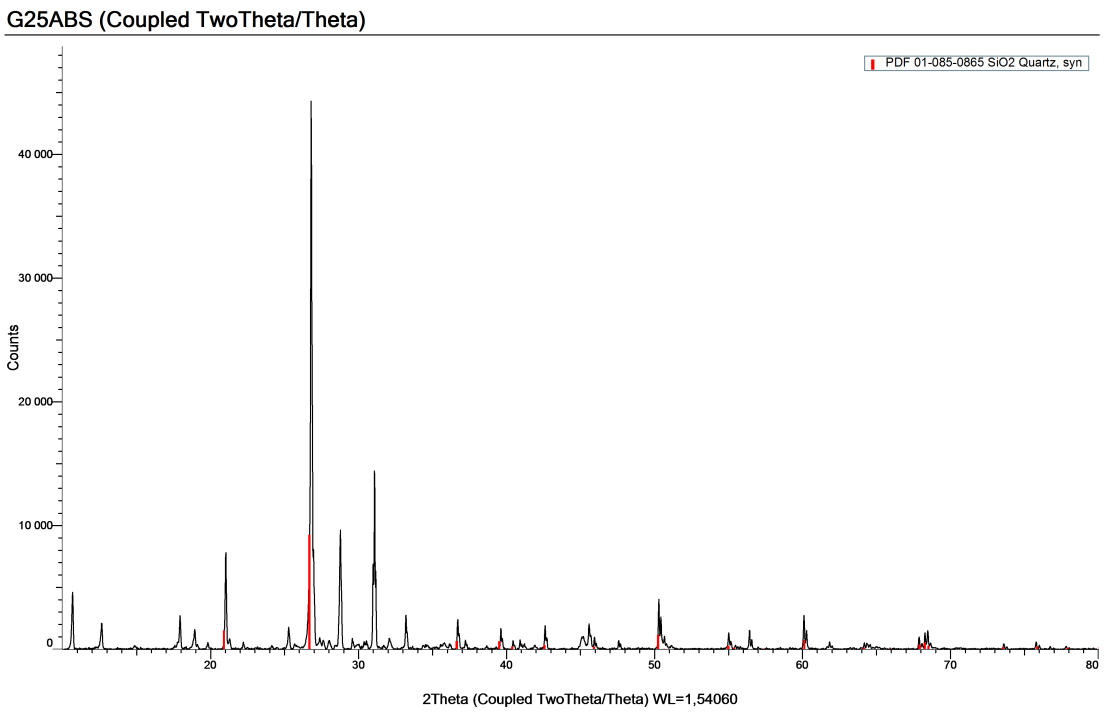

Figure B.10: Diffractogram for the leaching sample Garpenberg, ABS @ 25 °C.

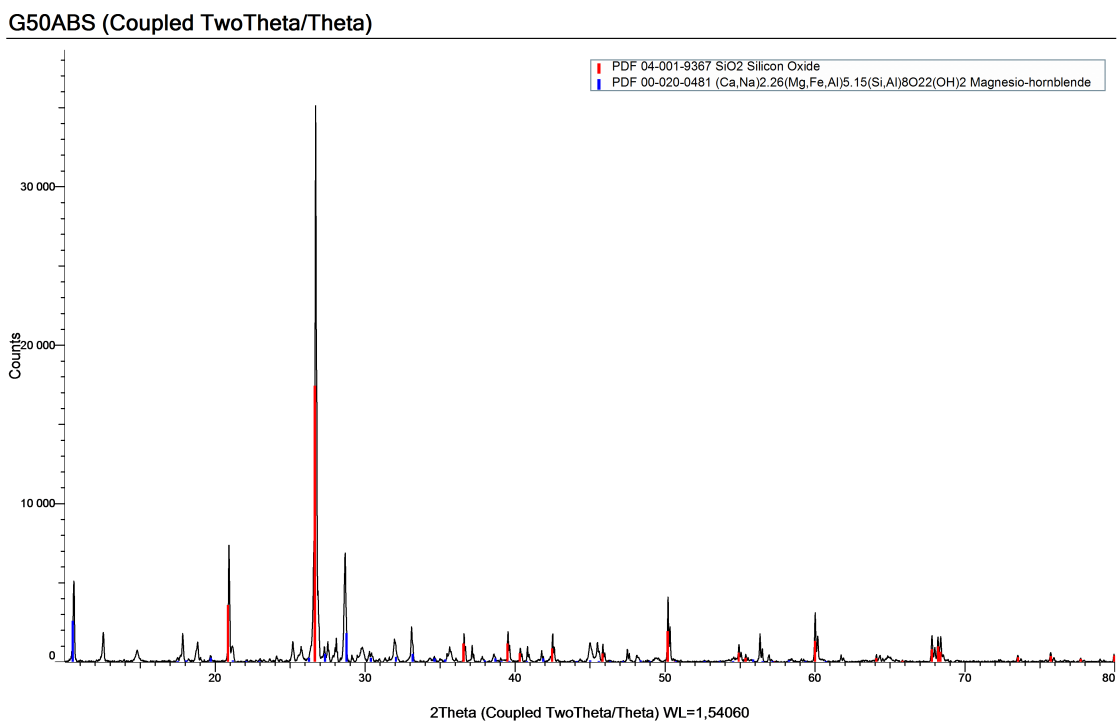

Figure B.11: Diffractogram for the leaching sample Garpenberg, ABS @ 50 °C.

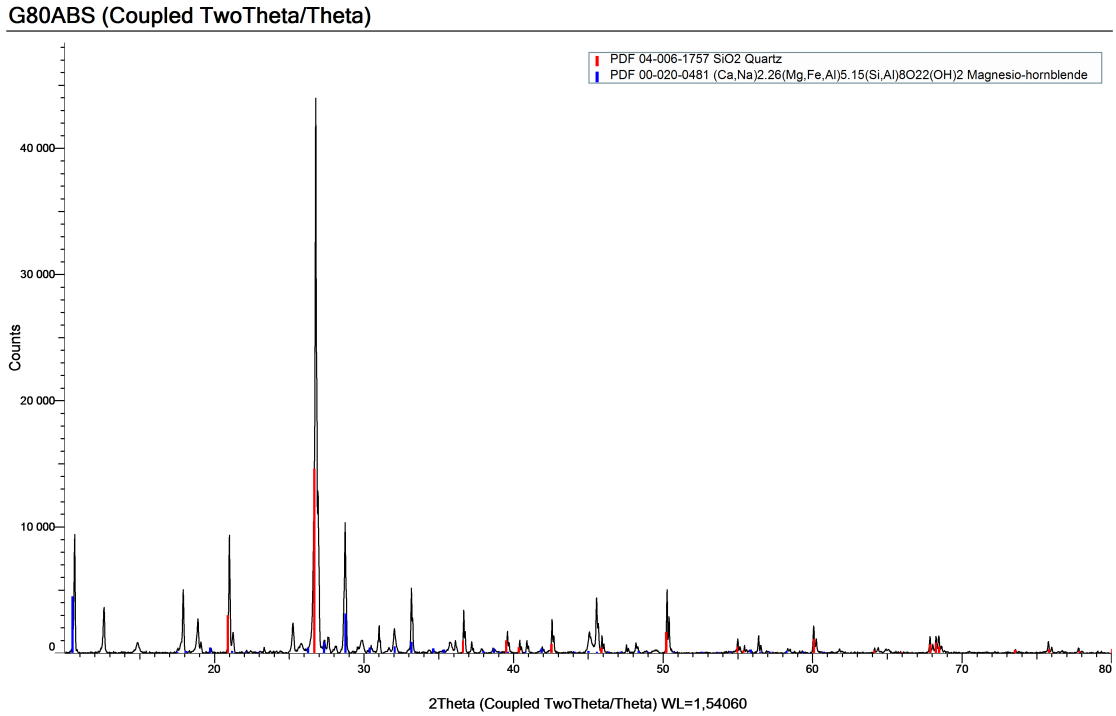

Figure B.12: Diffractogram for the leaching sample Garpenberg, ABS @ 80 °C.

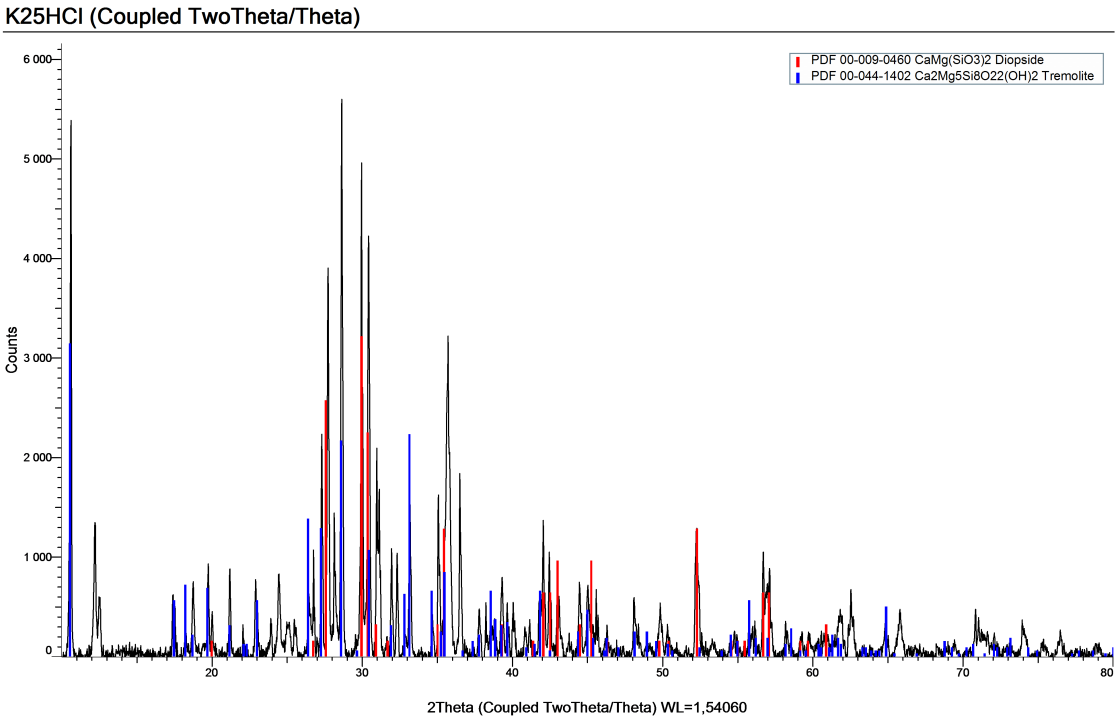

Figure B.13: Diffractogram for the leaching sample Kevitsa, HCl @ 25 °C.

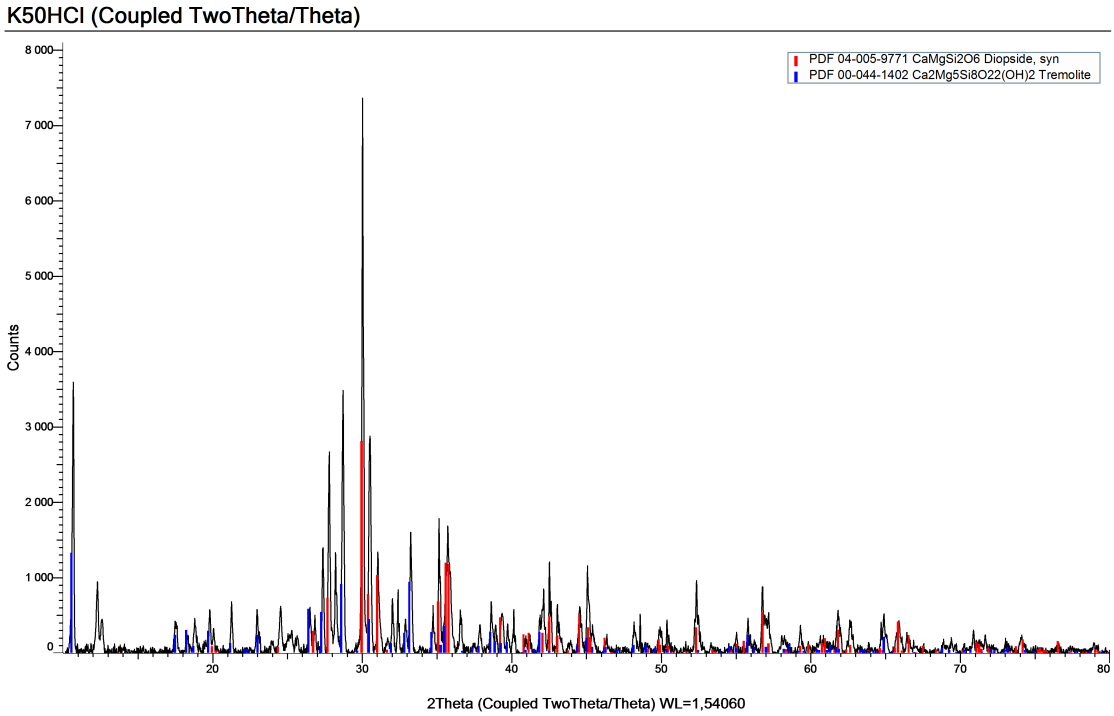

Figure B.14: Diffractogram for the leaching sample Kevitsa, HCl @ 50 °C.

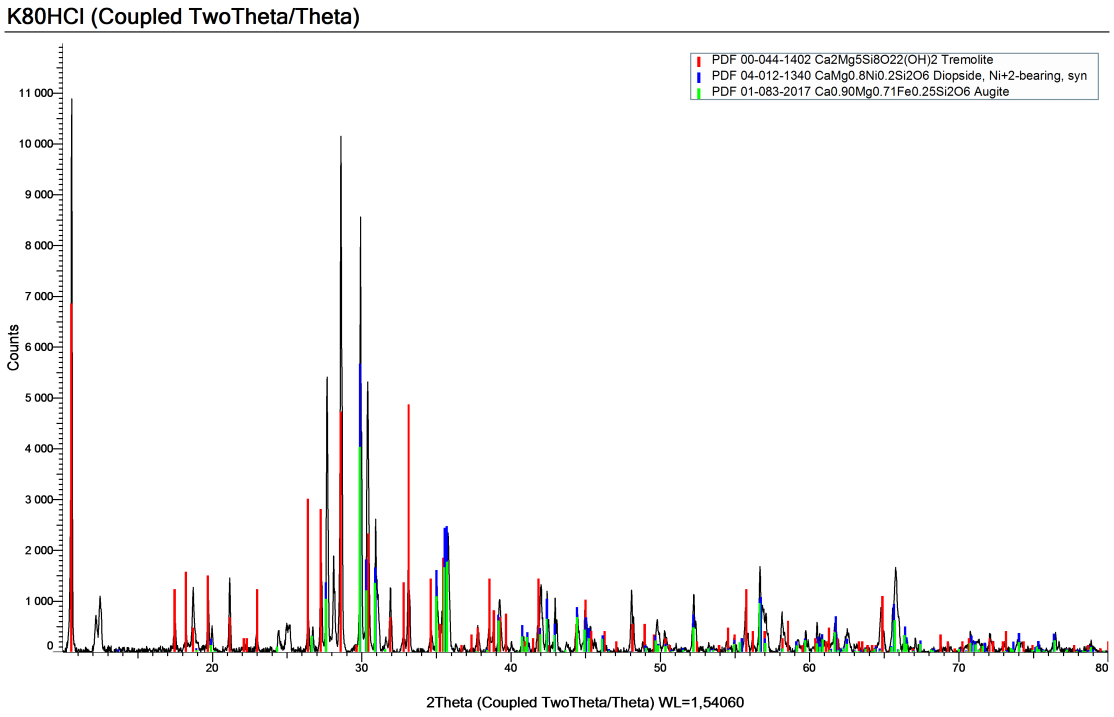

Figure B.15: Diffractogram for the leaching sample Kevitsa, HCl @ 80 °C.

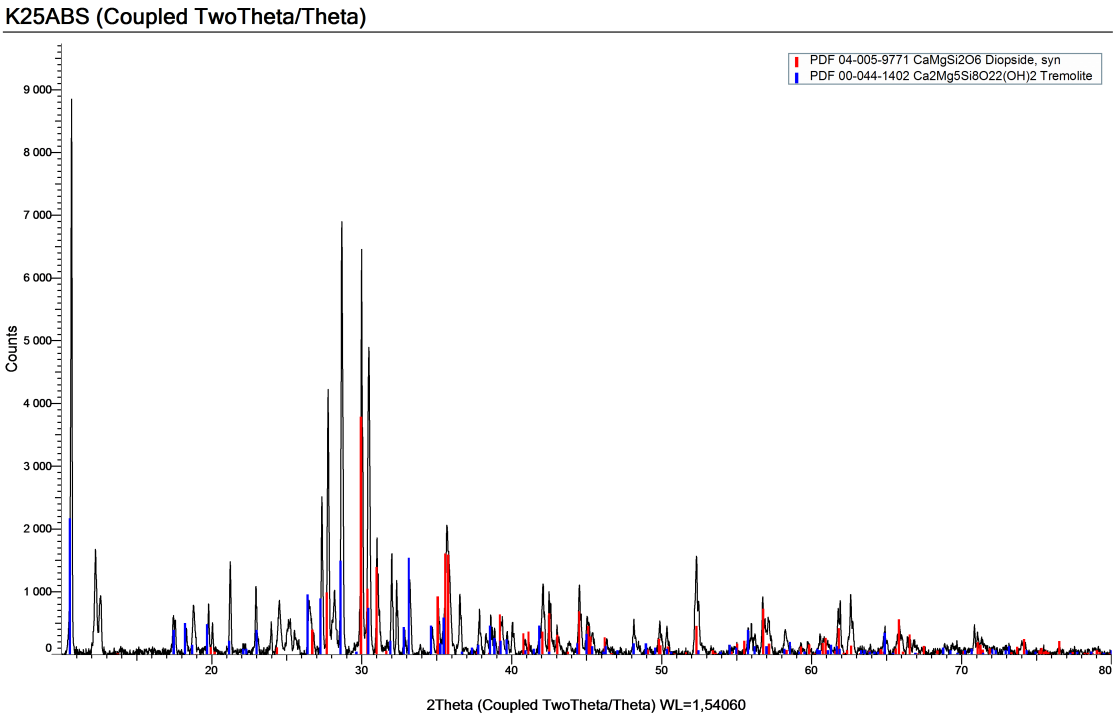

Figure B.16: Diffractogram for the leaching sample Kevitsa, ABS @ 25 °C.

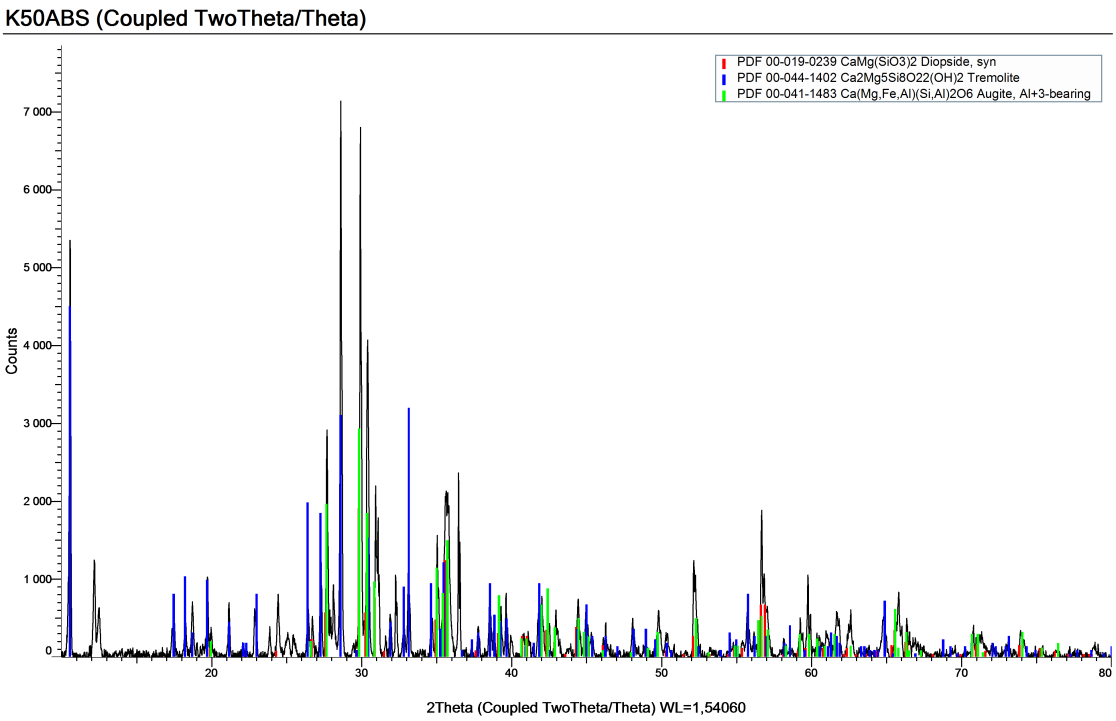

Figure B.17: Diffractogram for the leaching sample Kevitsa, ABS @ 50 °C.

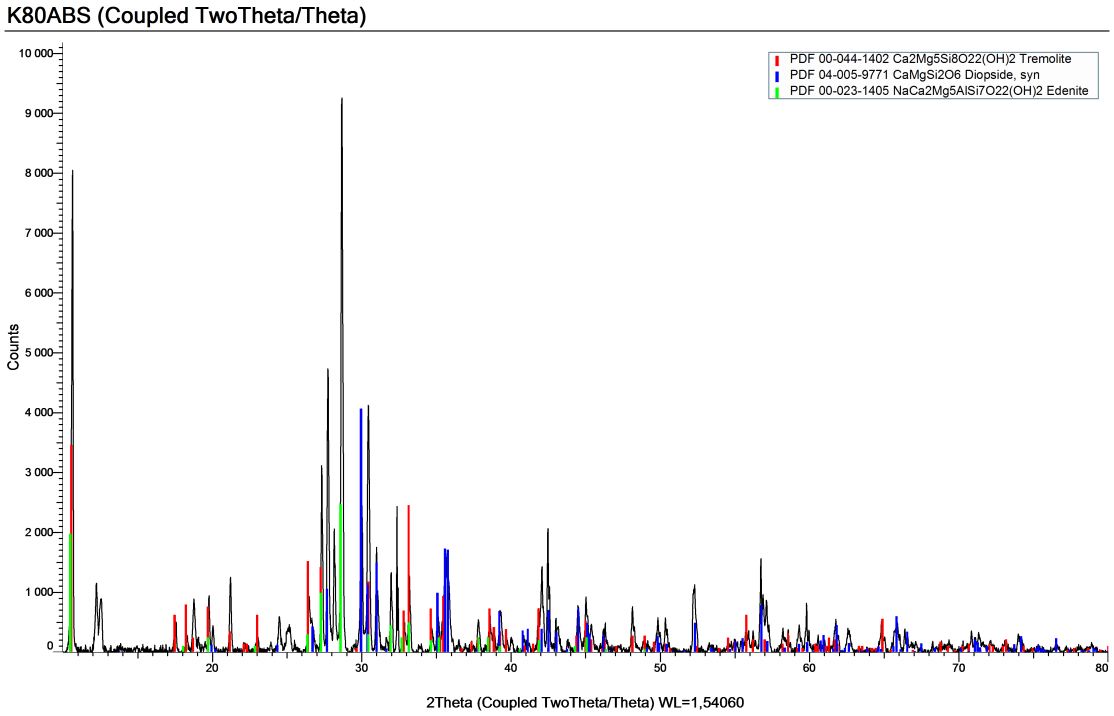

Figure B.18: Diffractogram for the leaching sample Kevitsa, ABS @ 80 °C.

B.2 Precipitates from the pH lift

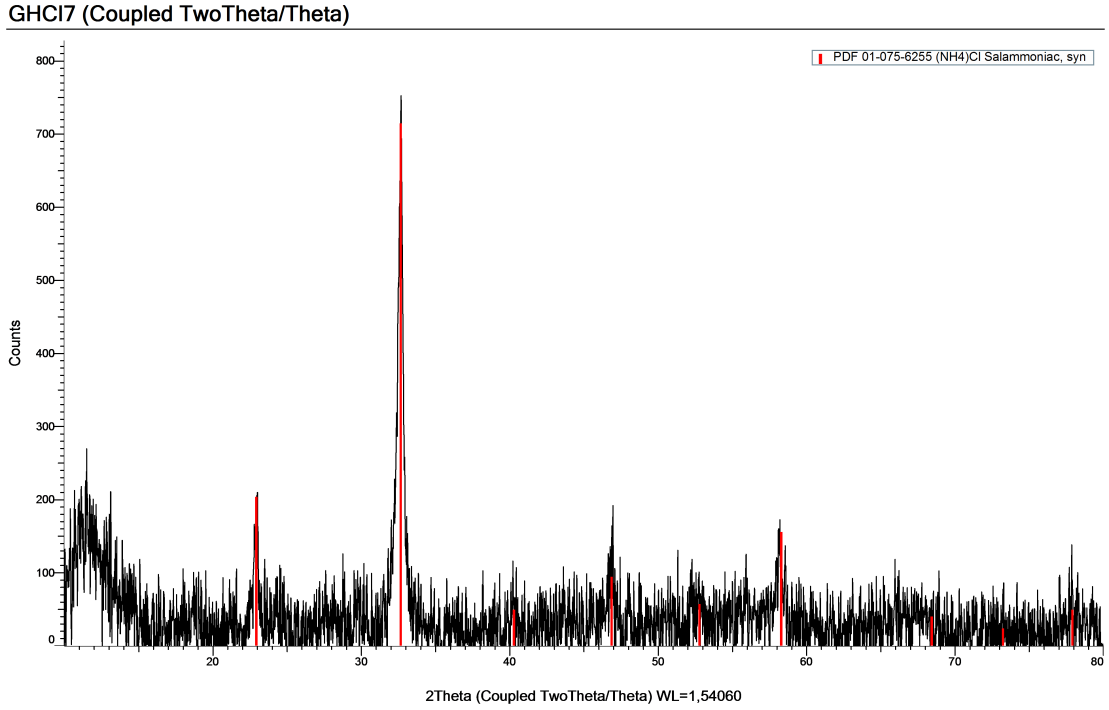

Figure B.19: Diffractogram for the precipitate from pH adjustment of the Garpenberg, HCl sample at pH 7.

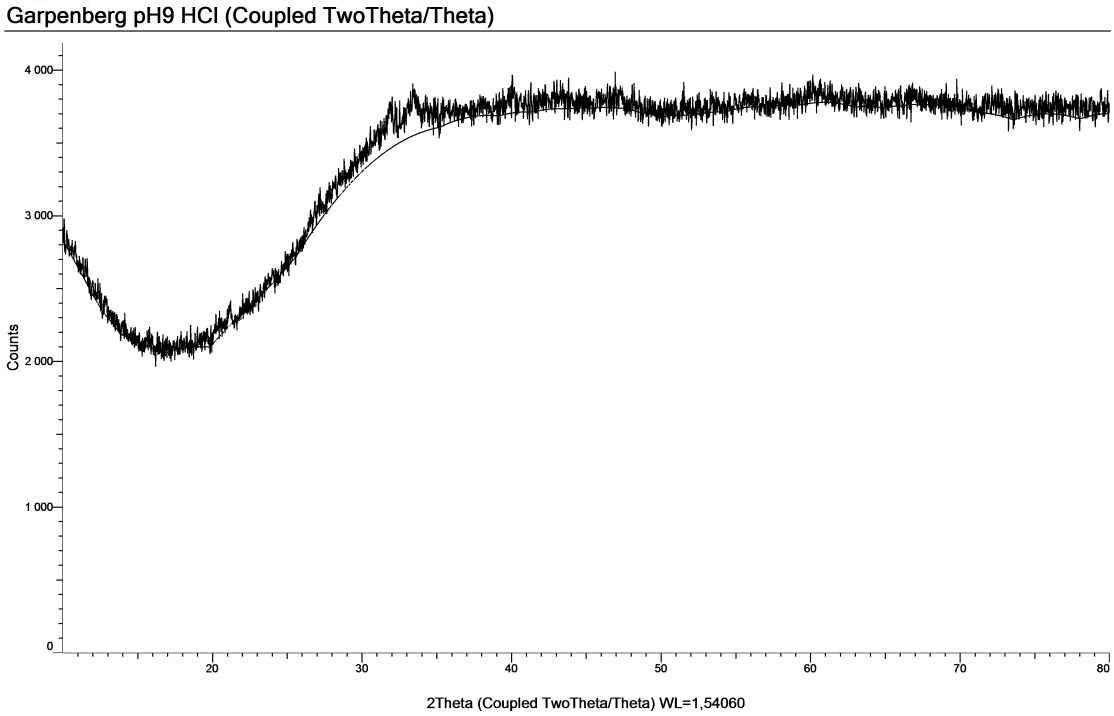

Figure B.20: Diffractogram for the precipitate from pH adjustment of the Garpenberg, HCl sample at pH 9.

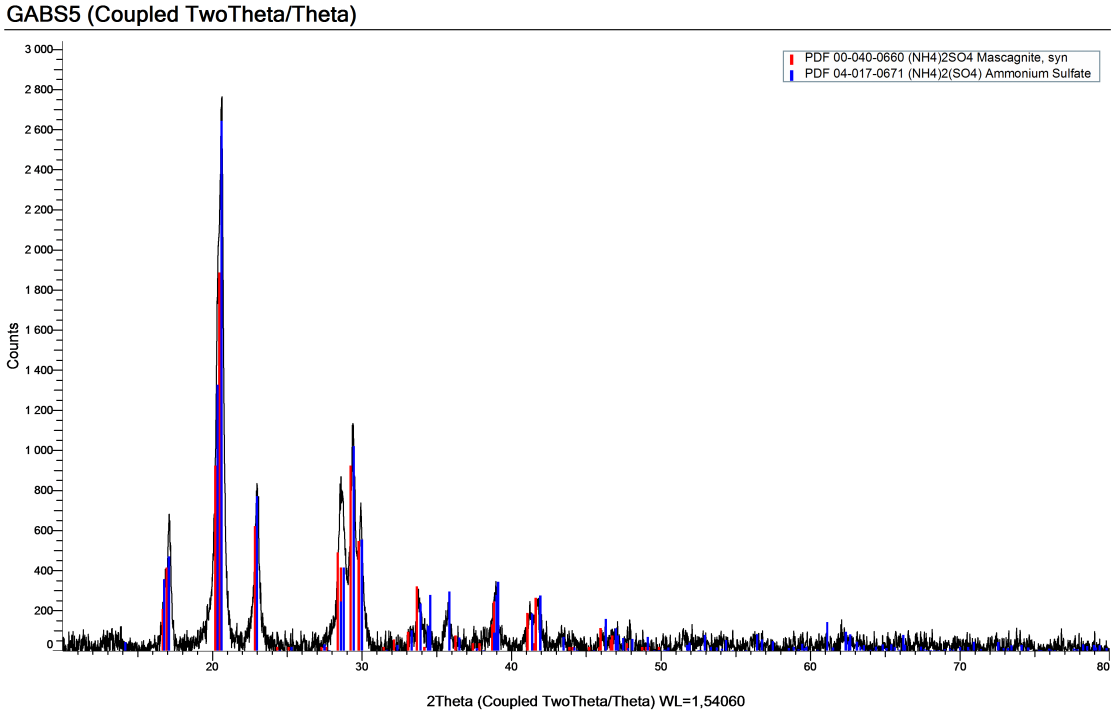

Figure B.21: Diffractogram for the precipitate from pH adjustment of the Garpenberg, ABS sample at pH 5.

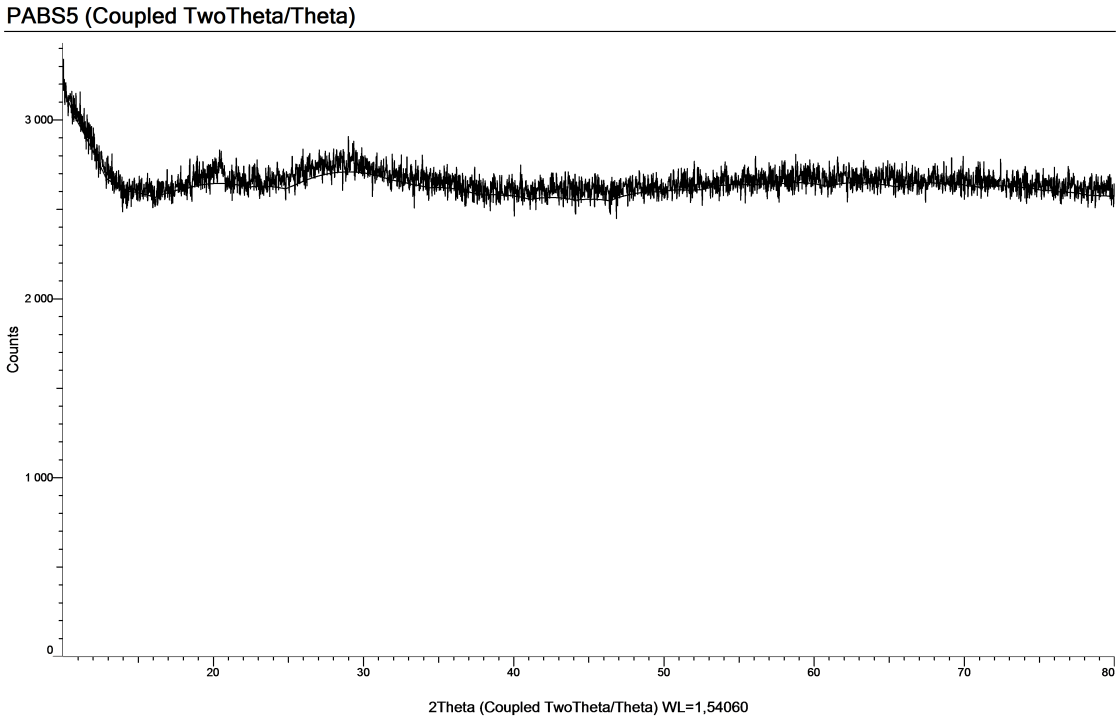

Figure B.22: Diffractogram for the precipitate from pH adjustment of the Pajala, ABS sample at pH 5.

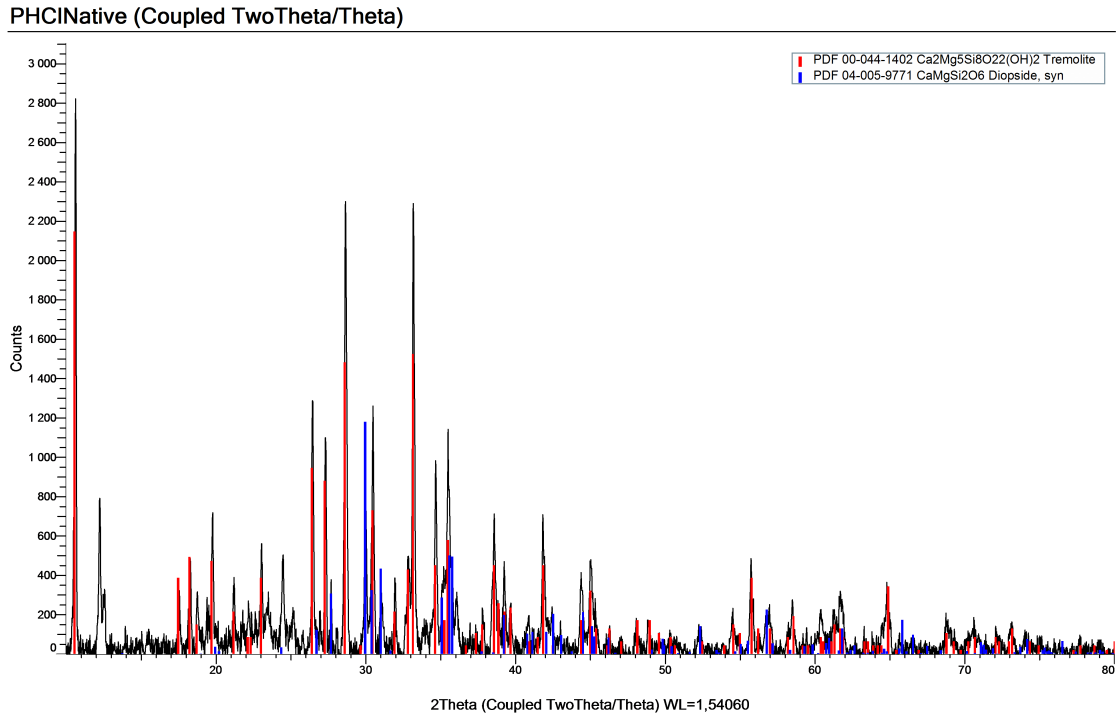

Figure B.23: Diffractogram for the precipitate from pH adjustment of the Pajala, HCl sample at native pH.

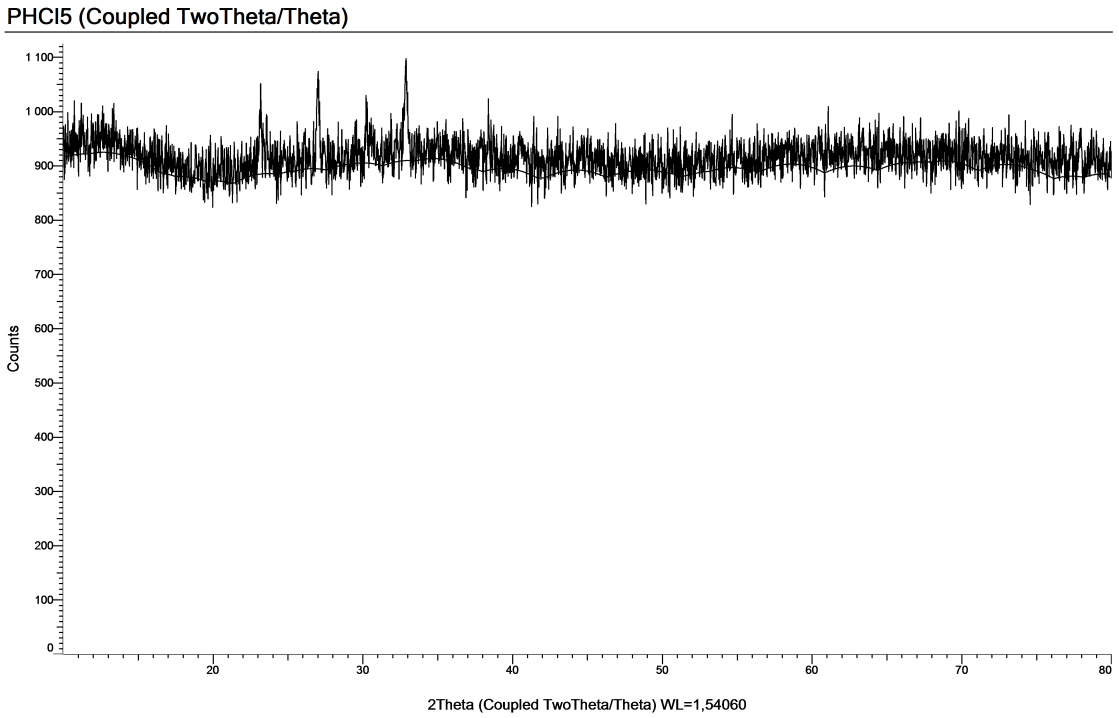

Figure B.24: Diffractogram for the precipitate from pH adjustment of the Pajala, HCl sample at pH 5.

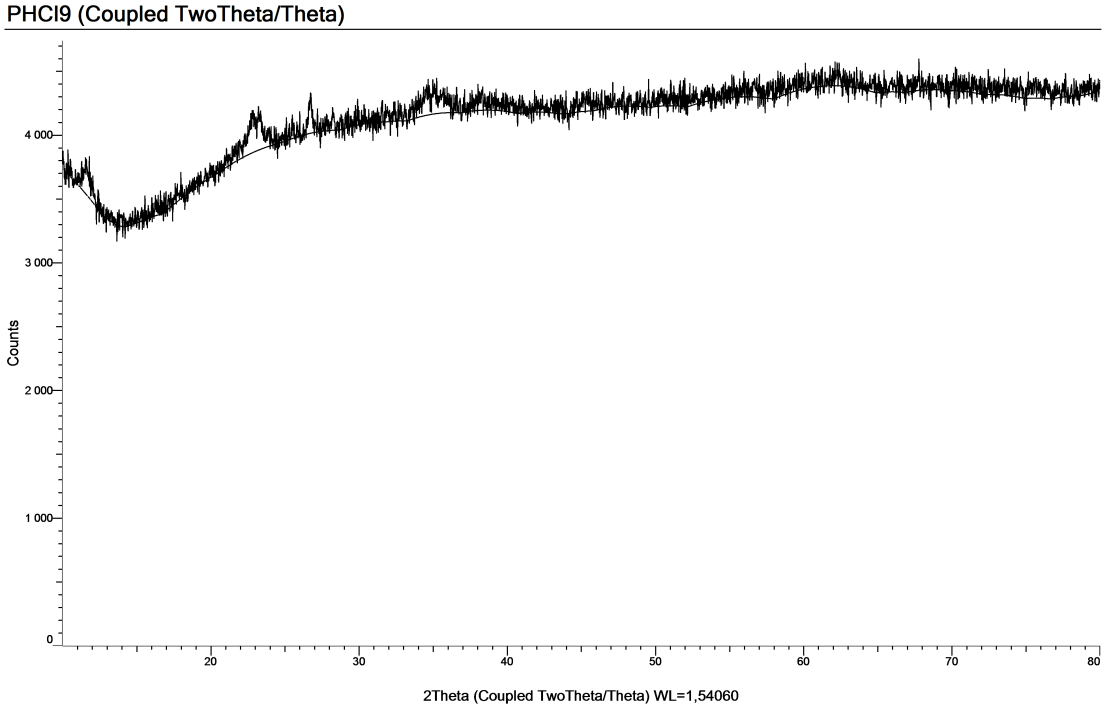

Figure B.25: Diffractogram for the precipitate from pH adjustment of the Pajala, HCl sample at pH 9.

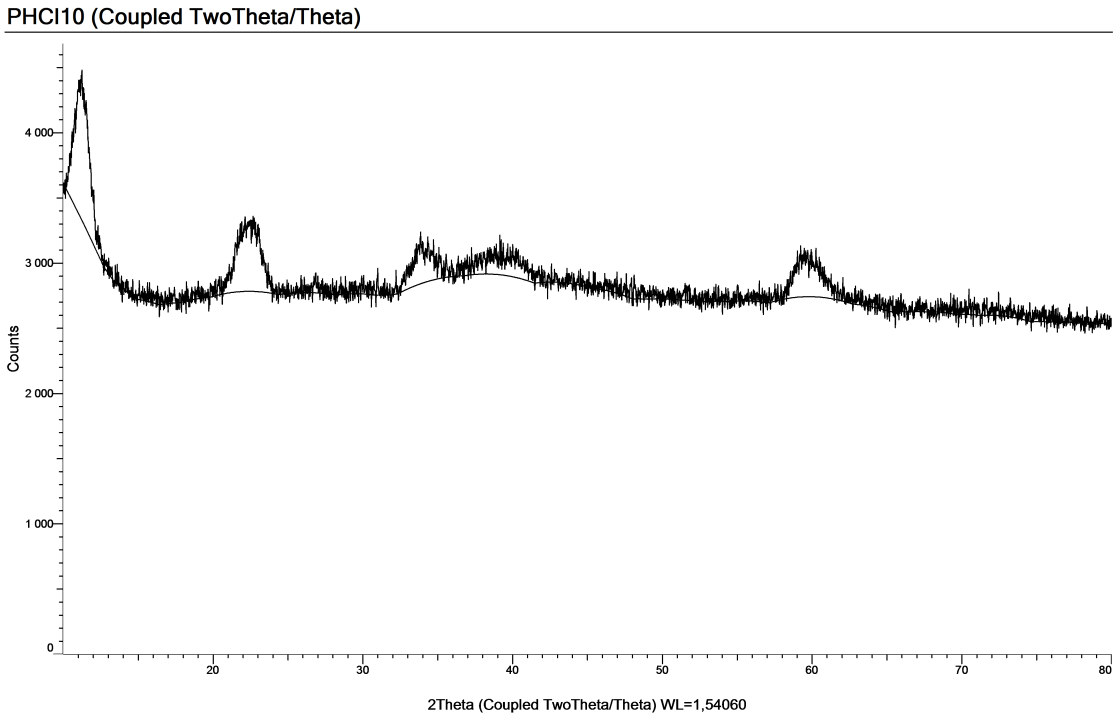

Figure B.26: Diffractogram for the precipitate from pH adjustment of the Pajala, HCl sample at pH 10.

B.3 Precipitates before pre-carbonation heating

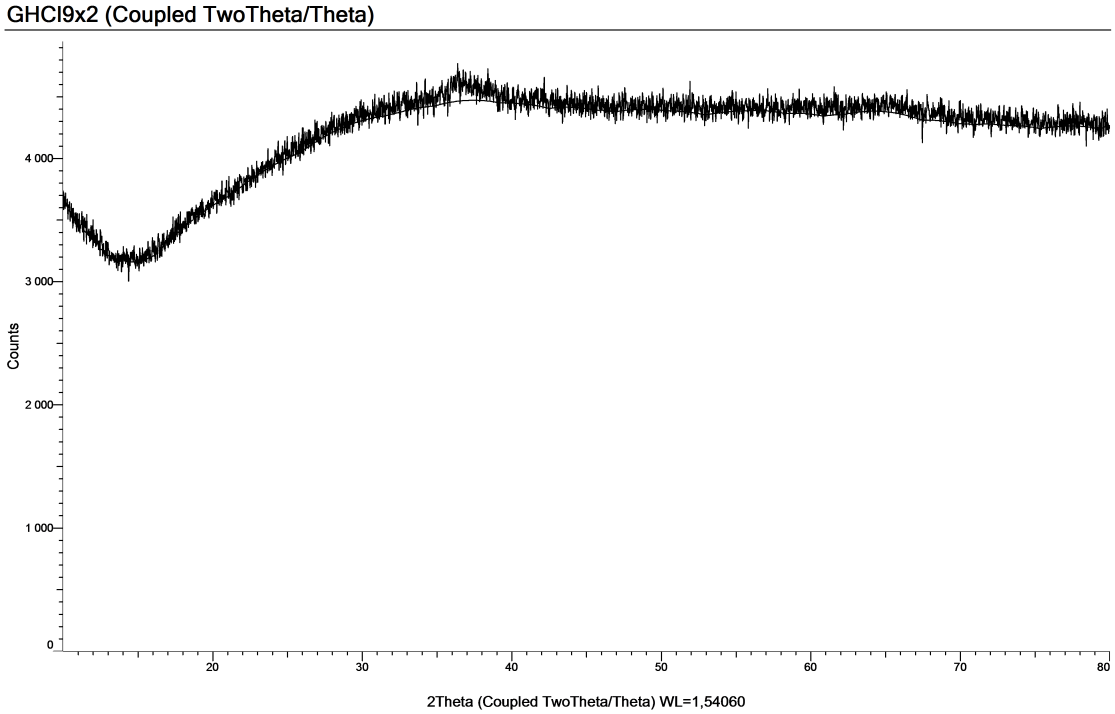

Figure B.27: Diffractogram for the precipitate prior to carbonation for the Garpenberg, HCl sample at pH 9.

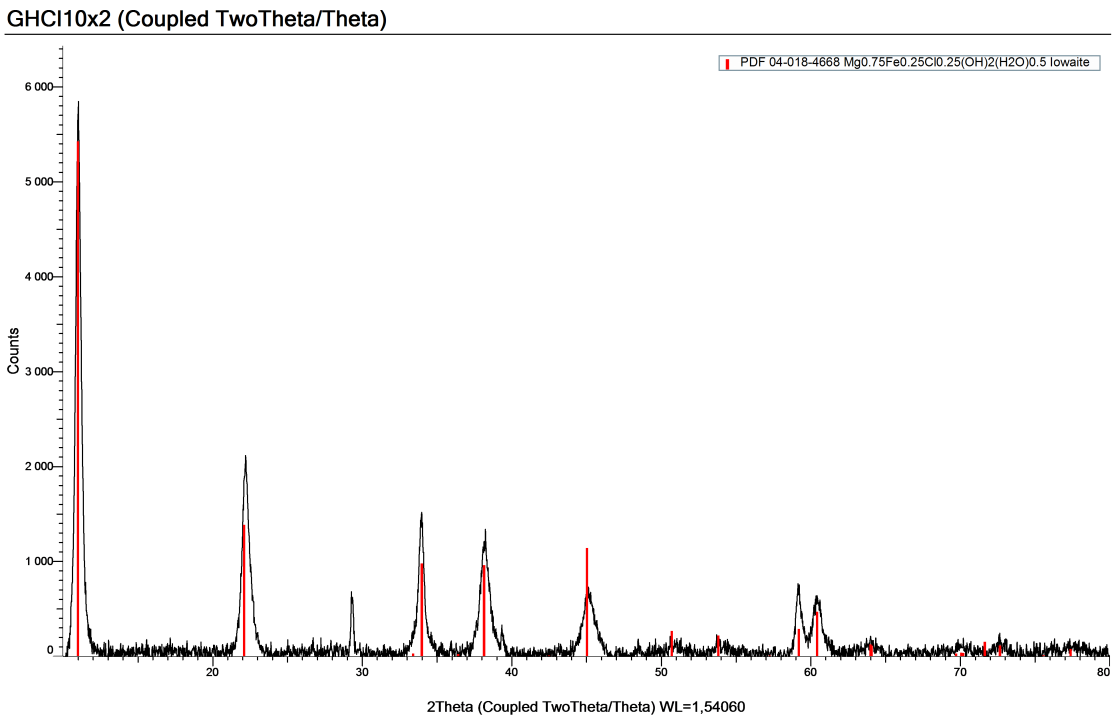

Figure B.28: Diffractogram for the precipitate prior to carbonation for the Garpenberg, HCl sample at pH 10.

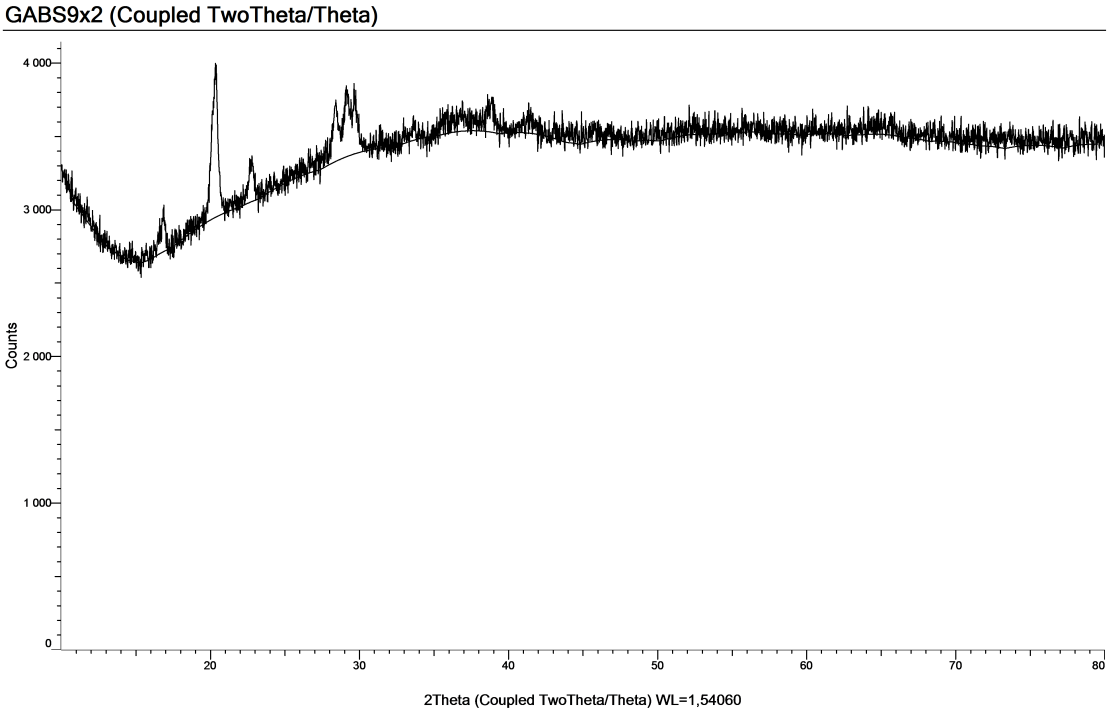

Figure B.29: Diffractogram for the precipitate prior to carbonation for the Garpenberg, ABS sample at pH 9.

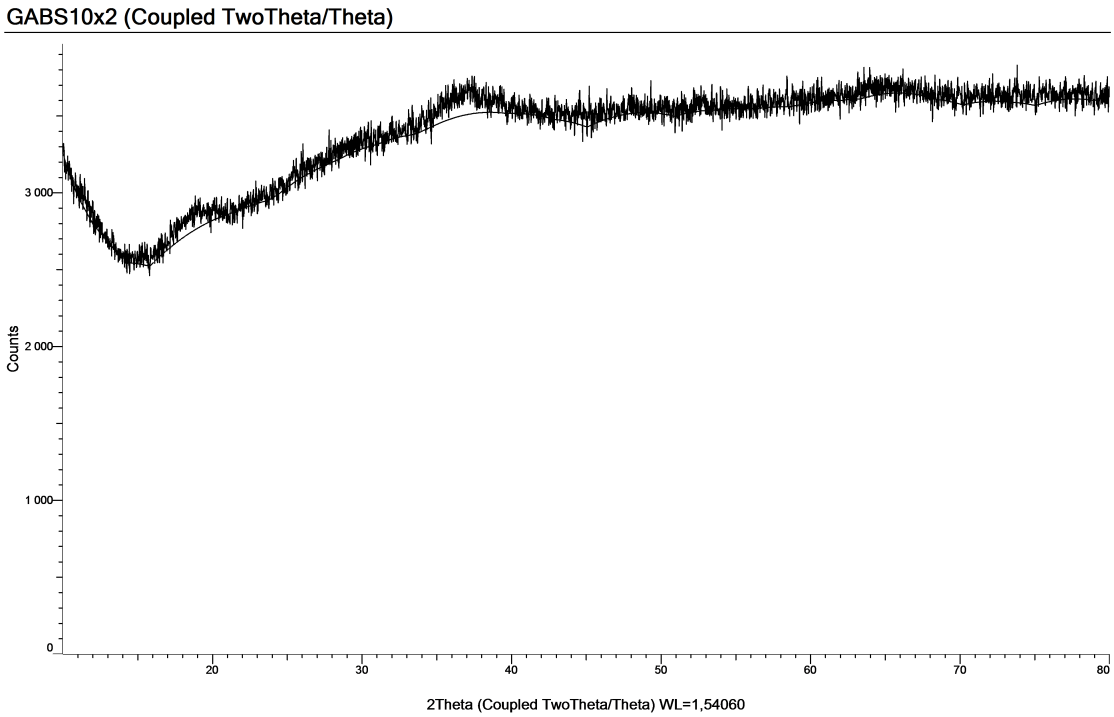

Figure B.30: Diffractogram for the precipitate prior to carbonation for the Garpenberg, ABS sample at pH 10.

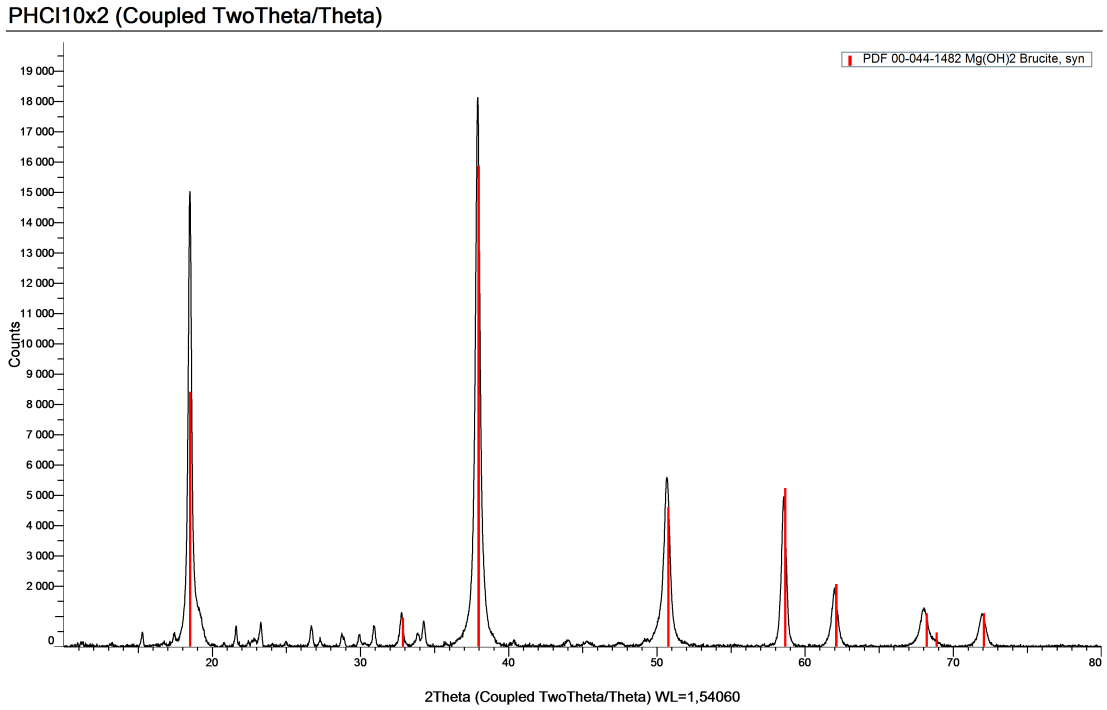

Figure B.31: Diffractogram for the precipitate prior to carbonation for the Pajala, HCl sample at pH 10.

B.4 Carbonation products

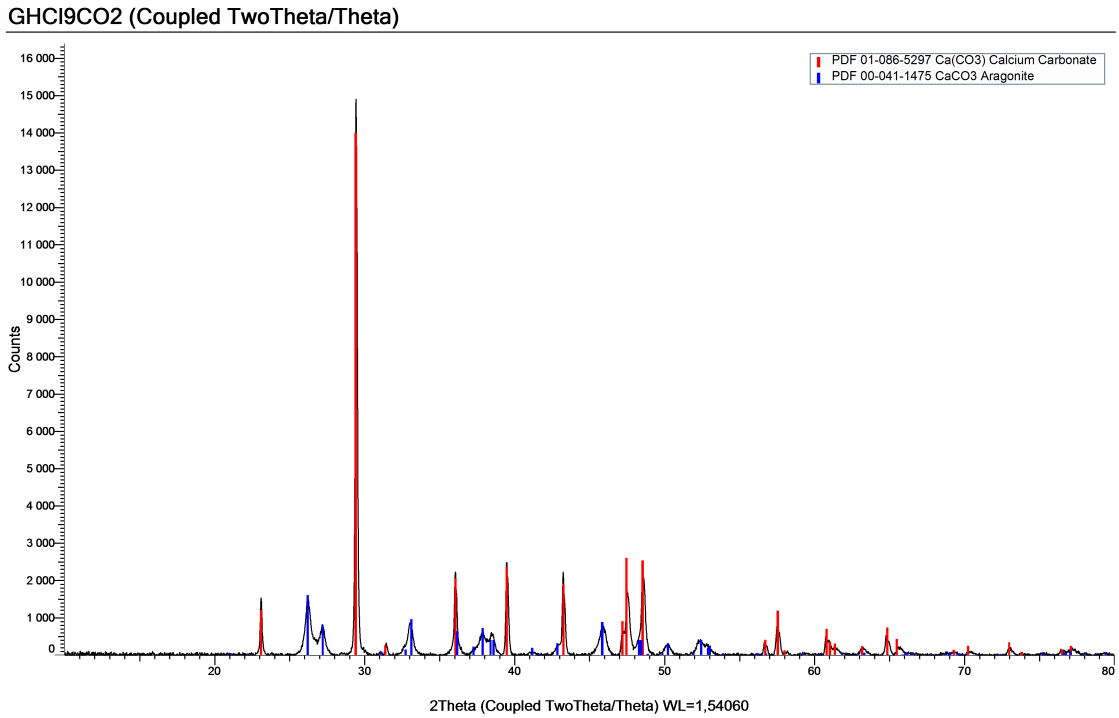

Figure B.32: Diffractogram for the carbonation product from the Garpenberg, HCl sample at pH 9.

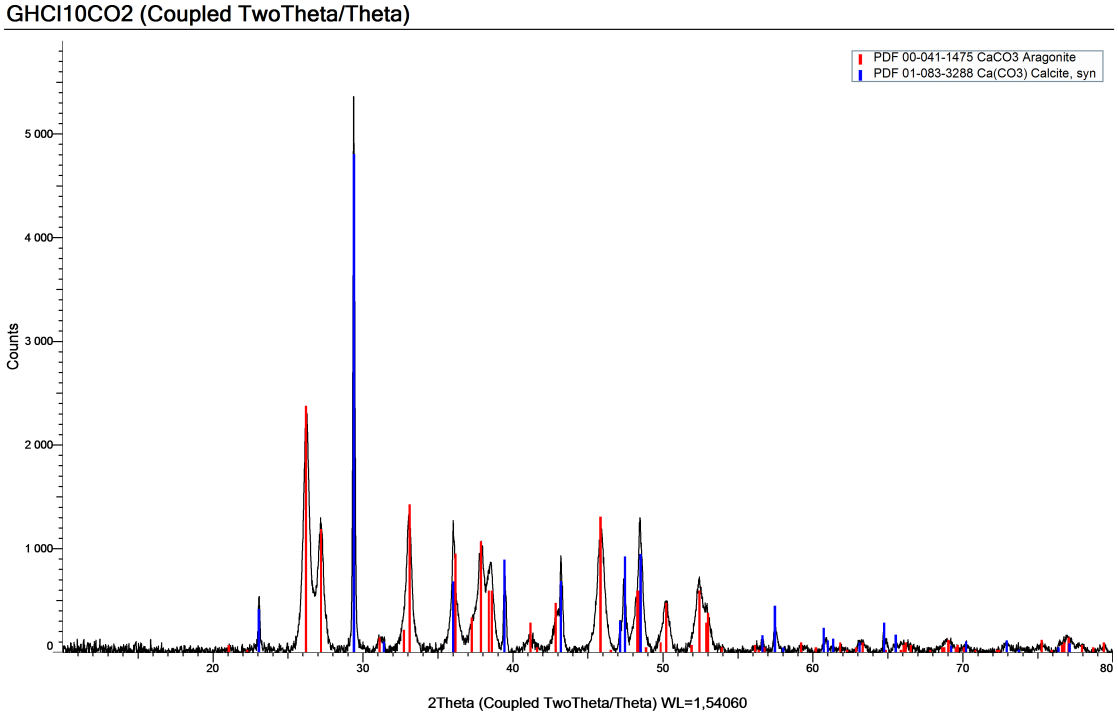

Figure B.33: Diffractogram for the carbonation product from the Garpenberg, HCl sample at pH 10.

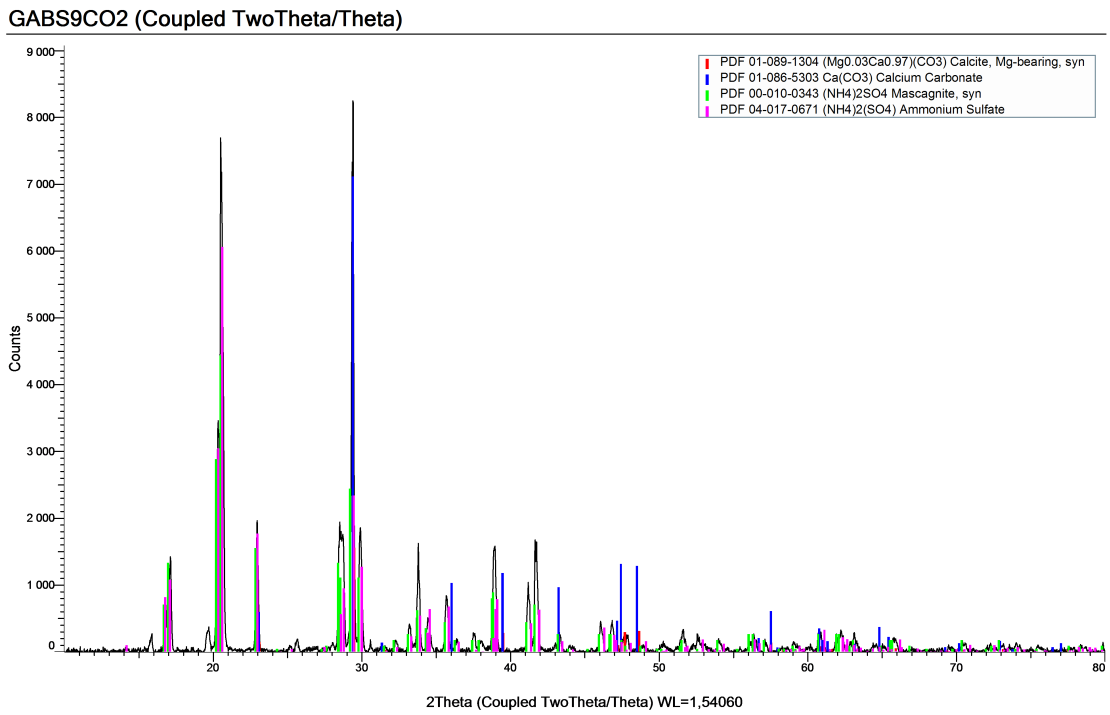

Figure B.34: Diffractogram for the carbonation product from the Garpenberg, ABS sample at pH 9.

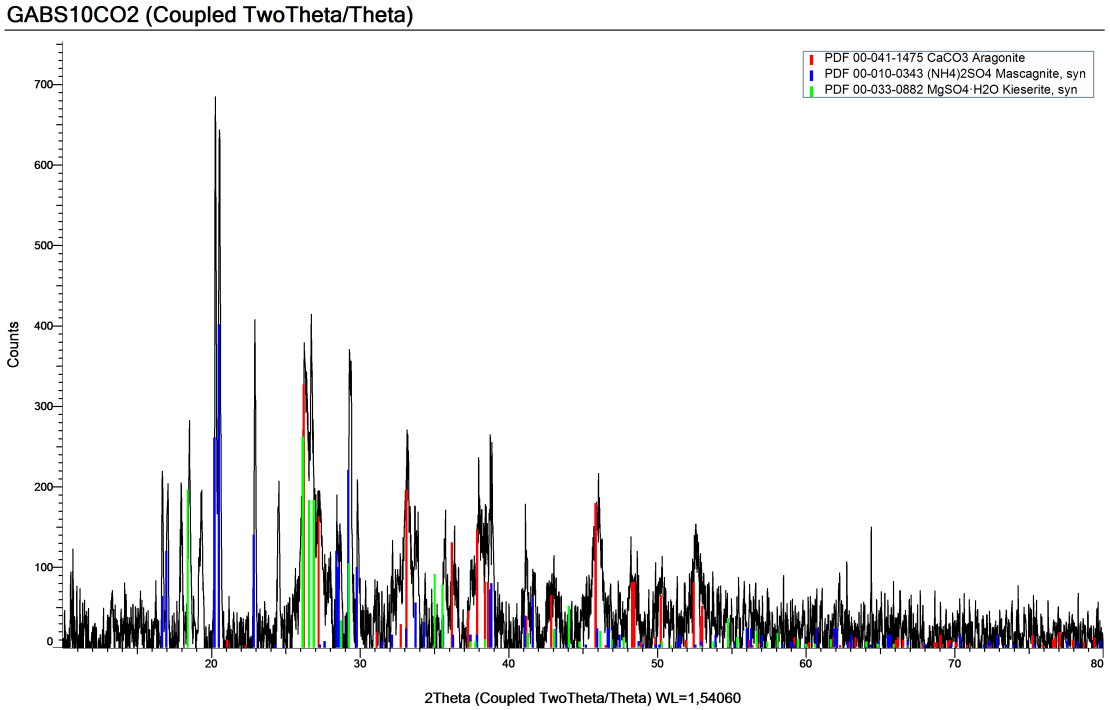

Figure B.35: Diffractogram for the carbonation product from the Garpenberg, ABS sample at pH 10.

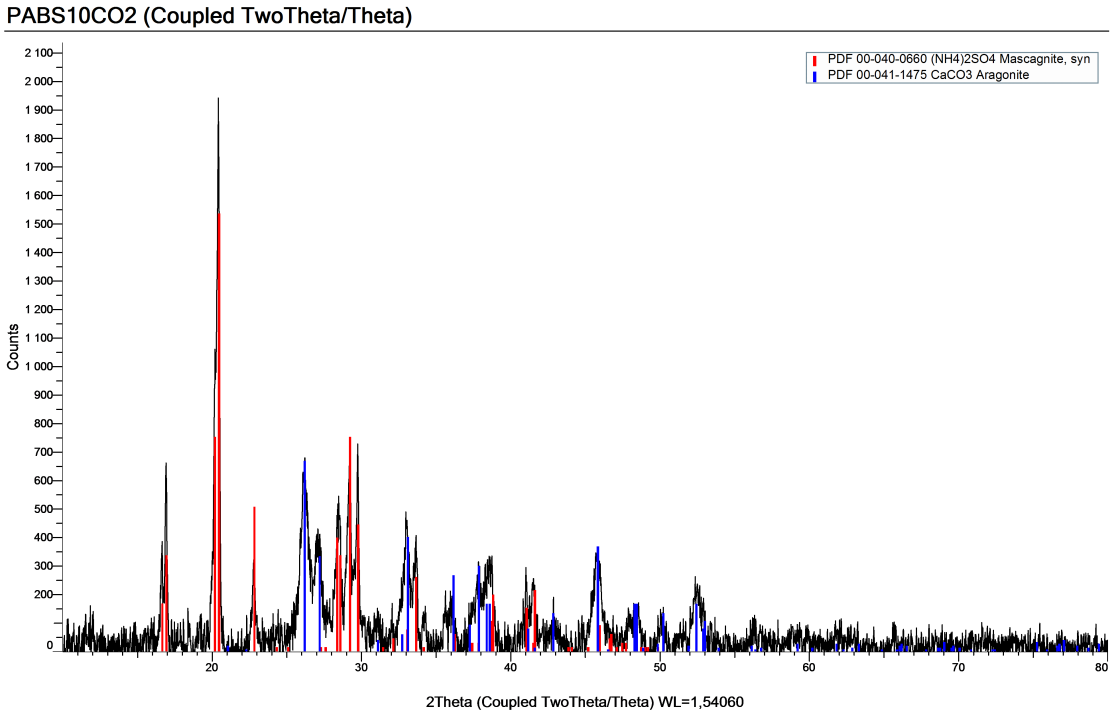

Figure B.36: Diffractogram for the carbonation product from the Pajala, ABS sample at pH 10.

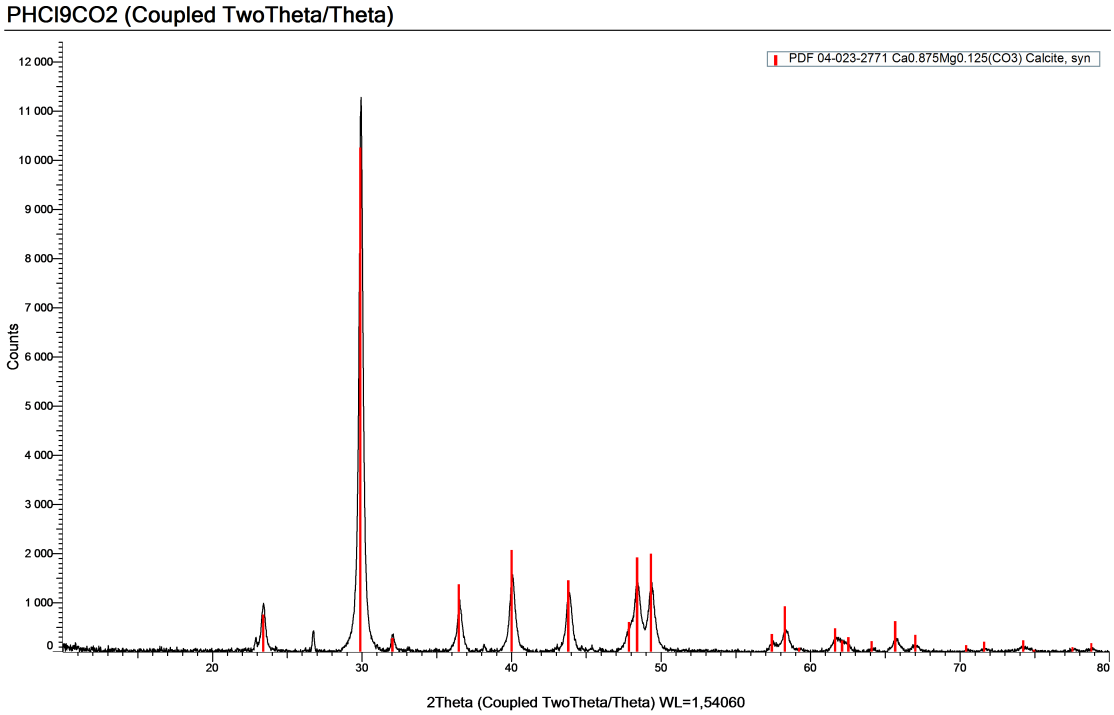

Figure B.37: Diffractogram for the carbonation product from the Pajala, HCl sample at pH 9.

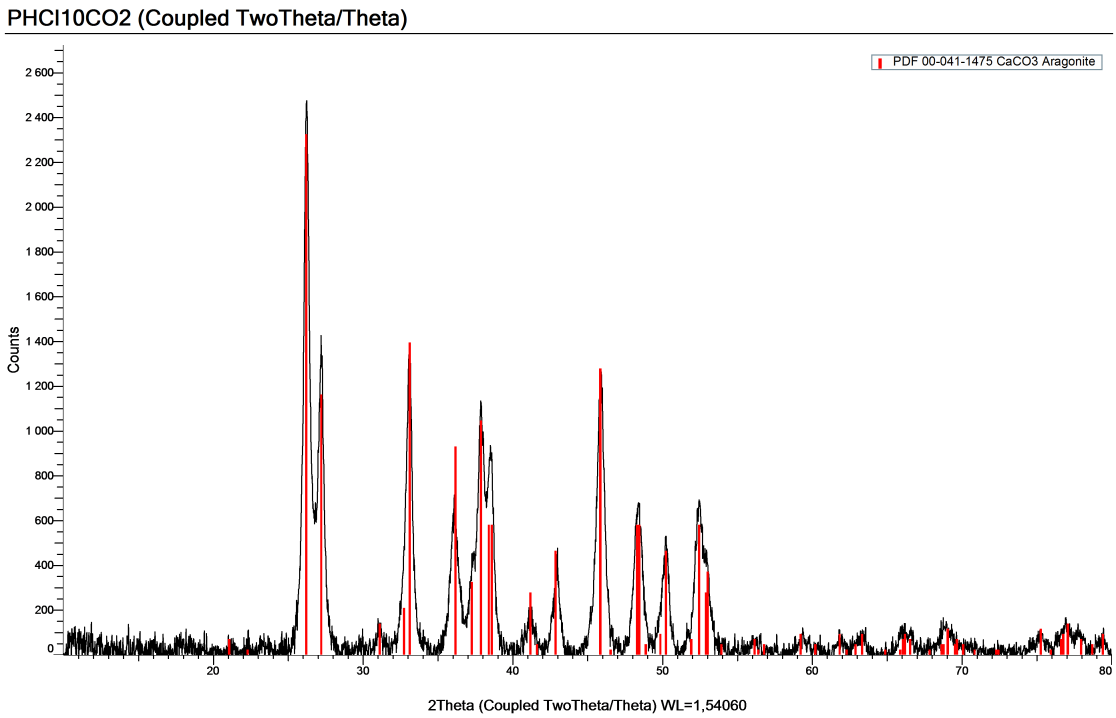

Figure B.38: Diffractogram for the carbonation product from the Pajala, HCl sample at pH 10.

DEPARTMENT OF CHEMISTRY AND CHEMICAL ENGINEERING
DIVISION FOR CHEMISTRY AND BIOCHEMISTRY
CHALMERS UNIVERSITY OF TECHNOLOGY
Gothenburg, Sweden 2023
www.chalmers.se

CHALMERS
UNIVERSITY OF TECHNOLOGY